UNIVERSITY OF PARDUBICE

FACULTY OF CHEMICAL TECHNOLOGY

Institute of Environmental and Chemical Engineering

THE USE OF NANOFILTRATION FOR SEPARATION OF HEAVY METALS FROM WASTEWATER

Doctoral Dissertation

2020

UNIVERZITA PARDUBICE

FAKULTA CHEMICKO–TECHNOLOGICKÁ

Ústav environmentálního a chemického inženýrství

POUŽITÍ NANOFILTRACE PRO SEPARACI TĚŽKÝCH KOVŮ Z ODPADNÍ VODY

Ing. Edwin Wallace

Disertační práce

2020

Prohlašuji:

Tuto práci jsem vypracoval samostatně. Veškeré literární prameny a informace, které jsem v práci využil, jsou uvedeny v seznamu použité literatury.

Byl jsem seznámen s tím, že se na moji práci vztahují práva a povinnosti vyplývající ze zákona č. 121/2000 Sb., o právu autorském, o právech souvisejících s právem autorským a o změně některých zákonů (autorský zákon), ve znění pozdějších předpisů, zejména se skutečností, že Univerzita Pardubice má právo na uzavření licenční smlouvy o užití této práce jako školního díla podle § 60 odst. 1 autorského zákona, a s tím, že pokud dojde k užití této práce mnou nebo bude poskytnuta licence o užití jinému subjektu, je Univerzita Pardubice oprávněna ode mne požadovat přiměřený příspěvek na úhradu nákladů, které na vytvoření díla vynaložila, a to podle okolností až do jejich skutečné výše.

Beru na vědomí, že v souladu s § 47b zákona č. 111/1998 Sb., o vysokých školách a o změně a doplnění dalších zákonů (zákon o vysokých školách), ve znění pozdějších předpisů, a směrnicí Univerzity Pardubice č. 9/2012 Pravidla pro zveřejňování závěrečných prací a jejich základní jednotnou formální úpravu, ve znění pozdějších dodatků, bude práce zveřejněna v Univerzitní knihovně a prostřednictvím Digitální knihovny Univerzity Pardubice.

V Pardubicích dne 30. září 2020

Ing. Edwin Wallace

DECLARATION

I hereby declare that the use of nanofiltration for the separating of heavy metals from waste water is my own work, it does not include any material published or written by another person or has been submitted for the award of any other university degree and that all the sources I have used and quoted have been indicated and acknowledged by complete references.

Pardubice, September 30, 2020

……

Ing. Edwin Wallace

ACKNOWLEDGEMENT

First, I am thankful to the Almighty God Jehovah for given me the necessary strength to complete this dissertation.

I would like to express my profound gratitude to Dr. Jiří Cuhorka for his entire assistant during my experiments at the lab and his guidance throughout my work.

I am particularly grateful to my supervisor, prof. Ing. Petr Mikulášek, CSc., Head of Institute of Environmental and Chemical Engineering, Faculty of Chemical Technology, University of Pardubice, for his valuable and constructive suggestion during the planning and development of this doctoral dissertation. In fact, without his support and guidance, this doctoral dissertation would not have been completed.

Finally, I would like to thank my family especially my mother, Mrs. Georgina Wallace who inspired me throughout my studies and all my friends who help me in diverse ways in writing my doctoral dissertation.

ABSTRACT

The aim of this research is to investigate the performance of two commercially available thin–film composite polyamide NF membranes (AFC 30 and AFC 80) for separating toxic heavy metals from wastewater. Structural parameters and charged surface properties of the membranes were estimated. Experiments with neutral aqueous solutions in conjunction with two independent pore models (Donnan Steric Pore and Steric Hindrance Pore model) were performed at various process conditions. The fixed charge density (ΦX) on the membrane surfaces were determined from different concentrations of sodium chloride (NaCl) experiment by using the Spiegler–Kedem model together with Teorell–Meyer–Sievers model (TMS). The dependence of charge density on NaCl concentration is represented by the known Freundlich isotherm.

The influence of the operating conditions such as transmembrane pressure, feed concentration, cross flow velocity, pH, and effect of composition solution on heavy metals were studied. The operating parameters have been used to find optimum conditions of the two tested commercially available nanofiltration membranes for the removal of heavy metals from wastewater. Heavy metals rejection was modelled using Spiegler–Kedem model and Steric Hindrance Pore model to estimate the reflection coefficient as well as the effective pore radius.

KEYWORDS

Heavy metals, rejection, nanofiltration, polyamide membrane, modelling

ABSTRAKT

Práce se zabývá separací toxických těžkých kovů z odpadní vody pomocí dvou komerčně dostupných tenkovrstvých polyamidových NF membrán (AFC 30 a AFC 80). Byly zjišťovány strukturní parametry a náboj membrán. V práci jsou použity dva nezávislé modely popisující porézní strukturu membrány (Donnan Steric Pore model – DSP model a Steric Hindrance Pore model – SHP model) společně s experimentálními výsledky separace neutrálních látek při různých pracovních podmínkách. Oba použité modely, DSP a SHP, přesně popsaly experimentálně stanovené rejekce různých neutrálních látek. Z toho lze usuzovat, že oba dva modely lze využít pro popis strukturních parametrů NF membrány. Hustota náboje na povrchu membrány (ΦX) byla určena pomocí experimentů s různými koncentracemi chloridu sodného (NaCl) s využitím modelu Spiegler–Kedemové a modelu Teorell–Meyer–Sieverse (TMS). Závislost hustoty náboje na koncentraci NaCl vystihuje známá Freundlichova izoterma.

Byl studován vliv provozních parametrů, jako tlakový rozdíl nad a pod membránou, koncentrace kovu v nástřiku, rychlost průtoku nástřiku a hodnota pH. K experimentům byly použity síran zinečnatý ($ZnSO_4$), dusičnan zinečnatý ($Zn(NO_3)_2$), dusičnan kobaltnatý ($Co(NO_3)_2$) a dusičnan nikelnatý ($Ni(NO_3)_2$). Zvolené pracovní podmínky sloužily k nalezení optimálních podmínek při odstraňování těžkých kovů na komerčně dostupných membránách.

KLÍČOVÁ SLOVA

Těžké kovy, rejekce, nanofiltrace, polyamidová membrána, modelování

Table of Contents

List of symbols and abbreviations

Symbols

A_k	membrane porosity	–
C_f	concentration of solute *i* in feed solution	mol m^{-3}
C_m	concentration of solute *i* in feed solution at the membrane surface	mol m^{-3}
C_p	concentration of solute *i* in permeate solution	mol m^{-3}
c	concentration of the 1–1 electrolyte	mol m^{-3}
$D_{i,\infty}$	bulk diffusivity of solute *i*	m^2 s^{-1}
D_s	diffusivity of the 1–1 electrolyte	m^2 s^{-1}
d_h	hydraulic diameter	m
J	permeate volume flux	m^{-2} s^{-1}
J_w	pure water flux	m^{-2} s^{-1}
K	mass transfer coefficient in polarization layer	m s^{-1}
$K_{i,c}$	hindrance factor for convection	–
$K_{i,d}$	hindrance factor for diffusion	–
L_p	pure water permeability	m s^{-1} Pa^{-1}
ΔP	transmembrane pressure difference	Pa
Pe	Peclet number	–
P	solute permeability	m s^{-1}
r_p	pore radius	m
R	real (intrinsic) rejection	–

R_o	observed rejection	–
Re	Reynolds number	–
Sc	Schmidt number	–
Sh	Sherwood number	–
u	fluid velocity in the channel	m s^{-1}
Δx	membrane thickness to porosity ratio	m

Greek symbols

α	transport number of cations in the free solution	–
η	dynamic viscosity	Pa s
λ_i	ratio of solute *i* radius to pore size	–
Φ_i	steric partitioning coefficient of solute *i*	–
ΦX	effective fixed charged density	mol m^{-3}
$\Delta\pi$	osmotic pressure	Pa
σ	reflection coefficient	–
ξ	electrostatic effect	V mol m^{-2}
ρ	density	kg m^{-3}

Abbreviations

AMX	Amoxicillin
BGW	Brackish ground water
BPA	Bisphenol A
CA	Cellulose acetate
CBTs	Coagulation bath temperatures
CDX	Carbadox
COD	Chemical oxygen demand
CS	Chitosan
CTABr	Cetyl trimethyl–ammonium bromide
DAF	Dissolved–air flotation
DETA	Diethlenetriamine
DOC	Dissolved organic carbon
DSPM	Donnan steric pore model
DSPM–DE	Donnan steric Pore model with dielectric exclusion
ED	Electrodiaysis
EDC/PPCPs	Endocrine disrupting compound/Pharmaceuticals and Personal Care Products
EDTA	Ethylenediaminetetraacetic acid
ENP	Extended Nernst–Plank
EPA	Environmental protection agency

EPD	Environmental protection department
EPS	Exopolymeric substance
FDFO	Fertilizer forward osmosis
IP	Interfacial polymerization
IT	Irreversible thermodynamic
IUPAC	International Union of Pure and Applied Chemistry
LPRO	Low pressure reverse osmosis
MCL	Maximum contaminant level
MED	Multi–effect distillation
MF	Microfiltration
MMMs	Mixed matrix membranes
MOFs	Metal–organic frameworks
MPD	M–phenylenediamine
MSF	Multi–stage flash
MUEF	Micellar enhnaced ultrafiltration
MWCO	Molecular weight cut–off
NF	Nanofiltration
NF–BW	Nanofiltration brackish water
NF–MBR	Nanofiltration membrane bioreactor
NOM	Natural organic matter
NPs	Nanoparticles

PA	Polyamide
PAC	Polyaluminium chloride
PAM	Polyacrylamide
PCD	Pollution control department
PEG	Polyethylene glycol
PEI	Polyetherimide
PES	Polyethersulfone
PFS	Polyferric sulphate
PIP	Piperazidine
PP	Polypropylene
PS	Polysulfone
PUEF	Polymer enhnaced ultrafiltration
PVDF	Polyvinylidene fluoride
RO	Reverse osmosis
ROS	Reactive oxygen species
SEM	Scanning electronic microscopy
SHP	Steric hindrance pore
SMX	Sulfamethoxazole
SW	Seawater
SWRO	Sea water reverse osmosis
TDS	Total dissolved solids

TEM	Transmission electron microscope
TEPA	Tetraethylenepentamine
TETA	Triethylenetetramine
TFC	Thin–film composite
TMC	Trimesoyl chloride
TMP	Transmembrane pressure
UF	Ultrafiltration
UV	Ultraviolet
WWTP	Wastewater treatment plant

List of Figures

List of Tables

1. Introduction

During the past decades, about 50–90 % of capital investments in the chemical industry are related to separation processes of heavy metals from wastewater. Yet, several concerns have been raised on heavy metals due to its recalcitrance and persistence into the environment. It has also become crucial that regulatory measures need to be set up on the effluent limit globally as the industries realize its potential environmental impacts (Geens et al., 2007; Zhao et al., 2016). Water shortage is one of the problems caused by global industrializtion. In developing countries, continued population expansion and urbanization leads to increasing water demand (Yang et al., 2019). According to the World Health Organization (WHO), two out of every three persons in the world may be living under water–stressed conditions if water pollution continues under the current condition. Today, nearly 1.2 billion people around the world drink unclean water. In addition, the United Nation (UN) confirmed that 2.7 billion people will lack access to water by 2025 (Ahuja, 2014). The UN–Water 2009 predicted that 70 percent of wastewater in developing countries is not treated before it is discharged into lakes, sea, and oceans. In similar manner, a report by the United Nations Environment Programme and UN–Habitat in partnership with members of UN Water estimated that two million tons of sewage, industrial and agricultural waste is discharged into the world's waterways without treatment and at least 1.8 million children under five–years–old die as a result every year. This attest to the fact, that one child dies every 20 second due to untreated water (Corcoran et al., 2010). Environmentally friendly process for separation of heavy metals from wastewater is paramount to save numerous humans lives, aquatic life, and the environment. Several alternative conventional processes for separation of heavy metal from wastewater have been extensively studied. However, the major setbacks of these processes are high capital and operational cost, incomplete removal, sludge production, highly sensitive to pH, slow metal precipitation, poor settling and use of chemicals (Fu and Wang, 2011). Therefore, an appropriate and pollution free separation process is necessary to eradicate such occurrences since wastewater is highly polluted and toxic to the environment. Membrane process is equal to the task because of its several advantages in comparison to conventional treatment. Some of the advantages are high performance, simple in operation, no chemical and sludge production (Wei et al., 2013).

This dissertation will be structured as follows: Chapter 2 focuses on the theoretical parts which deals with heavy metals; Chapter 3 is devoted to pressure driven membrane process specifically nanofiltration and its applications; Chapter 4 deals with phenomenon in

NF process; Chapter 5 focuses on the characterization and modelling of NF membrane; Chapter 6 examines the problems and outlines the objectives of my work; Chapters 7 and 8 is devoted to the experimental analysis and results; and Chapter 9 concludes this dissertation with summary of key findings and recommendations.

2. Theoretical part

2.1 Heavy metals and their effect in the environment

Heavy metals are defined as a group of elements having atomic weights between 63.5 and 200.6. The specific weight of heavy metal is over 5000 kg m^{-3} which makes the metal toxic even at low concentrations (Bilal et al., 2013; Otero–Fernández et al., 2017; O' Connell et al., 2008; Srivastava and Majumder, 2008). According to Tchounwou et al., (2012), heavy metals refer to any metallic element that has a relatively high density and is toxic or poisonous even at low concentrations. Heavy metals were further explained as a general collective term which applies to a group of metals and metalloids with atomic density greater than 4000 kg m^{-3}. Heavy metal is highly toxic, non–biodegradable and has the tendency to accumulate in living organism. Additionally, heavy metals cannot be degraded or destroyed. Toxic heavy metals of critical concerns found in wastewater treatment are cadmium (Cd), chromium (Cr), nickel (Ni), copper (Cu), lead (Pb), arsenic (As), cobalt (Co), mercury (Hg) and zinc (Zn). Heavy metals are usually found in wastewater from fuel industry, petroleum refining, mining, textile industry, fertilizer plants, battery manufacturing, paper industries, photographic process industry, automotive and electroplating (Gherasim and Mikulášek, 2014). Furthermore, although heavy metals are naturally occurring elements that are found throughout the earth's crust, most environmental contamination and human exposure result from anthropogenic activities such as mining and smelting operations, industrial production, domestic and agricultural use of metals, and metal–containing compounds. Heavy metals toxicity depends on several factors including the dose, route of exposure, and chemical species, as well as the age, gender, genetics, and nutritional status of exposed individuals. At least 20 metals are toxic, and almost half of these metals enter the environment which poses threat to aquatic life and human beings (Tchounwou et al., 2012).

The Czech government regulation no. 61/2003 Coll (Directive 2013/39/EU) states the permissible value of heavy metals in wastewater is approximately less than 5 mg L^{-1}. Many industries wastewater contains heavy metals having a concentration of up to 500 mg L^{-1}. Living organism including human beings, animals, and plants requires varying quantity of heavy metal to survive. Although heavy metals are needed in the human body, at higher concentration become toxic and harmful to the body. When the metals are beyond the allowed permissible concentration, serious health problems do occur. For instance, as children consume more food for them to gain body weight than adult, they are more defenceless to higher dose than adult (Barakat, 2011, Kurniawan et al., 2006). Such health disorders can be

diseases of the kidney, damage of the fatal brain, hypertension, reduced growth and development, nervous system damage, toxicity to the reproductive organs, and mental retardation (Lee et al., 2012). Table 1 gives evidence about the maximum contaminant level (MCL) of heavy metals and several health disorders associated to ingestion beyond permitted levels.

Table 1. The MCL standard for the most hazardous metal (Kurniawan et al., 2006)

Heavy metal	Toxicity	Maximum effluent discharge standards (mg/L)		
		EPA[a] (USA)	EPD[b] (Hong Kong)	PCD[c] (Thailand)
Cr (VI)	Headache, nausea, diarrhea, vomiting, carcinogenic to human	0.05	0.05–2.0	0.25
Zn	Depression, lethargy, neurologic signs such as seizures and ataxia, and increased thirst	1.00	0.60–5.00	5.00
Cu	Liver damage, Wilson disease, insomnia	0.25	0.05–4.0	2.00
Cd	Kidney damage, renal disorder, probable human carcinogen	0.01	0.001–0.2	0.03
Ni	Dermatitis, nausea, chronic asthma, coughing, human carcinogen	0.20	0.10–4.0	1.00

[a] Environmental Protection Agency (EPA), USA.

[b] Environmental Protection Department (EPD), Hong Kong SAR.

[c] Pollution Control Department (PCD), The Ministry of Natural Resources and Environment, Thailand.

Heavy metals are toxic to organic in soil, plants and aquatic life immediately when it enters the environment. With regards to plant, there is growth reduction because of changes in physiological and biochemical processes growing on heavy metal polluted soils. This continued decline in plant growth reduces yield which eventually leads to food insecurity (Chikuike and Obiora, 2014). The change of diversity, population size and overall activity of the soil microbial communities is because of the effect of heavy metal on soil micro–organism (Ashraf and Ali, 2007). Uptake of heavy metals by plants and subsequent accumulation along the food chain is a potential threat to animal and human health. Contaminants in aquatic systems, including heavy metals, stimulate the production of reactive oxygen species (ROS) that can damage fishes and other aquatic organisms. Heavy metals uptake by plants and successive accumulation in human tissues and biomagnifications through the food chain causes both human health and environmental concerns. Heavy metals containing agricultural runoff then enter the aquatic environment which is harmful to aquatic plants and animals (Singh and Kalamdhad, 2011). The impact of heavy metals on aquatic organisms is due to the movements of pollutants from various diffuse or point sources which gives rise to

coincidental mixtures in the ecosystem (Rajeswari and Sailaja, 2014). Among animal species, fishes are the inhabitant that cannot escape from the detrimental effects of these pollutants. Fishes are widely used to evaluate the health of aquatic ecosystems because pollutants build up in the food chain and are responsible for adverse effects and death in the aquatic systems (Baby et al., 2010). However, heavy metals undergo metabolic activation that induces a cellular change in affected fish. The tissue lesions and apoptosis arise from bioaccumulation stimulate necrotic alterations in the fish with an inflammatory defensive reaction (Roganovic–Zafirova et al., 2003).

Zinc is an essential element for human health but the permissible level for humans is 15 mg L^{-1}. It is necessary for the physiological function of living tissue and control countless biochemical processes. Mostly, zinc deficiency results in growth failure of organs in human beings. These are epidermal, gastrointestinal, central nervous, immune, skeletal, and reproductive systems (Oyaro et al., 2007; Roohani et al., 2013). The entry of zinc into the human body has three major routes. These are by inhalation, through the skin or by ingestion. Inhalation of zinc–containing smoke generally originates from industrial processes such as galvanization, primarily affecting several manufacture workers. This acute syndrome is an industrial disease which mostly occurs by inhalation of fresh metal fumes with a particle size <1 μm in occupational situations such as zinc smelting or welding. In addition, military smoke bombs contain zinc oxide or zinc chloride making soldiers vulnerable to inhalation of zinc–containing fumes. Serious health problem which occurs when zinc is excessive in human body are skin irritations, vomiting, stomach cramps; nausea and anaemia (Plum et al., 2010).

Cobalt is usually found in chemical and electroplating industries and by–product of nickel and copper mining (Gherasim et al., 2015). Cobalt and its compound are widely used for cosmetics products such as eye pencil, shadow, lipstick, skin cream, soap, etc. (Bocca et al., 2014). The use of Co and Co salts in cosmetics is forbidden by the EU regulation on cosmetics and intentional ingredients, but their presence is allowed as impurities when technically necessary. Although cobalt has a biologically necessary role as metal constituent of vitamin B_{12}, excessive exposure has end up in various adverse health effects. The four–exposure setting of Co sources are occupational, environmental, dietary, and medical. Cobalt health effects are categorized by a complex clinical syndrome mainly including neurological (e.g. hearing and visual impairment), cardiovascular and endocrine deficits (Leyssens et al., 2017). Studies in animals suggest that exposure to excessive amounts of non–radioactive cobalt during pregnancy might affect the health of the developing foetus. However, birth defects have not been found in children born to mothers who were treated with cobalt for

anaemia during pregnancy. Research has shown that the doses of cobalt used in the animal studies were much higher than the amounts of cobalt to which humans would normally be exposed. Other health effects to humans such as inhalation exposure to cobalt include cardiac effects such as functional effects on the ventricles and enlargement of the heart, congestion of the liver, kidneys, and conjunctiva (ATSDR, 2004).

Nickel is vital for the function of many organisms. But concentrations in some areas from both anthropogenic release and naturally varying levels may be toxic to living organisms. The concentration of Ni in the industrial effluent ranges from 3.4 to 900 mg L^{-1}. According to the standard set by the European community, the maximum limit of concentration of Ni in drinking water is 50 μg L^{-1}. In addition, Food and Agricultural Organization (FAO) of the United Nations (UN) suggested the maximum limit to be 200 μg L^{-1} (Hosseini et al., 2016). The health effect of nickel depends on the route of exposure such as inhalation, oral, or dermal. These routes are categorized according to systemic, immunologic, neurologic, reproductive, development or carcinogenic effects (Das and Buchner, 2007). For instance, inhalation exposure in occupational settings is a primary route for nickel–induced toxicity and may cause toxic effects in the respiratory tract and immune system. Nickel which goes beyond its critical level can cause serious lungs problem from gastrointestinal distress, skin dermatitis, kidney for oral exposure, cardiovascular system, pulmonary fibrosis, chronic asthma, and nausea (Cempel and Nikel, 2006).

2.2 Removal of heavy metals

There are several methods for removing heavy metal from wastewater. It has become paramount to separate heavy metals from wastewater due to its toxic nature to the environment as well as living organism. Because of the increase growing of heavy metals worldwide during the past decades, government regulation limit has been established to reduce the impact on the environment. The most used techniques to separate heavy metals from wasterwater include chemical precipitation, ion exchange, flotation, coagulation and flocculation, and membrane processes. In this preceding part, these methods will be discussed.

2.2.1 Chemical precipitation

Chemical precipitation is widely used for removal of heavy metal from wastewater due to its simple operation and low initial cost. Chemical precipitation processes produce insoluble precipitates of heavy metals such as hydroxide, sulphide, carbonate, and phosphate.

The mechanism of the process is to produce insoluble metal precipitation by reacting dissolved metals in the solution and precipitant (Gunatilake, 2015). Adjusting pH in a range from 9–11 is the major parameter that significantly improves the removal of heavy metals in wastewater by chemical precipitation (Barakat, 2011). Due to its availability in most countries, lime or calcium hydroxide is the most employed precipitant agent. Lime precipitation can be used effectively to treat inorganic effluent with a metal concentration of higher than 1000 mg L^{-1} (Kurniawan et al., 2006).

With hydroxide precipitation, the pH is sensitive which is in the range 9.5–10. Each metal has a narrow range of pH for the precipitation and beyond this range, the metal resolubilizes. The incorporation of coagulants such as iron salts, alum, and some polymers are very important as it improve the separation of heavy metals from wastewater. Alkaline agent can be useful to increase the pH of the water (Azimi et al., 2017). Tunay and Kabdasli (1994) analysis the mechanism of ligand–sharing effect of metals which was added to wastewater to ensure effective removal of complexed heavy metals. Heavy metals the authors considered were cadmium, copper, and nickel. The experimental results show that high pH precipitation is applicable to cases where organic ligand can be effectively bound by calcium or any other coagulant or pH adjustment agent. With those conditions, the heavy metals are free from forming hydroxide or carbonate solids.

Different results were obtained for the removal of Ni (II) uptake from a low–strength of real wastewater with a metal concentration of less than 100 mg L^{-1}. With pH adjustment at 7.5 and 10.5, the authors found that about 70.7 % and 85 % of Ni (II) was removed respectively, with an initial metal concentration of 51.6 mg L^{-1} which might be attained. This could be attributed to the fact that a greater portion of the Ni (II) was precipitated and removed in the form of insoluble hydroxide compounds with increasing pH (Papadopoulos et al., 2004; Kurniawan et al., 2006). Advantages are simple in operation, inexpensive equipment requirement, and convenient and safe operations. However, chemical precipitation involves excessive sludge production that requires additional treatment, the increasing cost of sludge disposal, slow metal precipitation, poor settling, the aggregation of metal precipitates, and the long–term environmental impacts of sludge disposal (Kurniawan et al., 2006).

2.2.2 Ion exchange

Ion–exchange processes have been generally used in removing heavy metals from wastewater because of its high treatment capacity, high removal efficiency and fast kinetics (Kang et al., 2004). Among all materials used in ion–exchange processes, synthetic resins are

mostly chosen as they are effective to nearly remove the heavy metals from the solution (Alyüz and Veli, 2009). The uptake of heavy metal ions by ion–exchange resins is rather affected by absolute variables such as pH, temperature, initial metal concentration and contact time (Gode and Pehlivan, 2006). Apart from synthetic resins, natural zeolites occurring in silicate minerals have been widely used in removal heavy metals from wastewater. This is due to it high abundance and low cost. Many studies have been conducted and the results show that zeolites exhibit good cation–exchange capacities for heavy metal ions under different experimental conditions (Taffarel and Rubio, 2009). Clinoptilolite is one of the natural zeolites, which has been studied recently due to its selectivity for heavy metals (Inglezakis et al., 2007; Argun, 2008). Ion exchange does not present any sludge disposal problems unlike chemical precipitation, thus lowering the operational costs for the disposal of the residual metal sludge. Their limitations are high capital and operational cost, highly sensitive to pH, suitable ion exchanger is not available for all heavy metals, and appropriate pre–treatment systems for secondary effluent such as removal of suspended solids from wastewater (Kurniawan et al., 2006).

2.2.3 Flotation

Flotation is employed to separate heavy metals from liquid phase using bubble attachment. To separate the attached particles from the suspended heavy metal, it is necessary to use bubble mechanism to raise the heavy metals. Flotation can be classified as: (i) dispersed–air flotation, (ii) dissolved–air flotation (DAF), (iii) vacuum air flotation, (iv) electroflotation, and (v) biological flotation. Among the several types of flotation, DAF is commonly used for the treatment of metal–contaminated wastewater (Kurniawan et al., 2006). The main flotation processes used to remove heavy metals from solution are dissolved air flotation (DAF), precipitation flotation and ion flotation (Fu and Wang, 2011).

The commonly used method for removal of heavy metal is ion flotation. The process of ion flotation is based on imparting the ionic metal species in wastewaters hydrophobic by use of surface–active agent and subsequent removal of these hydrophobic species by air bubbles (Polat and Erdogan, 2007). Low–cost material such as zeolite and chabazite are mostly effective collector with the removal efficiency highest than 95 %. Advantages of flotation are better removal of small particles, low operational cost, and high selectivity. High maintenance and initial cost are its limitations (Fu and Wang, 2011).

A study was conducted by Rubio and Tessele, (1997) to investigate the flotation of Zn (II) and Ni (II) from synthetic wastewater using chabazite as the adsorptive particulate.

The process efficient was depended on solution and interfacial chemistry and aggregation effectiveness. Results showed that almost complete removal (> 98 %) of the heavy metal ions using $Fe(OH)_3$ precipitates to aggregate the carrier. The results are like those of Blöcher et al. (2003), who combined flotation and membrane separations to remove Ni (II) cations from synthetic plating solution by using CTABr (cetyl trimethyl–ammonium bromide) as the cationic collector.

2.2.4 Coagulation and flocculation

Coagulation and flocculation followed by sedimentation and filtration are also used to remove heavy metal from wastewaters (Fu and Wang, 2011). It was noted by Chang and Wang, (2007) that coagulation–flocculation cannot remove heavy metal from wastewater completely. Plattes et al. (2007) applied precipitation, coagulation and flocculation processes using ferric chloride to remove tungsten from industrial wastewater. Tungsten removal was found to be most efficient (98–99 %) in acidic conditions (pH < 6). Bojic et al. (2009) explored spontaneous reduction–coagulation process using micro–alloyed aluminium composite in a laboratory semi–flow system to treat model heavy metal from wastewater. The research was performed on the removal of heavy metal by coagulation of combined sewer overflow with two commercial coagulants, a ferric chloride solution and a polyaluminium chloride (PAC). They found out that excellent heavy metal elimination was achieved within a narrow range of coagulant around the best coagulant concentrations (El Samrani et al., 2008). Many kinds of flocculants, such as PAC, polyferric sulphate (PFS) and polyacrylamide (PAM), are widely used in the treatment of wastewater. However, it was practically not possible to remove heavy metal very well from wastewater directly by these current flocculants. Limitations include high operational cost due to chemical consumption, high initial cost, and the increased volume of sludge generated (Kurniawan et al., 2006).

2.2.5 Membrane processes

Membrane technologies with different types of membranes show great future promise for heavy metal removal for their high efficiency, easy operation and space saving. The membrane processes used to remove metals from the wastewater are ultrafiltration (UF), reverse osmosis (RO), nanofiltration (NF) and electrodialysis (ED) (Fu and Wang, 2011). Cold separation using membrane technology is widely used in the food technology, biotechnology, and pharmaceutical industries. Membrane separation processes can be used for a wide range of applications and have advantages over conventional separation such as

chemical precipitation, floatation, ion exchange, adsorption since the separation is based on physical mechanism. In most membrane process, no chemical, biological, or thermal change of the component is involved. With these advantages, membrane separation is particularly attractive to the processing of food, beverage, and bioproducts where the processed products can be sensitive to temperature and solvent (Cui and Muralidhara, 2010; Uragami et al., 2007).

The word membrane originates from a Latin word '*membrana*' which means thin skin. According to Nath (2017) membrane can be defined as a barrier or interface that separate two phases and restrict transport of various chemicals in a selective manner. In another reserach, membrane was regarded as selective barriers separating two fluids and allowing the passage of certain components and the rejection of others from a given mixture which imply the concentration of one or more components (Mulder, 1997). A schematic representation of the two phases separated by a membrane can be seen in Fig. 1. The properties of separated particles of membrane can be in terms of size, charge, and shape. During the separation process, the feed stream to a membrane module is split into (i) the retentate stream, which is the stream that has been retained by the membrane containing both the material that has been rejected by the membrane and a quantity of material that would not be rejected by the membrane but has yet not been given the opportunity to pass through the membrane; and (ii) the permeate stream, the stream that has passed through the membrane containing much less or no bigger molecules or particles than the pores. Similar to any separation processes, membrane separation processes can be estimated by two important parameters, efficiency and productivity. The productivity is characterized by the parameter permeate flux which descibes the rate of mass transport across the membrane. In general terms, the local mass transport of a component through a membrane element is related to its concentration on the feed side and the permeate side. The flow of a component through a membrane element can be referred to as its flux (Cui and Muralidhara, 2010). Transport through the membrane takes place when the driving force is established across the membrane. In most membrane processes, the driving force depends on the difference in pressure, concentration, temperature, chemical and electric potential (Mulder, 1997).

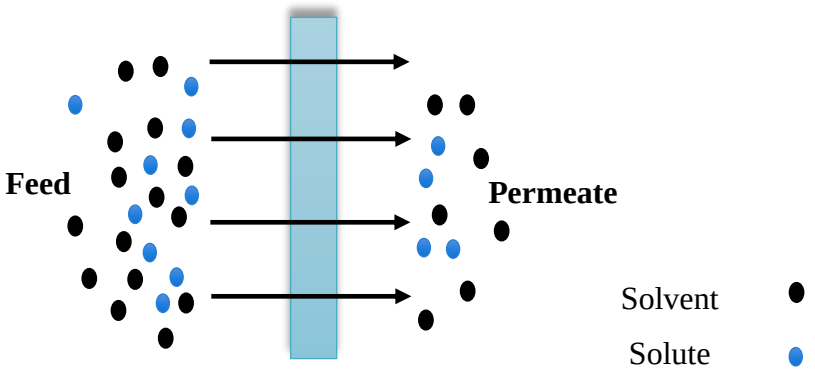

Fig. 1 Schematic representation of the two–phase system separated by a membrane (Mulder, 1997).

As already discussed, conventional methods such as chemical precipitation, coagulation–flocculation, flotation, and ion exchanger have been used for separating of heavy metals from wastewater. However, these methods have several limitations that can lead to other problem when separating heavy metals. When such methods are used, it poses a threat to humans, aquatic life, and the environment. Sludge productions, chemical used are some of the limitations which make such treatment not environmentally friendly methods. Membrane process such as pressure driven has been determined as feasible and promising option due to its high efficiency, no phase change, convenient operation, and many advantages over the conventional methods (Wei et al., 2013).

3. Pressure driven membrane processes

Pressure driven membrane process are subset of membrane separation processes which includes microfiltration (MF), ultrafiltration (UF), nanofiltration (NF), and reverse osmosis (RO) (Baker, 2004). Pressure driven membrane processes can be classified by several criteria such as the characteristics of the membrane (pore size), size and charge of the retained particles or molecules, and pressure exerted on the membrane. The pore size of the membrane is usually indicated by membrane manufacturers through its molecular weight cut–off (MWCO) which is usually expressed in Dalton (1 Da = 1g mol^{-1}) (Coutinho et al., 2009). Molecular weight cut–off or nominal molecular weight cut–off is defined as the minimum molecular weight of a solute that is 90 % retained by the membrane (Drioli et al., 2016). Particles and dissolved components are (partially) retained based on properties such as size, shape, and charge. These membrane processes use the pressure differences between the feed and permeate side as the driving force to transport solvent (usually water) through the membrane (Van der Bruggen et al., 2003). The driving force in pressure driven membrane separation is of course the pressure or the pressure difference between the upstream and the downstream of the membrane or between the feed and the permeate. This pressure difference is known as transmembrane pressure. The Fig. 2 gives a clear overview of classification on the applicability of different membrane separation processes based on pore size, pressure and their application (Hung et al., 2017).

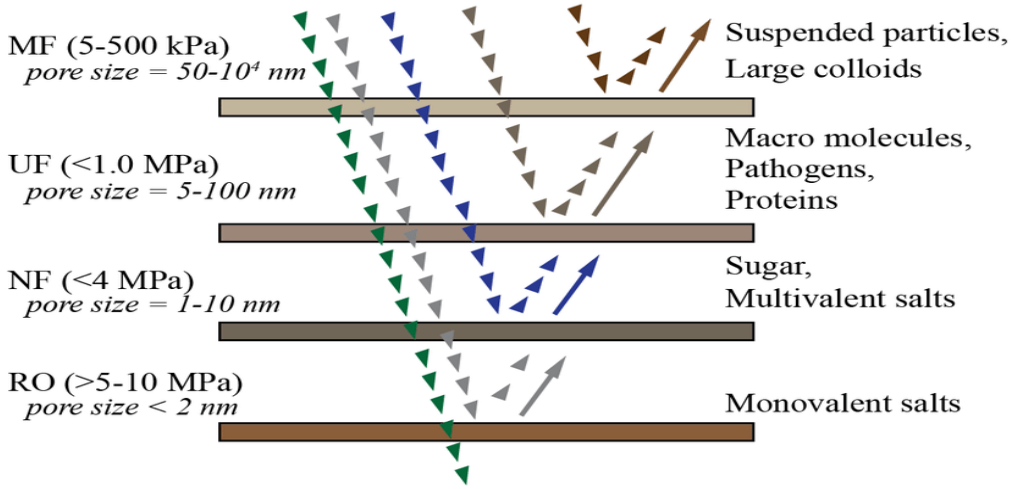

Fig. 2 The ranges of pore sizes, applied pressure, and applications of pressure driven membrane processes (Hung et al., 2017)

Pressure driven processes can be operated in two different mode. These are cross–flow and dead–end operations. In the cross–flow operation, the feed stream moves parallel or tangential on the surface of the membrane. During this process only portion of the feed passes throught the membrane under the operating driving pressure. There are two streams leaving the membrane module with one for the retentate flow and the other for the permeate flow. The tangential flow in the cross–flow mode can help to shear away the accumulated rejected species at the membrane which limit the height of cake layers and hence maintain the permeate flux. In addition, the material deposited on the surface of the membrane can be removed by back washing ultrasound vibration or periodic flow prolonging the life span of the membrane (Cui and Muralidhara, 2010; Fane et al., 2010). The dead–end (conventional) is the opposite to the cross flow. The feed flow perpendicular to the membrane surface at a constant pressure leaving solids behind on the membrane. The dead end is also referred to as batch process because the filter will be accumulated which may cause significant pressure drop as the filter surface is plugged. The filter is then cleaned or replaced which makes the proces expensive (Kucera, 2010). Hence, dead–end mode is often applied for feed water that pose a low risk of membrane fouling such as pre–treatment in wastewater recycling and seawater desalination whereas cross–flow operation is practiced in applications to treat feed water with high content of organic matter, colloidal component, and suspended solids (Hung et al., 2017). Schematic diagrams of the dead–end and the cross–flow mode and their effects on the permeate flux and the height and resistance of the cake layer are shown in Fig. 3.

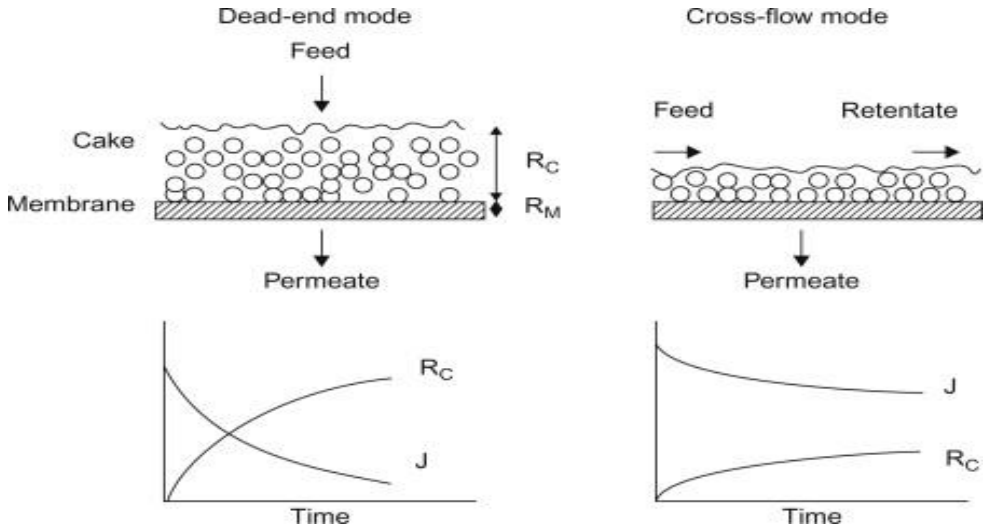

Fig. 3 The schematic diagrams of the dead–end mode and the cross–flow mode, and their effects on the permeate flux (J) and the height of the cake layer (R–resistance) (Cui and Muralidhara, 2010).

3.1 Basic description

Microfiltration is a physical separation process that uses porous membrane with an average pore size between 0.1 and 10 μm. It promotes the separation of particles and dissolved components from fluids by a sieving mechanism based on size exclusion. The membrane separating a feed solution from permeate has a symmetric or asymmetric porous structure. Since only large particles with diameters more than 0.1 μm are separated by the membrane, the diffusion of particles and the osmotic pressure difference between the feed and permeate solution are negligibly low (Giorno et al., 2015). The main industrial applications are cold sterilization of beverages and pharmaceutical products, clarification of fruit juice, cell harvesting, and separation of oil–water emulsions, wine, and wastewater treatment (Mulder 1997). Microfiltration can be used for treatment of anoxic pond (Al–Malack et al., 1998), removal of arsenic from drinking water (Mólgora et al., 2013), improving of the quality and shelf life of ultra–high temperature milk (Zhang et al., 2015) and pre–treatment of sea water (Vial and Doussau, 2003).

Ultrafiltration (UF) utilizes permeable membrane to separate heavy metals, macromolecules and suspended solids from inorganic solution on the basis of the pore size (5–20 nm) and molecular weight of the separating compounds (10^3–10^6 Da). These unique specialties enable UF to allow the passage of water and low–molecular weight solutes while retaining the macromolecules which have a size larger than the pore size of the membrane (Barakat, 2011). Application of ultrafiltration can be found in food and dairy industry, textile industry, chemical industry, pharmaceutical (enzymes, antibiotics, and pyrogen), and metallurgy (Mulder, 1997). In addition, ultrafiltration was useful in the pulp and paper industry for the removal of metals and white–water reuse (Oliveira et al., 2007).

There are two types of UF technique used to obtain high removal of heavy metals from wastewater. These are the micellar enhnaced ultrafiltration (MEUF) and polymer enhanced ultrafiltration (PEUF). In MEUF, the separation is based on the addition of surfactants to wastewater. When the surfactant molecules agregate into the micelle, they bind the metal ions to form large–surfactant structures (Renu et al., 2017). The micelles containing heavy metals can be retained by a UF membrane, whereas the untrapped heavy metals pass through the UF membrane. To obtain the highest rejection, surfactants of electric charge opposite to that of the ions to be removed have to be used. Sodium dodecyl sulfate (SDS), an anionic surfactant is often selected for the effective removal of heavy metal ions in MEUF. MEUF has several advantages such as it gives high flux, high removal, and low energy cost.

However, it has disadvantage of increasing the operating cost. (Landaburu–Aguirre et al., 2009, 2010). Metal removal efficiency by MEUF depends on the characteristics and concentrations of the metals and surfactants, solution pH, ionic strength, and parameters related to membrane operation (Fu and Wang, 2011).

The second is the PEUF which uses water–soluble polymer to complex metallic ions and form a macromolecular having a higher molecular weight than the MWCO of the membrane (Fu and Wang, 2011). Aroua et al. (2007) investigated the removal of chromium ions from aqueous dilute solutions using PEUF process by three water–soluble polymers namely chitosan, PEI (polyetherimide), and pectin. For Cr (III), high rejections approaching 100 % were obtained at pH higher than 7 for the three tested polymers. The main parameters affecting PEUF are metal and polymer type, the ratio of metal to polymer, pH and existence of other metal ions in the solution. The advantages of PEUF include high removal efficiency, high binding selectivity and highly concentrated metal for reuse (Fu and Wang, 2011). The Table 2 shows the effective technique of UF for the removal of heavy metals from wastewater.

Table 2. Removal of heavy metal from wastewater by MUEF and PEUF

UF type	Complexing agent	Heavy metal	pH	Removal efficiency (%)	References
MUEF	PVA	Co^{+2}	–	99.98	Uzal et al., 2011
MUEF	SDS	Cd, Zn^{+2}		92–98	Huang et al., 2010
MUEF	PEI	Cu^{+2}	4–5	92	Camarillo et al., 2010
PEUF	Carboxyl methyl cellulose	Cu^{+2},Cr^{+3}, Ni^{+2}	6–7 5–6	97.6, 99.5, 99.1	Barakat and Schmidt, 2010
PEUF	Polyvinylamine	Hg	–	99	Huang et al., 2015
PEUF	Poly (ammonium acrylate)	Cd (II)	6.32	99	Ennigrou et al., 2009

Nanofiltration (NF) process lies between ultrafiltration (UF) and reverse osmosis (RO). In all pressure driven processes, a pressure is applied to transport a molecular mixture to the surface of a membrane. Generally, the solvent and some low molecular weight solutes permeate the membrane while other components are retained. The main difference between nanofiltration and ultrafiltration is the pore size of the membrane and thus the molecular weight of the components that are retained by the membrane. In nanofiltration process, it is assumed that all components permeate the membrane exclusively through geometrically well–defined pores. However, it is assumed that in reverse osmosis the different components

permeate the membrane by diffusion through a homogeneous polymer matrix and the separation is due to the solubility and the diffusivity in the polymer matrix. The main difference between nanofiltration and reverse osmosis is the transport mode in the membrane (Strathmann et al. 2006). Nanofiltration is widely used for the removal of micropollutant, desalination of brackish water, wastewater treatment, rejection of dyes (textile industry), water softening and treatment of chloride rich steel plant effluent (Baker, 2004; Mulder, 1997).

Wei et al., (2013) studied the performance of thin–film composite (NF) hollow–fibre for removal of heavy metal from electroplating wastewater. The researchers tested the rejection rates for chromium, copper, and nickel. They observed that at 4 bars, the rejection rates of chromium, copper and nickel were 95.76 %, 95.33 %, and 94.99 %, respectively. The removal of heavy metal ions using a commercial nanofiltration membrane (NF 270) was studied by Al–Rashdi et al. (2013). Three heavy metals namely manganese, cadmium and lead were tested at 1000 mg L^{-1} concentration. It was found that the rejection rate was 89 %, 74 % and 99 %, respectively. In another research, Wang et al., (2007) used three NF membranes, DL, DK, and NTR–7450, for investigation of electroplating wastewater containing Cu and Cr. Considering the DL membrane, the Cr and Cu rejection increased from 91.2 % and 91.1 % to 97.3 % and 94.5 %, respectively. For DK membrane, the Cr and Cu rejection increased from 91.7 % and 91.3 % to 98.8 % and 97.2 %, respectively. Bennani and M'hiri (2013) studied the rejection of heavy metals Cu (II), Cd (II), and Zn (II) using two commercial nanofiltration membranes (DL and DK). The rejection sequence was identical for both membranes ($R_{Cu} < R_{Zn} < R_{Cd}$). The results show that the DL membrane rejections of Zn, Cu, and Cd were 93, 90, and 86%, respectively. Similar high rejection of heavy metals from wastewater can be seen in various literatures (Ahmad and Ooi, 2010; Mirbagheri et al., 2016; Nguyen et al., 2009). The Table 3 shows the removal of some heavy metals using NF membrane.

Table 3. Heavy metal removal using NF membrane

Membrane material	Heavy metal	Removal efficiency (%)	References
Dual–layer (PES/PVP), PBI	Cd, Cr, Pb	95, 98, 93	Zhu et al., 2014
TFC–NF 270	Cd, Mn, Pb	99, 89, 74	Al–Rashdi et al., 2013
AFC 80 (Polyamide TFC)	Pb	>98	Gherasim et al., 2013
TFC–NF 300	Ni	98	Murphy and Chaudhari, 2009
NE 4040–90	Cu, Zn, Cd, Pb	97.5	Mehdipour et al., 2015
TFC NF hollow fibre	Cr, Cu, Ni	95.76, 95.33, 94.99	Wei et al., 2013

The heart of RO based separation is the semi permeable membrane which preferentially allows water molecules to pass through it by obstructing the passage of salts under the influence of externally applied pressure (Shenvi et al., 2015). Reverse osmosis uses pressures between 4 and 10 MPa and concentrates particles with molar masses below 350 Da (Coutinho et al., 2009). The rejection of RO membrane is due to size exclusion, charge exclusion and physical–chemical interactions between solute, solvent, and membrane (Malaeb and Ayoub, 2011). The efficiency of the membrane depends on the operational parameters, membrane, and feed water properties (Bunani et al., 2015). RO membrane has been widely used for water treatment such as the production of ultrapure water and boiler pure water for industrial use. Other uses of osmosis membrane are treatment of seawater and brackish water desalination for drinking water and agricultural water use, wastewater reclamation for industrial purposes, agricultural and indirect drinking water use (Kurihara and Tomioka, 2010).

Integration of a membrane bioreactor (MBR) coupled with reverse osmosis was used by Dialynas and Diamadopoulos (2009) for advancement of municipal treatment. It was observed that the removal of nickel, chromium and copper were 100 %, 89 % and 49 % respectively. Therefore, the combination of MBR and RO provided a quality effluent devoid of heavy metals and with very low organic matter concentration. Ipeak, (2005) used reverse osmosis for the removal of zinc and nickel from aqueous solution. The author combined pre–treatment units and reverse osmosis. It was found that the removal of nickel and zinc were 92.2 % and 98.8 % respectively. When the EDTA was added into the aqueous solution, the removal of nickel and zinc increases to 99.7 % and 99.6 %, respectively.

3.2 Nanofiltration

Nanofiltration membrane had made remarkable progress globally during the past decades due to outstanding mechanism used in the removal of contaminant from water. In this part of the research, the overview of nanofiltration, applications of nanofiltration, and recent progress during the past years will be discussed. The overview of nanofiltration includes separation mechanism, membrane material, structure, and module.

3.2.1 Overview of nanofiltration

Nanofiltration membrane which falls into a transition region between reverse osmosis (RO) membranes and ultrafiltration (UF) has received greater attention in the past years. As compared to other pressure driven membrane processes, NF is characterized by a membrane

pore size (<1 nm) corresponding to a molecular weight cut–off approximately 300–500 Dalton (Baker, 2004). Moreover, nanofiltration membrane has specific advantages over reverse osmosis which makes the separation mechanism attractive. These are less energy consumption, lower operating pressure than RO, higher flux, inexpensive compared to reverse osmosis and monovalent ions partly passes through the membrane whiles multivalent ions are rejected to a substantial degree determined by the feed stream (Mikulášek and Cuhorka, 2016). The membrane can be positively or negatively charged depending on the material from which is formed. Moreover, the membrane charge is because of dissociation of ionizable functional group(s) in the membrane surface and pores. This group can be acidic or basic in nature or a combination of both; depending on the material used in manufacturing and fabrication processes (Gherasim et al., 2014).

NF plays a significant role in many separation and purification applications such as seawater and brackish water desalination (Silva et al., 2011), industrial wastewater treatment (Aouni et al., 2012) and food and pharmaceutical industries (Bes–Pia et al., 2010). NF is usually operated in cross–flow mode as opposed to the dead–end mode to reduce the build–up of filter cake on membrane surface or fouling. The performance and effectiveness of metal ion removal by nanofiltration membrane depend on many factors. These include the type and surface charge characteristics of the membrane, geometry module and configuration, mode of operation, operating pressure, temperature, feed pH, feed flow rate, feed concentration and product recovery rate among others (Hosseini et al., 2016). Rejection in NF membrane may be attributed to solution diffusion, Donnan effect, dielectric exclusion, electro migration or a combination of them (Mohammad et al., 2015). The separation of NF membrane is very complex and till now not fully understood.

3.2.2 Separation mechanism of nanofiltration

To fully understand the fundamental principle behind the separation mechanism, it is paramount to have in–depth knowledge of the mechanism that is involved in the performance of NF membrane. The driving force for the separation in NF is the pressure difference between the feed and permeate side of the membrane. NF is associated with a combination of steric, Donnan, dielectric and transport effects. The transport of neutral solutes is by steric mechanism (size–based exclusion). The classical Donnan effect plays a role in describing the equilibrium maintenance and membrane potential interactions at the charged and the interface of the charged membrane (Donnan, 1995). The membrane charged is based on material used for manufacturing and fabrication. However, the membrane charge is because of dissociation

of ionizable functional group in the membrane surface and pore structure. These groups can be acidic or basic in nature or a combination of both depending on the material used in manufacturing and fabrication process. The dissociation of these surface groups is strongly influenced by the pH of the contacting solution and where the membrane surface chemistry is amphoteric in nature, the membrane may exhibit an isoelectric point at a specific pH. In addition to the ionizable surface groups, NF membranes have a weak ion–exchange capacity and in some cases, ions from the contacting solution may adsorb to the membrane surface causing a slight modification of the membrane charge (Childress and Elimelech, 1996; Oatley et al., 2012). Electrostatic repulsion or attraction known as dielectric effect takes place in the membrane due to variation in ionic surroundings between the ion and the membrane surface. There are two main competing hypotheses as to the exact nature of the interaction and is less understood. These are the image forces phenomenon and the, salvation energy barrier mechanism. These interactions have been reviewed in detail in this literature (Oatley et al., 2012). Because nanofiltration is pressure driven process the movement of solute is pressure dependent which is known as drag force. The drag force takes care of the removal of the solute through the porous membrane which leads to hindrance of its transport. The transport of solvent and solutes is due to three effects namely, convective, diffusive and electro migration (Kumaran and Bajpai, 2015).

3.2.3 Material of membrane

Synthetic membranes are produced from large varieties of materials which are classified in terms of their physical structure and material they are made from. These materials can be polymeric or organic and ceramic or inorganic. These typical organic membranes are made up of several polymers which include cellulose acetate (CA), polyamide (PA), polysulfone (PS), polyether sulfone (PES), polyvinylidene fluoride (PVDF), polypropylene (PP), etc. Polymeric membranes are relatively cheap, easy to manufacture, available in a wide range of pore sizes, and they have been widely used in various industries (Cui and Muralidhara, 2010; Strathmann et al., 2006). Most commercial NF membranes are made of synthetic polymers containing fully or slightly charged on the surface due to the dissociation of surface functional groups or adsorption of charged solutes. These properties make them effective for the separation of metal ions present in the aqueous solutions (Mohammad et al., 2015).

Inorganic membranes are generally divided into five groups: glass membranes, ceramic membranes, metallic membranes, carbon membranes, and zeolitic membranes

(Ladewig and Al–Shaeli, 2016). Inorganic membranes have been commercialized since the early 1980s due to its numerous advantages. They have high mechanical strength, and chemical and thermal stability over the conventional polymeric membranes, as well as other application of membrane technology into many new areas. However, inorganic membranes are very brittle, so the membranes can be easily damaged by dropping or unduly vibrating and are more expensive than polymeric membranes. Additionally, the availability of such membranes is only limited to mostly UF membranes and MF membranes today (Cui and Muralidhara, 2010).

3.2.4 Structure of membrane

Membranes can be classified according to the cross–sectional structure and the material they are made from (Strathmann, 2011). They can be classified according to their morphology, as shown in Fig. 4.

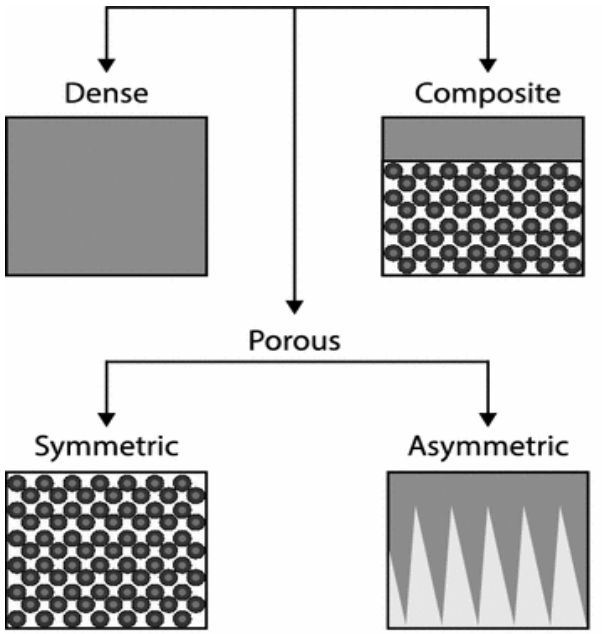

Fig. 4 Membrane classifications according to morphology (Ladewig and Al–Shaeli, 2016)

The first group can be identified as a dense homogeneous polymer membrane. Generally, they are prepared (i) from solution by solvent evaporation only or (ii) by extrusion of the melted polymer. Nevertheless, dense homogeneous membranes only have a practical meaning when made of highly permeable polymers such as silicone. Usually, the permeant flow across the membrane is quite low since a minimum thickness is required to give the

membrane mechanical stability. Almost the current available membranes are porous or consist of a dense top layer on a porous structure (Nunes and Peinemann, 2006).

The second type is porous membranes which can be further divided into two main groups. These groups are divided according to their pore diameter of the membrane. The first and second groups of the membranes are symmetric (isotropic) and the asymmetric (anisotropic) membranes, respectively. Within the asymmetric membranes, there are various distinctly different structures including integrally skinned membranes. These pore structure gradually changes from very large pores to very fine pores, essentially forming a "skin" on top of the membrane which is called "integrally skinned". Alternatively, the skin may be nonporous. A third and industrially very important type of asymmetric membrane is the thin–film composite membrane where a dense, selective, and thin layer is deposited or polymerised at the surface/interface of a porous substrate (Ladewig and Al–Sheli, 2017).

The symmetric membrane has both structure and transport properties being identical over the whole section. In addition, the flux can be evaluated by the thickness of the entire membrane. These membranes are used today in dialysis and electro dialysis (Strathmann, 2011). The pores are of uniform size (isotropic) or non uniform size (anisotropic). These membranes are designed to reject all the species above their ratings (Cui and Muralidhara, 2010). Asymmetric membranes have a gradient in structure and consist of a 0.1–5 μm thick "skin" layer on a highly porous 100–300 μm thick structure. The skin represents the actual selective barrier of the asymmetric substructure. Separation properties of asymmetric membrane are completely determined by the nature of the material or the size of pores in the skin layer. The porous substrate layer serves as a support for the mostly very thin top layer, or "skin" (relatively dense) and has little effect on the separation properties of the membrane or the mass transfer rate of the membrane (Ladewig and Al–Shaeli, 2017). The dense surface layer is considered to be responsible for the membrane selectivity. Asymmetric membranes are usually used in pressure driven processes such as reverse osmosis, ultrafiltration, gas separation and sometimes in microfiltration. A skinned asymmetric membrane is known as composite membrane. Asymmetric membrane has distinctive properties such as high fluxes and mechanical stability (Strathmann, 2011; Nunes and Peinemann, 2006).

Nevertheless, the top layer and sublayer originate from different polymeric materials to enhance each layer separately. Almost all NF membrane is composite or thin–film composite (TFC) due to its unique properties (Mulder, 1997). These properties the structure exhibit is heat stability, good strength, high elongation, good hydrolytic stability, high chemical stability, and engineering thermoplastic (Hosseini et al., 2016). TFC membranes are

composed of at least two layers (with different (polymeric) materials) with a very selective membrane material being deposited as a dense ultra thin layer formed upon a more or less porous support layer (sublayer) which usually is an ultrafiltration membrane and serves as support (Ladewig and Al–Shaeli, 2017). Several methods are established to prepare NF membranes such as phase inversion, interfacial polymerization, solution coating, hot–melt spinning, leaching, track–etching, sintering, and sol–gel techniques (Mulder, 1997). All these methods are necessary to produce membrane with high selectivity, rejection tendency and overcoming fouling issues. The development of thin–film composite (TFC) membrane through interfacial polymerization which involves phase invasion has received attention recently due to significantly better improvement of membrane characteristics such as selectivity and fouling resistance (Mohammad et al., 2015).

3.2.5 Membrane modules

Membranes are packed in a small unit which is called a membrane module and is the central part of a membrane installation. The utmost important of development of these modules is to provide maximum membrane area in relatively smaller volume so that the permeate flux i.e. the productivity of the system is maximum (Ahmad et al., 2004; Mulder, 1997). The major criteria needed to be considered during membrane module selection are cost, concentration polarization, operational parameters (particularly pressure) and resistance to fouling (Shenvi et al., 2015). Up till now, there are four kinds of membrane modules that have been widely used in industry. They are (i) tubular modules, (ii) hollow fibre modules, (iii) flat sheet modules, and (iv) spiral–wound modules (Cui and Muralidhara, 2010).

In most nanofiltration process, the tubular modules are used due to its various characteristics over the rest of the modules. The tubular modules have some important characteristics: (i) due to their large internal diameters, tubular modules can deal with the feed stream containing large particles. Additionally, they can be easily cleaned by using either mechanical or chemical cleaning methods; (ii) they need large pumping capacity because they are usually operated under the turbulent flow conditions with the Re > 10,000; (iii) they have the lowest surface area–to–volume ratio among all the four membrane configurations (Cui and Muralidhara, 2010).

3.2.6 Applications of nanofiltration

NF had gained interest as well as popularity worldwide due to excellent removal of the contaminant; lower energy consumption, decreasing prices for the membranes, and

enhanced membrane lifetime when compared to RO. NF is used for environmental applications for treatment of ground water, surface water and wastewater reclamation. In addition, NF membranes have been used for many interesting applications such as desalination, non–water application, food industry, and pharmaceutical and biotechnology application (Mohammad et al., 2015).

The softening of ground water has been studied by many researchers. Rahimpour et al. (2010) prepared an asymmetric polyether sulfone and a thin–film composite NF were used for water softening. It was concluded that thin–film composite rejected 90 % of $MgSO_4$ and 67 % of NaCl, respectively. This means that this membrane shows a higher capability to softening water. Preparation of polysulfone nanofiltration membrane by UV–assisted grafting polymerization for water was proposed by Homayoofal et al. (2010). The results imply that by increasing irradiation time and monomer concentration in the photo grafting process, pure water flux declines and salt rejection increases. During their studies, additive such as acrylic acid solution and PEG–4000 as additive was added to the membrane for 180 min, the rejection of Na_2SO_4, $MgSO_4$, NaCl and $CaCl_2$ follows a decreasing in order of 100 %, 77.9 %, 49.9 % and 35.9 %, respectively.

Remarkable progress has been made in NF membrane in surface water application for removal of pesticides, disinfection by–products, and hormones. Fang et al. (2013) developed composite nanofiltration hollow fibre membranes under low operating pressure which were desirable for water softening. The resulting membrane developed possesses a positively charged thin–film selective layer with pure water permeability (PWP) of about 17 L m^{-2} h^{-1} bar^{-1} and a molecular weight cut–off 500 Da. With combined separation mechanisms of Donnan exclusion and steric hindrance, $MgCl_2$ and $MgSO_4$ rejection were 96.7 % and 80.6 % respectively when tested for 1000 ppm feed solutions at 2 bar operating pressure. In addition, for a 3000 ppm total dissolved salt (TDS) feed stream containing salt mixtures, the membrane rejection for Mg^{2+} and Ca^{2+} ions were 90 % while the pure water flux was 20 L m^{-2} h^{-1} at 2 bar pressure suggest that the potential of the newly developed composite hollow fibre was effective for water softening application. As an extension of these newly composite NF hollow fibre membranes, Fang et al. (2014) fabricated a mixed polyamide – based composite NF hollow fibre membrane. The resultant hollow fibre membrane was used to improved low–pressure water softening capability. The newly pure water permeability and MWCO were 18.2 L m^{-2} h^{-1} bar and 380 Da, respectively. Under an

operating pressure of 2 bar, the membrane displayed a rejection of 96.3 % and 93.8 % to 1000 ppm $MgCl_2$ and $MgSO_4$ feed solution, respectively.

Numerous studies have been performed on nanofiltration in the removal of pharmaceutical from wastewater as well as personal care products that are difficult to be removed by conventional treatment and the results are very encouraging. Moarefian et al. (2014) investigated the performance of a self–made nanofiltration membrane for the removal of amoxicillin from wastewater. This was done under changing operating conditions such as pH, initial feed concentration, operating pressure, and temperature. The results indicated that the AMX rejection and permeation flux by the self–made membrane varied from 56.49 % to 99.09 % and from 15.14 L m^{-2} h^{-1} to 110.29 L m^{-2} h^{-1}, respectively. Feed concentration is the only parameter that affects adversely rejection of AMX. The AMX rejection efficiency was 99.09 % which confirms a higher rejection at the initial concentration of 20 ppm. This shows that modified membrane can be suited for removals of AMX at a very low concentration and highly recommended. In a similar research, Shahtalebi et al. (2011) investigated the separation of amoxicillin from pharmaceutical wastewater. Polyamide spiral wound NF membrane was used for this treatment. The effect of the operating conditions was examined. Since NF is a pressure driven process, operating pressure is very important factor which influences the rate of rejection. Increase in pressure will tend to increase the permeation flux. They observed that the effect of amoxicillin concentration has greater effect on NF membrane performance. This shows that the decreasing the concentration will tend to increase the amoxicillin rejection. Amoxicillin rejection was adequate and, in most cases, exceeds 97 % whereas COD reached a maximum of 40 % rejection. This means that NF membrane process is suitable for recovery of amoxicillin from pharmaceutical wastewater.

Apart from this advanced treatment of separating pharmaceutical from wastewater, it is necessary to consider strategies for the reduction of input into the aquatic environment. However, the presence of pharmaceuticals in the environment together with evident on the effects give an idea that precautionary measure had to be taken to reduce the release into the environment (Kümmerer, 2009). Opportunities for reducing the input of pharmaceutical are possible when different approaches are applied. Combination of management strategies is likely to be the most effective way of mitigating the risks presented by pharmaceuticals. Furthermore, Kümmerer (2007) stated that there are three principal strategies that can be used to reduce chemicals in the environment. These are technical approach, education together with training and substitution of critical compounds. The focus had always been advanced treatment of pharmaceuticals from wastewater. The second approach deals with

environmental protection that is seeking for solution that protects the environment. This can be from patients, doctors, and nurses. Until now, the third approach is usually ignored. However, it seems to be the most promising one. The long run when we substitute critical compound to reduce pharmaceuticals found in wastewater.

Desalination technology with membrane–based process has increased throughout the world to resolve water scarcity. It is also considered as a solution to the problem of potable water deficiency in various developing countries. According to the World Health Organization, more than 12,000 desalination plants are in operation throughout the world since 2005 producing about 40 million m^3 of water per day. These numbers are growing rapidly as the need for fresh water supplies grows more acute, technologies improve, and unit costs decrease (Diawara, 2008). Conversely, there are several issues which need to be addressed in the operation of large desalination plant. Two major obstacles of desalination are membrane fouling and energy consumption. Membrane fouling will affect and reduce the productivity of the plant at a given period. High energy consumption due to high operating pressure hinders the acceptance of membrane desalination process especially in developing countries as it accounts for around 44 % of the cost of the water produce. Hence, few suggestions have been proposed to tackle the problems of membrane fouling and energy consumption with research relevant to these obstacles has been carried out. NF membrane has shown high potential to be an alternative process to reduce those obstacles in desalination process. Basically, NF has shown its usefulness as pre–treatment for seawater (SW) desalination, replacement for RO in water treatment process and it can be integrated with other processes for better overall performance (Mohammad et al., 2015).

The integration of NF as part of the pre–treatment process also led to a higher water production (around 60 %) and resulted in about 30 % cost reduction for RO and MSF plants as well as the environmentally friendly process. These findings encourage further research to improve the application of NF as pre–treatment in desalination process (Mohammad et al., 2015). Scaling is one of the problems encountered by membrane processes. It does not only reduce flux but increases pressure drop along the membrane element. Experiments were performed to evaluate scale potential in a pilot–scale NF–SWRO integrated seawater desalination system. The pilot test provided very valuable and promising results for commercial application of NF membrane in seawater softening process. It was found that the application of NF–SWRO system and the further hybridization of NF integrated membrane technology with thermal desalination would help increase overall water recovery and decrease desalination costs considerably. In addition, it was observed that the scaling effect of NF was

totally different from the traditional SWRO desalination process. More research study needs to be conducted because the scaling potential prediction method in NF module could also be useful in this NF application (Song et al., 2013).

3.2.7 Recent progress in nanofiltration

A major area to the development of NF membrane technology in past decades has been in terms of creating better technologies to separate inorganic and organic substances from solution in a liquid (Mohammad et al., 2015). The chemical structures and physical properties of nanofiltration membranes determine water permeability, solute selectivity, mechanical/ thermal stability, and antifouling properties which greatly influence the separation efficiency and operation cost in nanofiltration applications. With the increased interest in this field, a remarkable progress has been made in the development of high performance nanofiltration membranes based on nanomaterials (Ji et al., 2017).

Since the past two decades, polymeric membranes have been the main research object due to their properties such as good film–forming, suitable flexibility, and mechanical strength. These membranes are usually used in wastewater treatment and seawater desalination due to their well–developed and outstanding performance. Nowadays, commercially available nanofiltration membranes are mainly prepared with polymers such as polyamides (PA) and cellulose acetate (CA) (Ji et al., 2017; Yang et al., 2019; Werber et al., 2016). Some other polymers like polyether sulfone (PES), sulfonated polysulfone (SPSF), polyimide (PI), polyvinyl alcohol (PVA), and chitosan (CS) have been studied and used for preparing nanofiltration membranes (Fane et al., 2015; Mohammad et al., 2015). There has been great outstanding achievement for the development of nanofiltration technologies. For more complicated applications, the nanofiltration membranes with superior separation performance and anti–fouling property are essential. The polymer selective layer which rejects solutes while allowing water/solvent molecules to pass is the crucial part that is expected to render high productivity/selectivity coupled with anti–fouling properties. Nevertheless, the membranes constructed with the highly cross–linked and restrained polymer chains resist further enhancing membrane performance, and there is more research to be done to improve the properties (Ji et al., 2017).

Recently, membrane scientists have come out with new approach in modifying conventional polymeric membranes with nanoparticles where nanoparticles were incorporated into/onto membranes. Introducing nanoparticles into monomer/polymer solution before membrane formation, the resultant nanoparticle–blended membranes or nanoparticle–

entrapped membranes are often called mixed matrix membranes (MMMs) (Pendergast and Hoek, 2011). In addition, nanoparticles are self–assembled onto membrane surface by dip–coating or pressurized deposition on the prepared membrane. Most of studies embedded nanofillers into polyamide thin film layer to form MMMs which are usually referred to as thin film nano composite membranes (TFNMs) (Li et al., 2016). In the last few years, remarkable progress in fabrication of nanomaterial based nanofiltration membrane does not only demonstrates promising potential in overriding the "trade–off" between solvent permeability and solute selectivity but also showed excellent mechanical/thermal stability and antifouling properties.In addition, MMMs to combine the low manufacturing cost, outstanding selectivity and high packing density of polymeric materials with long–term stabilities, and regeneration capability of ceramic materials (Jhaveri and Murthy, 2016; Yang et al., 2019; Goh et al., 2016).

Nanofiltration membrane based on nanomaterials has been improved in terms of its preparation. NF membrane is prepared with metal and metal oxide nanoparticles such as zeolite, silica, titanium dioxide and silver nanoparticle which have been incorporated into polymeric matrix for preparing nanofiltration membranes (Ji et al., 2017). Carbon–based nanomaterials such as carbon nanotubes (CNTs) (Zhao et al., 2016) and graphene (Bano et al., 2015) have been used to prepare nanofiltration membrane. Also, research have been made to use metal–organic frameworks (MOFs) in preparation of nanofiltration membrane and comprehensively summarized in previous review (Seoane et al., 2015). Other authors have achieved excellent results using metal–organic frameworks (Wang et al., 2015). With the development of new techniques for synthesizing nanoparticles, an alternative research has been introduced for the preparation of nanocomposite membrane with polymeric micro/nanoparticles (Ji et al., 2017). Some polymeric micro/nanoparticles have been used for the preparation of mixed matrix material (MMMs) and reported by (Kotte et al., 2014). The Fig. 5 shows an overview of a wide range of nanomaterials such as the metal and metal oxide nanoparticles, carbon–based nanomaterials, metal–organic frameworks, water channel proteins, and organic micro/nanoparticles which have been adopted to prepare nano–based nanofiltration membrane.

Apart from nanofiltration membranes based on nanomaterials, there have been many advances in NF mostly due to the creation of better membranes through methods such as interfacial polymerization (IP), nanoparticles (NPs) incorporation, UV treatment and many more. The goal of these methods used in developing membrane is to prepare membranes with higher selectivity, rejection tendency and overcoming fouling issues. These techniques can be

grouped into IP and grafting polymerization. IP method typically involved phase inversion followed by interfacial polymerization to produce thin–film composite (TFC) membranes. The thin film composite membrane has dominated in the marke due to its outstanding performance. Recent advancement included the incorporation of additives such as nanoparticles in the thin–film layer which lead to thin film nanocomposite (TFN). However, grafting polymerization focused more on UV/photo–grafting, electron beam (EB) irradiation, plasma treatment, and layer–by–layer (LbL) methods (Mohammad et al., 2015).

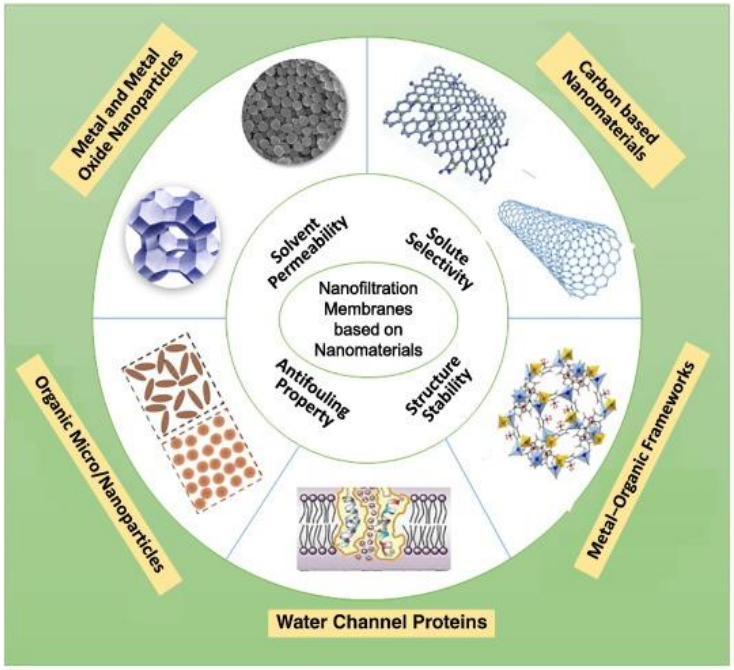

Fig. 5 Overview of nanofiltration membranes based on various nanomaterials with improved permeability, selectivity, stability, and anti–fouling properties (Ji et al., 2017).

There are different types of monomers that have been used in IP process such as bisphenol A (BPA), tannic acid, m–phenylenediamine (MPD), polyvinyl amine reacting with trimesoyl chloride (TMC) or isophthaloyl chloride to form the thin active film layer, diethylenetriamine (DETA), triethylenetetramine (TETA), tetraethylenepentamine (TEPA) and piperazidine (PIP) (Mohammad et al., 2015). A combination of two or more monomers can be used to achieve a great result. Tsuru et al. (2013) applied two steps interfacial polymerization with two monomers (TMC and MPD) to increase the water permeability of membrane. To improve the anti–fouling properties and performance of membranes, Abu Seman et al. (2011) combined BPA and TMBPA to develop modified membranes. The additive can be useful during IP process to increase the pure water fluxes of a composite NF

membrane. Fan et al. (2014) used additive such as calcium chloride ($CaCl_2$) in aqueous solution to improve the performance of composite nanofiltration membranes during interfacial polymerization process. Other types of additives such as organic acids with different structures which include ascorbic acid, citric acid, malic acid, and acidic are used to improve the rejection performance (Ghaemi et al., 2012) Several methods that have been introduced to improve membrane performance during interfacial polymerization included surface fluorination of polyamide membrane (Li et al., 2014), limiting the thickness of membranes (Veerababu et al., 2014), and hyper–branching of polyester (Wei at al., 2013). The UV–assisted grafting polymerization has been applied in wide surface modification works. With the high–energy EB irradiation, the beam penetrates the polymer layer and active sites could be formed which are effective and requires no additive.

Several studies have found the electron beam useful to improve on the performance of the membrane (Linggawati et al., 2012). Plasma surface modification is effective way to increase surface hydrophilicity and wettability. This treatment was used only when the physical and chemical properties of polymeric surface will be altered without changing the bulk properties (Mohammad et al., 2015). The method used nitrogen–containing plasma that can be applied to polymer membrane to produce nitrogen functional groups which improve membrane anti–fouling properties due to increase in hydrophilicity (Kim et al., 2014; Mohammad et al., 2015). Lajimi et al. (2011) used LbL surface modification to evaluate the effect on the characteristics and performance of cellulose acetate membranes. The results show that layer–by–layer surface treatment makes CA membranes less sensitive to protein fouling with 15 adsorbed bilayers. Other authors used this layer by layer method and had provided an alternate way in membrane preparation (Hu and Mi, 2014; Zhu et al., 2014). Although there has been tremendous progress, there are still technical and scientific problems that need to be solved before more benefits can be realized. New research directions for barrier layers are being performed to improve the fouling resistance as well as chemical and thermal stabilities (Yang et al., 2019).

4. Phenomena in NF process

Nanofiltration (NF) has attracted much attention over the past few years due to the reduced energy consumption compared to reverse osmosis (RO) and better separation performance compared to ultrafiltration (UF). This is because of its efficiency, less energy consumption and environmentally friendly nature compared to the conventional techniques. The efficiency of NF separation process does not depend only on membrane properties but also on process operational condition (Boussu et al., 2008). There are four main phenomena in NF process such as rejection, concentration polarization, osmotic pressure and fouling which will be discussed.

4.1 Rejection (neutral and charged substances)

In nanofiltration process, rejection of solutes depends strongly on the solute type including charge valency, diffusion coefficient, and hydration energy (Agboola et al., 2015). Rejection of neutral molecules in nanofiltration is mainly affected by molecule shape and size, chemical nature along with hydrophobicity and hydrophilicity. The major factors affecting rejection of neutral molecules are molecular size or steric exclusion and diffusion. The size exclusion is based on sieving mechanism and diffusion which is because of concentration gradient across the membrane. NF membrane selectivity layer could be three–dimensional network of polymer chains. Membrane selectivity and permeability are usually determined by the free space inside the polymer network (Schafer et al., 2005).

The charge in NF membrane is created when the membrane is in contact with aqueous solutions. Various mechanisms such as dissociation of functional groups, adsorption of polyelectrolytes, ions, ionic surfactants and charged macromolecules contribute to charge in NF membrane (Schaep et al., 2001). The rejection of charged species have been explained to depend on the valency, concentration and chemical nature of the compounds in solution and on the surface charge, charge density, and the chemical nature of the groups on the membrane surfaces (Mänttäri et al., 2006). In NF membrane, rejection of charged species process is mostly Donnan effect and dielectric exclusion. The significant of the Donnan equilibrium effect is that solutes with the same sign (co–ions) as that of the fixed membrane charge is repelled while solutes with opposite charge (counter–ions) are attracted. Furthermore, membranes show a higher rejection to multivalent co–ions than monovalent co–ions whereas less rejection to multivalent counter–ions than monovalent counter–ions (Zhao and Li, 2006; Donnan, 1995).

4.2 Concentration polarization

By measuring the solute concentrations in the feed and permeate, the separation process in nanofiltration is evaluated by calculating the observed rejection as follows:

$$R_o = 1 - \frac{c_p}{c_f} \quad (1)$$

The observed rejection indicates the extent of separation with respect to the solute concentration in the feed. The rejection is very dependent upon the pressure and the hydrodynamic conditions of the system in the membrane feed channel. This rejection is estimated by experimental measurement. If the membrane is semi permeable, the permeate concentration is almost close to zero and that of the retained component is close to 1. The rejection is usually lower than 1 because the concentration increases toward the membrane wall surface (Beier, 2015).

In nanofiltration processes, the pressure applied on the feed side of the membrane allows solvent to flow through the membrane pores which is accompanied by a partial permeation of the solutes. Therefore, the solutes retained by the NF membrane are accumulated near the membrane surface, which makes the concentration of solute in the bulk differs from the concentration of solute near membrane wall due to boundary layer build up. This phenomenon is called concentration polarization as seen in Fig. 6 and is basically described by the film theory. The film theory is used to correct the experimental rejection rates (Zydney, 1997). It has or can have the following effects:

- Increase in osmotic pressure of the solution,
- Formation of gel over the membrane surface,
- Increase in the viscosity of the solution,
- Solute enters into the pores and pores are blocked partially or completely.

The first phenomenon decreases the driving force. Second and third increases the resistence of membrane and for this reason decrease the flux. The latter decreases the membrane permeability. All the above factors lead to a decrease in the permeate flux. It should be noted that concentration polarization can only be minimized but cannot be eliminated. One of the ways of reducing concentration in cross–flow separation is by imparting more turbulence in the flow channel. For cross–flow separation, the feed flows tangentially over the membrane surface and the growth of the concentration boundary layer is arrested. Also, turbulence can be achieved by using membrane spacer which disrupts the fluid

flow. Pulsing the feed fluid flow through the membrane module is another technique (Baker, 2004).

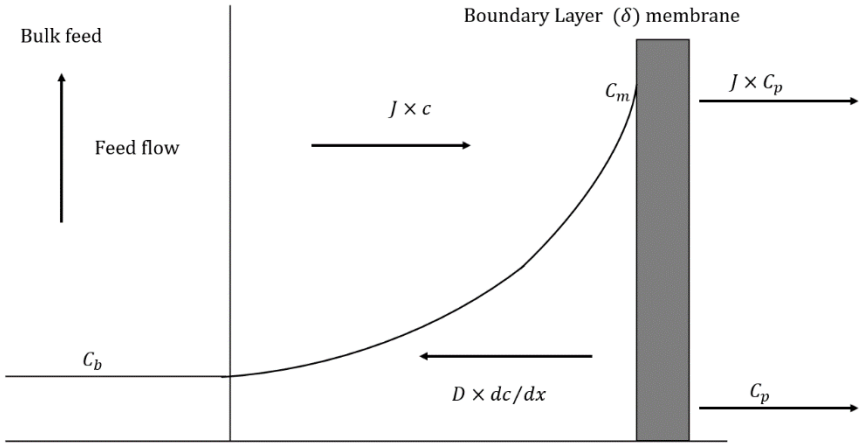

Fig. 6 Schematic of concentration polarization (Lin et al., 2005)

The Fig. 6 describes the concentration polarization profile. Near the membrane surface, there is the formation of a boundary layer where the mass transfer occurs. The concentration in the layer varies from maximum at the membrane surface to the minimum in the bulk (Lin et al., 2005). The film theory equation describes the correlation between the bulk, permeate and membrane surface concentrations and the flux. From Fig. 6, the permeate flux can be expressed in terms of:

- Convection solute transport towards the membrane in the film layer: $J.C$
- Diffusion transport in the boundary film layer back into the bulk:$-D\frac{dC}{dy}$
- Transport of solutes in the permeate away from the membrane: JC_p

The diffusion coefficient is *D*, and $\frac{dC}{dy}$ is the concentration gradient in the boundary film layer, and *C* is the bulk concentration.

At steady state, the sum of the three fluxes should be zero.

$$\sum J_s = 0$$

$$JC - \left(-D\frac{dc}{dx}\right) - JC_p = 0 \qquad (2)$$

By integrating and using the boundary conditions $\begin{Bmatrix} x = -\delta\ C = C_f \\ x = 0\ C = C_m \end{Bmatrix}$,

the Eq. (2) becomes

$$\ln\left(\frac{C_f - C_p}{C_m - C_p}\right) = -J\frac{\delta}{D} \tag{3}$$

where $\frac{\delta}{D}$ is the mass transfer coefficient and (k^{-1}) is express as $= \frac{D}{k}$

Therefore, inserting k into Eq. (3) we obtain the following equation:

$$\left(\frac{C_m - C_p}{C_f - C_p}\right) = exp\left(\frac{J}{k}\right) \tag{4}$$

The concentration near the membrane (C_m) can be simplified as:

$$C_m = C_p + \left[C_f - C_p\right]exp\left(\frac{J}{k}\right) \tag{5}$$

The mass transfer coefficient (k) can be calculated from the appropriate Sherwood number relation.

For turbulent flow in tubular membrane,

$$Sh = 0.023\ Re^{0.875}Sc^{0.25} \tag{6}$$

where the Reynolds number (Re), Schmidt (Sc) and the Sherwood (Sh) numbers are given by

$$Re = \frac{u\rho d_h}{\eta} \qquad Sc = \frac{\eta}{\rho D_{i,\infty}} \qquad Sh = \frac{kd_h}{D_{i,\infty}} \tag{7}$$

where u is the fluid velocity in the channel whose hydraulic diameter is d_h, $D_{i,\infty}$ is the bulk diffusivity of the solute i, and η and ρ are the dynamic viscosity and density of the solution, respectively.

The salt diffusion coefficient (D) was computed based on the diffusion coefficient (D_+, D_-) and valences (z_+, z_-) of the individual ions (cations and anions) by using the following equation (Vanýsek 2005).

$$D = \frac{(z_+ - z_-)D_+D_-}{z_+D_+ - z_-D_-} \tag{8}$$

4.3 Osmotic pressure

Osmosis refers to the movement of fluid across a membrane in response to different concentrations of solutes on the two sides (permeate and retentate) of the membrane. The movement of fluid is toward the more concentrated solution. Osmotic pressure can be explained as the pressure that must be applied to the solution side to stop fluid movement when a semipermeable membrane separates a solution from solvent (water). Now, the semipermeable membrane is permeable to water but not to solute. The osmotic pressure for dilute ideal solutions obeys van't Hoff's law. The actual pressure developed across a membrane which separates a solution from pure water depends on the interaction of the solute with the membrane. Osmosis and osmotic pressure (π) are a thermodynamic concept that exists independently of mechanism. It is found that this reduces the pressure on the solution side of the pore by π for a semipermeable membrane (Feher, 2012). Osmotic pressure depends on solute concentration, solution temperature and the type of ions present. To counteract osmotic pressure in nanofiltration membrane, greater hydraulic pressure is needed to minimize the effect. Therefore, increasing of osmotic pressure is negative phenomenons due to the reduction of permeate flux (Cath et al., 2006).

4.4 Fouling and its mitigating

The IUPAC Working Party on Membrane Nomenclatures has defined fouling as the process resulting in loss of performance of a membrane due to deposition of suspended or dissolved substances on its external surfaces at its pore openings or within its ‘‘pores’’ (Koros et al., 1996). Fouling is one of the main problems associated with membrane separation processes. Nanofiltration might be more complex because the interaction leading to fouling happen at nanoscale and difficult to understand (Agenson and Urase, 2007). Fouling of the membrane causes deterioration of membrane materials and decreased membrane performance (in terms of flux decline). Fouling leads to several factors including drop in productivity, increase in costs of maintenance, high energy consumption, chemicals for cleaning, frequent cleaning, and shorter lifespan of membrane as well as a replacement of membrane. Fouling mechanism and types of fouling must be understood (Peinermann and Nunes, 2010; Lin et al., 2010). Fouling may exist several in different forms:

- Cake layer formation: Deposit of particle may develop layer by layer on the membrane surface. This usually happens in particles of a size larger than the pore size membrane.
- Adsorption: This occurs when there is an interaction between solutes and membrane. It may happen on the surface of the membrane or in pores.

- Gel layer formation: It is caused by concentration polarization in the immediate proximity of the membrane surface.
- Pore blocking: Solutes passing through the membrane may block and clog the pores. Size particle determines whether the pore membrane is partially or fully blocked.

Fouling mechanism is closely associated with another two phenomena, concentration polarization and osmotic pressure. Concentration polarization accumulates retained solute in the boundary of the feed side. As a result, the solute will increase the osmotic pressure of the solution and lead to a decrease of effective TMP and permeate flux. Concentration polarization contributes to fouling mechanism such as adsorption, gel, and cake layer formation (Sablani et al., 2001). According to Mohammad et al. (2015), it is interesting to know that a lot of studies had been carried out on fouling mechanism. But until now, it remains difficult to predict which mechanism involves in a membrane operation. Fouling can change from one to another after membrane process. This can be attributed by operating the membrane for sometimes or affected by feed properties.

Generally, fouling can be grouped into four major categories: organic fouling, colloidal (particulate) fouling, scaling (inorganic fouling) and biofouling (biological fouling). The Fig. 7 shows the schematic of the types of fouling. The existence of organic matter will lead to producing organic fouling at the same time it becomes a nutrient for the microorganism to survive and adhere to the membrane surface. Studies conducted show that the presence of certain foulants might suppress the other fouling propensity. Inorganic fouling is related to scaling. This involves precipitation of salts on the membrane surface (Van der Bruggen et al., 2008). Nanofiltration membranes retain ions which cause an increase of the concentration at the membrane surface that may exceed the solubility limit at a certain point in the membrane module. The most common constituents of scale are calcium carbonate, gypsum, barium/strontium sulphate and silica although other potential sealants exist (Schafer et al., 2005). Scaling is a purely thermodynamic process involving a phase change which requires a degree of super saturation. Biofouling is associated to all biologically active organisms mainly bacteria and fungi. This involves the formation and growth of a biofilm attached to the membrane. The biofilm may reduce the water flux and eventually prevent water passage. For nanofiltration of wastewater, the biofilms were found to have a thickness of 20–30 μm (Ivnitsky et al., 2010). Biofouling is not a major problem for nanofiltration in contrast to scaling and adsorption of small organic solutes. These may (partly) penetrate the membrane and since the bacteria are too large, it will remain in the superficial biofilm.

According to Kim and Jang (2006), the real cause of flux decline when biofouling occurs is due to the formation and accumulation of exopolymeric substances (EPS). Developing membrane with lower surface charge or surface charge like that of the foulant and increasing the hydrophilicity will help reduce colloidal fouling. Surface roughness is essential to increase membrane fouling by increasing the rate of attachment onto the membrane surface. It should be noted that membrane with a rough surface are more prone to fouling than membranes with a smoother surface. Biological fouling can be reduced by the addition for example, silver nanoparticles in the membrane structure (Van der Buggen et al., 2008). The Fig. 7 shows all the types of fouling in membrane process.

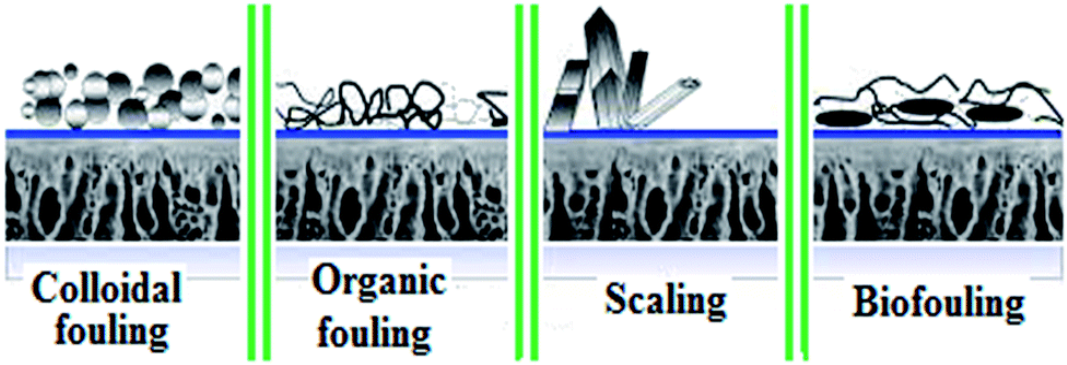

Fig. 7 Types of fouling (Choudhury et al., 2018)

Operating conditions such as recovery rate and flow velocity contribute to fouling propensity of a membrane process. In fact, fouling is a complex phenomenon where it involves the interaction between the feed solution, membrane properties and operating conditions. Fouling studies provide useful information on what can be done to reduce fouling and offer valuable guides for membrane process design and development in the industrial application for higher rejection. It must be noted that fouling can be prevented or controlled by taking necessary measures during water treatment. These are feed pre–treatment and early prediction, membrane selection, module design and operation mode, and cleaning processes when the performance of the membrane is dropped to a certain level. Different types of pre–treatment help reduce the foulants in feed and decrease fouling in many operations. Pre–treatment method also makes use of pressure driven membrane process such as ultrafiltration and microfiltration (Kim et al., 2007). Other methods include ozonation or UV/H_2O_2 oxidation, adsorption, and flocculation (Shon et al., 2005).

Back–flushing or pulsing is another approach to remove cake layers on the feed side and hence decrease the influence of fouling. It is carried out by reversing the flow of permeate through the membrane and therefore, dislodges the foulant and re–establishes the flux at a

high level. To maintain a high flux, back–flushing is carried out periodically and requires module types with a high–pressure resistance to overcome fouling (Cui and Muralidhara, 2010). The Fig. 8 shows the schematic diagram of back–flushing. The time of the back–flushing must be reduced to seconds which implies that the cake formation remains very low since there will be no time to build up layer (Mulder, 1997).

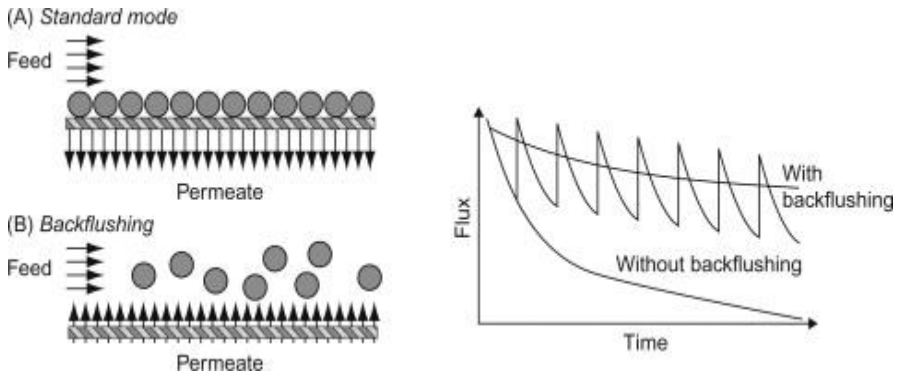

Fig. 8 Schematic of back–flushing and flux behaviour over time (Cui and Muralidhara, 2010).

After some operating period, NF membrane will be fouled by contaminants in the feed solution. Hence, the cleaning process must be conducted from time to time to ensure proper performance of the membrane. Conversely, selection of the cleaning agent is very important. Inappropriate selection of cleaning agents may result in membrane damage or ineffective performance by the membrane. Thus, usually cleaning efficiency will be used to determine the suitability of cleaning agent. Cleaning efficiency depends on the ability of cleaning agent to break down the integrity of the fouling layer with the membrane. For example, in a study of NF for municipal wastewater treatment, an amount of foulants extracted with alkaline solution (0.1 N NaOH) was significantly higher than acid solution (0.1 N HCl) (Chon et al., 2011). The layer on the membrane surface studies shows that alkaline cleaning was a more effective cleaning process to remove fouling. Wei et al. (2010) compares the effectiveness of NaOH, HCl, citric acid and EDTA cleaning agent for NF used to treat complex pharmaceutical wastewater. EDTA was found to be the most favourable cleaning agent as it managed to achieve about 99 % of membrane flux recovery ratio. However, examining the effect of the cleaning on membrane surface properties should be taken into consideration. According to Simon et al. (2013) caustic cleaning had created changes in NF membrane surface properties and solute separation efficiency due to an increment in the membrane pore size. Although cleaning agent reduces fouling in membrane process, precautionary measures should be taken on the selection of these chemical agents to avoid damage on the membrane.

5. Characterization and modelling of NF membrane

Basically, the characterization method used in the prediction of NF membrane is essential in the design and operation of the membrane processes. The current membranes used in NF are mostly either negatively charged or neutral (Fadaei et al., 2012). For better understanding and performance of the separation mechanism during nanofiltration, it is paramount to characterize a membrane. Furthermore, membrane characterization plays a vital role in three related aspects such as guiding membrane fabrication, obtaining specified membrane morphology, and achieving the desired membrane performance. From a practical point of view, membranes are usually characterized to assist in membrane selection, membrane process diagnosis, and new membrane material design (Tung et al., 2014). In addition, characterization is very important because the design of nanofiltration depends on reliable data relating to the membrane chemical structures and properties (Agboola et al., 2015). NF membrane is characterized by finding the structural (pore size and membrane thickness) and charge properties of the membrane. This is necessary to estimate the membrane suitability for application in different industries. Several NF membranes solely depend on the information provided by the manufacturers. Limited information is given in terms of membrane permeability, solute rejection, and neutral solute rejection. Such available information cannot give preliminary values on the structure and electrical properties of the membrane (Bowen and Mohammad, 1998). Many studies have been carried out on the physical and chemical properties of nanofiltration. The characterization methods and membrane characteristics can be seen in Table 4.

Table 4. Characterization methods used for NF membrane (Luo and Wan, 2013)

Characterization methods	**Membrane characteristics**
Atomic force microscopy (AFM)	Surface roughness, pore size distribution, active layer thickness, adhesion force
Scanning electronic microscopy (SEM)	Surface morphology, active layer thickness
Transmission electron microscopy (TEM)	Active layer thickness
Contact angle measurements	Surface hydrophilicity
Streaming potential measurement	Membrane charge
Mathematical modelling based of solute rejection data	Pore size, membrane thickness, charge

Predictive modelling is a very essential step used for membrane performance and determining membrane characteristics. A good predictive model is necessary to facilitate the performance of the membrane to be predicted accurately without involving tedious and complicated procedures. This will be neccessay to obtain raw data for prediction and enhance the efficiency of the modelling process. Using reliable modelling will result in a smaller number of experiments and consequently a reduction in cost and time (Hilal et al., 2004). These models are used to describe and predict flux as well as rejection at different operating conditions of both neutral and charge species by NF membrane. It has become crucial to develop practical and reliable models to better predict the flux and rejection of a membrane as the process is complicated. Modelling is developed to select appropriate membrane, separation mechanism, design process, and improve the efficiency of membrane (Agboola et al., 2015). Several theories and models have been proposed for membrane transport mechanisms to derive an acceptable model. The models used for each membrane might be different due to the difference in membranes properties during fabrication (Ang and Mohammad, 2015). The mathematical models can be divided into several classes which are non–equilibrium thermodynamic (IT) model, pore models and non–porous models (Wang et al., 2012). Most often, membrane characteristics (pore size, membrane thickness to porosity) are analysed by the neutral solutes and salt rejection experiment using structure models such as Donnan steric partitioning model (DSPM) (Bowen and Mukhtar, 1996) and Spiegler–Kedem model in combination with steric hindrance pore model (SHP). Other complex models are Teorell–Meyer–Sievers model, space charge (SC) (Szymczyk et al., 1999), electrostatic and steric hindrance (ES) model used to estimate the charge of the membrane. DSPM and dielectric exclusion (DSPM–DE) model (Bowen and Welfoot, 2002), steric, electric, and dielectric exclusion (SEDE) model (Szymczyk and Fievet, 2006) have been proposed. It should be emphasize that uptil now, there is no mathematical modelling (universal accepted model) that is valid for wide range applications. Most of the established models are only applicable for certain and specific conditions (Ang and Mohammad, 2015). The Table 5 gives a description of the main models for calculation of membrane parameters and their applications.

Table 5. Summarization of structural model used in nanofiltration process (Wang et al., 2012)

Model type	Description	Application in membrane characterization
Steric Hindrance Pore (SHP) model	Modelling the transport of neutral solutes through membrane based on the Stokes–Maxwell friction model	Estimation of the pore structure (pore radius and the ratio of membrane porosity to membrane thickness)
Teorell–Meyer–Sievers (TMS) model	Based on Donnan equation, Nernst–Planck equation and electroneutrality conditions	Evaluation of the electrical properties (charge density)
Space charge (SC) model	Based on Navier–Stokes equation, Poisson–Boltzmann equation and extended Nernst–Planck equation	Calculation of streaming and membrane potential, and transport coefficients
Electrostatic and steric–hindrance (ES) model	Combining SHP with TMS model	Estimation of the pore structure and charge properties
Donnan steric pore model (DSPM)	In contrast to ES model, considering the hydrodynamic and lag coefficients, and the steric effect of ion distribution	Estimation of the pore structure and charge properties
DSPM and dielectric exclusion (DSPM–DE) model	Considering dielectric exclusion	Estimation of the pore structure and charge properties
Steric, electric, and dielectric exclusion (SEDE) model	Considering dielectric exclusion	Estimation of the pore structure and charge properties

As studied by Moros et al. (2008), suitable model–based process stimulation tools are paramount for modelling of nanofiltration processes in a way to design, analyse and enhance the membrane system. To predict membrane performance using model, it is necessary to consider the separation properties of NF membrane. These are the structure and electrical properties. To determine their structure, the pore size and membrane thickness to porosity must be considered. The electrical properties apply to the sign and magnitude of the charge active layer (Mohammad et al., 2015). The most known NF models are based on the extended Nernst–Planck equation. It describes the mass transfer and an equilibrium partitioning which gives us in–depth knowledge about the distribution of ions at both the inlet and outlet pores. There are several setbacks associated with the use of such models which will be discussed.

5.1 Donnan Steric Pore model (DSPM)

This model was first developed by Bowen and Muhktar (1996), subsequently revised by Bowen et al. (1997) and by Bowen and Mohammad (1998). It is influenced by both electrical (Donnan) and sieving (steric) effects. Combining these two effects will lead to separation of wide range of mixture of organic and salt. The DSPM is entirely based on the extended Nernst–Planck equation modified to include steric effects for hindered transport in pores (Gherasim et al., 2014). Three main ion transportation mechanisms are involved. They are diffusion, electro–migration, and convention mechanism. The solute transfer is described by the following steps: first, a distribution of charged species at the membrane–solution interface resulting from both steric effects and Donnan exclusion, and second, a transfer by a combination of convection, diffusion and electro–migration through the membrane (Szymczyk and Fievet, 2005). The NF membrane was characterized by finding the structural properties (effective pore radius (r_p), effective thickness over porosity ($\Delta x/A_k$) and the effective membrane charge density (X_d). Numerous studies were carried out to test the validity of the DSPM model. Research work was conducted using DSPM to model a diafiltration process involving a mixture of dye and NaCl. It was found that an excellent prediction of rejection of Cl^- and Na^+ was in good agreement with the experimental results obtained if it was assumed that X_d was dependent on the total concentration of negative charges in the solution (Bowen and Mohammad, 1998; Bowen et al., 1997). The following assumptions were made for this model:

- The solution is assumed to behave ideal.
- Transport inside the pore is due to convection, diffusion, and electro–migration.
- Transport effects with convection and diffusion are corrected with hindrance factors.
- Nanofiltration (NF) membrane has a porous structure; Hagen–Poiseuille type relationship was used for solvent velocity.
- The flow inside the pore is assumed laminar.
- The chemical potential of solute depends on operating pressure.
- The solvent within the pores consist of one layer of oriented water molecules.
- Variation of solvent viscosity and dielectric constant inside the pore are considered.
- Concentration polarization across the surface of the membrane is neglected.
- Partial molar volume and diffusion coefficient inside pore are independent of concentration.

- The separation at the pore interface is due to steric, Donnan effect and dielectric exclusion.
- Electro viscous term is neglected for velocity of ions in the solvent.

In terms neutral solutes, the Donnan Steric Pore Model (DSPM) is used to describe the structural characteristics of the membrane that is the effective pore radius (r_p) and thickness to porosity ratio ($\Delta x/A_k$). The NF membrane can be modelled by considering the membrane as bundles of cylindrical pore radius r_p and length Δx or as a bundle of slits with length and the half width. The structural parameters which are the effective pore size (r_p) and membrane thickness to porosity ratio ($\Delta x/A_k$) were estimated through independent experiments of neutral solutes rejections by considering both slit–like and cylindrical pore geometries. In NF membrane, the rejection of neutral solutes can only be determined by steric mechanism (size–based exclusion). The pore radius (r_p) and membrane thickness to porosity ratio ($\Delta x/A_k$) can be obtained by using the Donnan Steric Partitioning Model (DSPM). This model calculates the structural parameters by fitting the rejection rates using the following equation (Bowen and Mohammad 1998; Cavaco et al., 2008):

$$R = 1 - \frac{C_p}{C_m} = 1 - \frac{\phi_i K_{i,c}}{1 - [(1 - \phi_i K_{i,c}) \exp(-Pe)]} \tag{9}$$

where C_p is the solute concentration in permeate, C_m is the solute concentration in feed solution at the membrane interface, $\phi_i = 1 - \lambda_i$ which is the steric portioning coefficient of the solute i. and λ_i is defined as the ratio of the solute radius (r_s) to pore radius (r_p). $K_{i,c}$ and $K_{i,d}$ are the hindrance factors for convection and diffusion for slit–like pores

The Peclet number (Pe) is defined by the expression:

$$Pe = \frac{K_{i,c} J}{K_{i,d} D_{i,\infty}} \frac{\Delta x}{A_k} \tag{10}$$

where A_k is the membrane porosity and Δx is the effective membrane thickness.

The hindrance factors for convention and diffusion (slit–like pores) can be evaluated by the following equations (Dechadilok and Deen, 2006). These hindrance factors are valid for all range of solutes to pore radius (of different pore geometries). These equations can be found in Table 6.

Also, the thickness to porosity ratio from the water flux using the Hagen–Poiseuille equation for different pore geometries is as follow:

$$J_w = L_p \Delta P = \frac{{r_p}^2}{3\eta(\Delta x/A_k)}\ \Delta P \quad \text{for slit} - \text{like pores} \tag{11}$$

$$J_w = L_p \Delta P = \frac{{r_p}^2}{8\eta(\Delta x/A_k)}\ \Delta P \quad \text{for cylindrical pores} \tag{12}$$

where J_w is the pure water flux L_p, is the pure water permeability ΔP, is the transmembrane pressure and η is the solution viscosity.

Table 6. Hindrance factors for diffusion and convection (Dechadilok and Deen, 2006)

Slit–like pores	Cylindrical pores
$\phi_i = (1 - \lambda i)$	$\phi_i = (1 - \lambda i)^2$
$\lambda i = \frac{r_{i,s}}{r_p}$	$\lambda i = \frac{r_{i,s}}{r_p}$
Diffusion	Diffusion
$K_{i,d} = \frac{H(\lambda i)}{\phi i}$	$K_{i,d} = \frac{H(\lambda i)}{\phi i}$
$H(\lambda i) = 1 + \frac{9}{8}\lambda i \ln \lambda_i - 1.19358\ \lambda_i + 0.4285\ \lambda i^3 - 0.3192\ \lambda i^4 + 0.08428\ \lambda i^5$	$H(\lambda i) = 1 + \frac{9}{8}\lambda i \ln \lambda_i - 1.56034\ \lambda_i + 0.528155\ \lambda i^2 + 1.91521\ \lambda i^3 - 2.81903\ \lambda i^4\ 0.270788\ \lambda i^5 + 1.10115\ \lambda i^6 - 0.435933\ \lambda i^7$
Convection	Convection
$K_{i,c} = \frac{W(\lambda i)}{\phi i}$	$K_{i,c} = \frac{1 + 3.867\ \lambda_i - 1.907\ \lambda i^2 - 0.834\ \lambda i^3}{1 + 1.867\ \lambda_i - 0.741\ \lambda i^2}$
$W(\lambda i) = 1 - 3.02\ \lambda i^2 + 5.776\ \lambda i^3 - 12.3675\ \lambda i^4 + 18.9775\ \lambda i^5 + 15.21185\ \lambda i^6 - 4.8525\ \lambda i^7$	

Gherasim et al. (2014) investigated the structural and charge properties by using a polyamide thin–film composite NF membrane (AFC 80). The DSPM model was used for the characterization of the membrane. The authors used four neutral solutes and found out that the structural parameters values were almost similar to each other irrespective of different solutes. The real rejection and the fitted rejection using DSPM were similar which confirm a good

agreement between the experimental and calculated rejection. Other authors found similar results using this model to estimate the structural parameters (Otero et al., 2006; Bowen and Mohammad, 1998; Bowen et al., 1997).

Characterization of NF membrane using neutral solutes is to improve its efficiency to save time by performing less experiment. Therefore, such method is a better choice which can be used to characterize the structural properties of a membrane without any damage on the structure of the membrane. There have been several drawbacks of DSPM and other models which are related to steric/electric exclusion. First, in most instances, these models are not able to fit experimental rejection rates of different electrolytes with a single value of the membrane thickness to membrane porosity ratio (Bowen et al., 1997; Schaep et al., 1999; Labbez et al., 2002). Second, the Donnan exclusion theory cannot predict successfully the high rejection rates observed with all NF membranes which contain ionic solutions of divalent counter or opposing ions although the ion size effect is not taken into consideration (Vezzani and Bandini, 2002).In almost all research performed using DSPM and other related models; the membrane volume charge density is used as a fitting parameter. Such a fitting parameter will probably produce unrealistic high–volume charges or to a ratio of the volume charge density like that of the salt concentration increasing with concentration (which contradict with common adsorption isotherms). This shows that additional phenomena must be accounted for to give a better understanding and prediction of NF membrane performance (Labbez et al., 2002; Bowen and Welfoot, 2002).

5.2 Spiegler–Kedem model (SKM)

The Spiegler–Kedem model makes use of irreversible thermodynamics (IT) for describing the transport of single solute and solvent in both NF and RO. It was first derived by Kedem and Katchalsky (1963) and Spiegler and Kedem (1966). This model describes the membrane as an empirical ‘‘black box’’ by neglecting the porosity of the membrane as well as detail transport mechanism (Agboola et al., 2015). The solvent and solute transport is described by a sum of convective (due to the pressure gradient) and diffusive (due to the concentration difference existing at the membrane sides) fluxes. The three transport coefficients which satisfy the Spiegler–Kedem model are: the reflection coefficient (σ), the solute permeability (P), and the water permeability (L_p) (Hidalgo et al., 2013). By applying linear relationship on a local level, the following equations can be expressed:

$$J_v = -L_p \left(\frac{dp}{dx} - \sigma \frac{d\pi}{dx}\right) \quad (13)$$

$$J_s = -P \frac{dc_s}{dx} + (1 - \sigma) c_s J_v \quad (14)$$

where (J_v) is the volume flux and (J_s) solute flux.

Assuming constant fluxes and constant coefficient is integrated through the membrane thickness. The Spiegler–Kedem equation describes the solute rejection with solvent volumetric flux.

The intrinsic rejection can be calculated by the following equation below:

$$R = 1 - \frac{c_p}{c_m} = \frac{\sigma\,(1 - F)}{1 - \sigma F} \qquad \text{where } F = \exp\left(-\frac{1 - \sigma}{P} .\ J_v\right) \quad (15)$$

where R is the real rejection, J_v is the permeate volume flux, σ is the reflection coefficient, and P is the solute permeability.

The reflection coefficient is the measure of the capability of the membrane to separate solutes during experiment. It has values between 0 and 1, σ = 0 means totally unselective membranes (no solute separation), and σ = 1 means ideally semi permeable membrane (no solute transport). The Eq. (15) shows that the rejection increases with increasing in permeate volume flux and has a limiting value R = σ at infinitely high permeate volume flux (Gherasim et al., 2013; Spiegler and Kedem, 1966).

This model is usually criticized for providing little knowledge into the physiochemical processes which include the transport mechanisms across the membrane. In addition, this model does not completely describe water flux for some solute system usually for some dilute organics which have lowered water fluxes. Several authors have used developed models based on the Spiegler–Kedem model or combined Spiegler–Kedem–Katchalsky model (SKK). Studies were conducted on the separation of (i) aqueous dye salt solution (Levenstein et al., 1996), (ii) organic solute from water (Van der Bruggen and Vandecasteele, 2002) and the result was quite successful.

The following assumptions were made:

- The Spiegler–Kedem model predicts only the transport of solute. The type of solute and its charge, solvent and membrane are not taken into consideration.

- Solute in the system is semi permeable to the membrane.
- Pressure and concentration are the driving forces.
- In the concentration polarization layer thickness, the solute value that is independent of the diffusion and mass transfer coefficient.

Even though this model has its limitations, numerous studies had been made using the Spiegler–Kedem model. It has achieved great result to an extent when compared to experimental values (Gherasim et al., 2013; Gherasim et al., 2015; Musbah et al., 2014). For instance, Mikulášek and Cuhorka (2016) and Gherasim et al. (2013) investigated the removal of toxic Pb (II) ions from aqueous solutions by using two commercially thin–film composite polyamide NF membrane (AFC 40 and AFC 80). The influence of operational variables such as applied pressure, feed solution pH, and feed solution concentration were evaluated. The Spiegler–Kedem model was used to compare the experimental data. It was found that the fitting experimental data are in good agreement with the Spiegler–Kedem model for operational variables even at different lead concentrations (25, 150, 400 mg Pb L^{-1}). This shows that the Spiegler–Kedem model can be used to predict toxic Pb (II) at a wider range of concentration.

5.3 Steric Hindrance Pore (SHP) model

As previously discussed, the real rejection of neutral solutes against the volume flux was used to estimate the membrane parameters (σ and *P*) with the help of the best fit method using the Spiegler–Kedem model (SKM). The Steric Hindrance Pore (SHP) model was proposed by Nakao and Kimura and was modified from pore model to determine the structural parameters. These parameters are the pore radius, and membrane thickness to porosity ($\Delta x/A_k$) by using error function method (Nakao and Kimura, 1982).
The equations used were as follow:

$$\sigma = 1 - (1 + \frac{16}{9}\,\lambda^2)\,(1-\lambda)^2\,[2 - (1-\lambda)^2] \tag{16}$$

$$P = D_s\,(1-\lambda)^2\,(A_k\,/\Delta_x) \tag{17}$$

where λ is the ratio of the solute radius to pore radius, D_s is the diffusivity coefficient, and ($\Delta x/A_k$) is the membrane porosity to thickness ratio.

Wang et al. (1995) used the steric hindrance pore (SHP) model to evaluate the structure parameters (pore radius and membrane porosity ratio) of four different NF membranes. Alcohol (ethyl alcohol, isopropyl, n–butyl alcohol, and t–butyl alcohol) and saccharides (glucose, saccharose, raffinose and cyclodextrin) were chosen as neutral solutes. It was shown that the pore radius of the neutral solutes was almost the same considering the four different membranes. The authors advised that selection of neutral solutes for the determination the pore radius is important when considering the molecular weight of each solute. For membrane thickness to porosity ratio, the values were similar with exception of neutral solutes with highly restriction permeation. The authors concluded that the reflection coefficient of more than 0.90 should be excluded from the results. The SHP is not a good model for solutes with reflection coefficient very close to unity. For instance, lactose has high rejection close to unity and this model is not useful for this solute. Comparable results were obtained by several authors (Nakao and Kimura, 1982; Tsuru et al., 1991).

5.4 Donnan–Steric Pore model with dielectric exclusion (DSPM–DE)

The DSPM–DE model is sometimes referred to as the transport model. Despite its complexity, this model has been used worldwide for modelling nanofiltration and proves successful in literature to model experimental membrane performance (Bowen and Welfoot, 2002; Bowen and Mohammad, 1998; Roy et al., 2015). This model was gradually developed from the hindered transport theory of neutral solutes in pores proposed by Anderson et al. (1974). The model was later extended for ionic species by including the electrochemical potential gradient in the solute transport equation leading to electrokinetic models that use the extended Nernst–Planck equation (Roy et al., 2017). The DSPM–DE model provides information about the magnitudes of the different modes of solute exclusion occurring at the membrane–solution interfaces namely steric exclusion (size–based exclusion at the pore opening or relative size ratio of ions to the membrane pores), dielectric exclusion (resistance to the solute entering the membrane pores due to an energy barrier associated with shedding of the solute hydration shell in order to enter the pore) and Donnan effect (repulsion or attraction effect due to membrane potential) (Geraldes and Alves, 2008; Bowen and Welfoot, 2002; Bandini and Vezzani, 2003). The Fig. 9 shows the ionic transport properties that mainly depend on a combination of these three exclusion mechanisms considered in the DSPM–DE model.

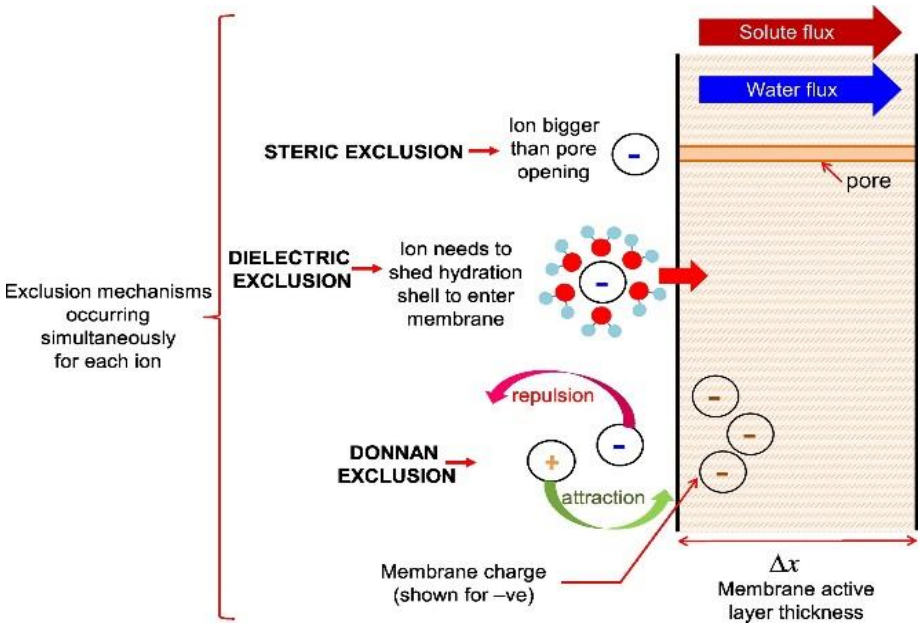

Fig. 9 Schematic representation of solute exclusion mechanisms in nanofiltration as per the Donnan Steric Pore model with Dielectric Exclusion (DSPM–DE) (Roy et al., 2017).

In addition, the model uses the Nernst–Planck equation to describe solute transport through the membrane and hence gives useful information on the individual modes of transport within the membrane namely diffusion (movement of solute down a concentration gradient), convection (solute transported by bulk fluid motion) and electro–migration (ion movement due to the membrane potential gradient). As inputs to this model, the membrane is characterized by certain structural parameters (pore radius and effective active layer thickness) and electrical parameters (membrane charge and pore dielectric constant) (Bowen and Welfoot, 2002; Bowen and Mohammad, 1996). These nanofiltration membrane properties are affected by operational parameters such as feed composition, pH, concentration, and temperature (Oatley et al., 2012). The Fig.10 schematically describes each of the modes of solute transport considered in the extended Nernst–Planck equation.

The DSPM was previously used but considered only the steric and Donnan exclusion mechanisms. This model quickly became popular and was useful in modelling nanofiltration of a wide variety of solutions even those consisting of multivalent co–ions (ions with the same charge as the membrane) (Geraldes and Alves, 2008; Bowen and Mohammad, 1996; Vezzani and Bandini, 2002).

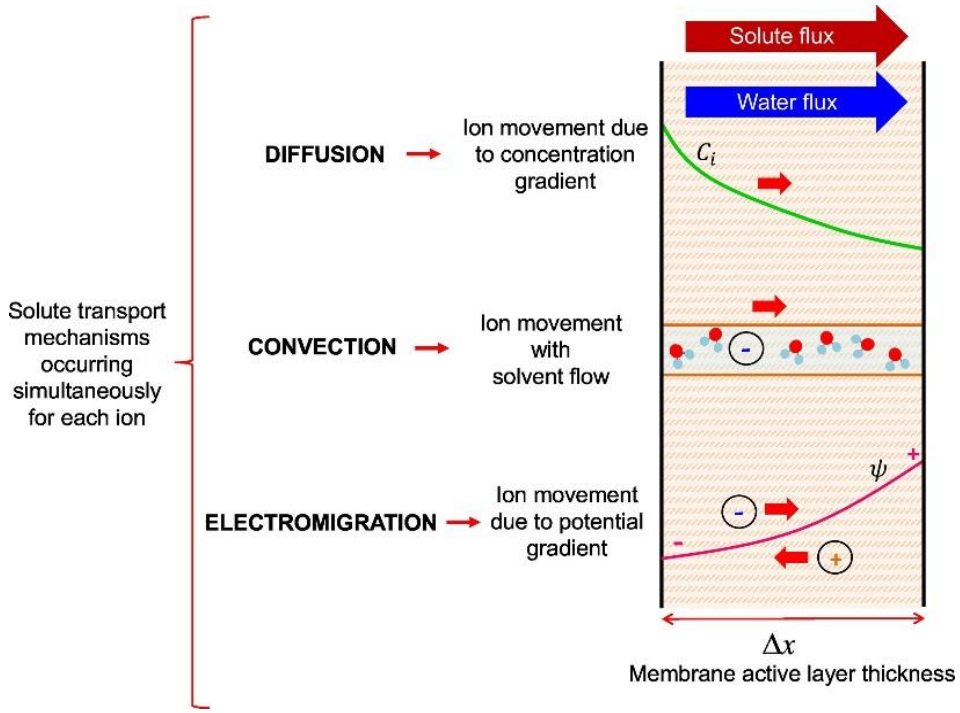

Fig. 10 Schematic representation of solute transport mechanisms in the current model described by the Extended Nernst–Planck (ENP) equation, which is a component of the Donnan Steric Pore model with Dielectric Exclusion (DSPM–DE*)* (Roy et al., 2017).

However, its major setback was the failure to predict multivalent or divalent counter ions. The failure was because there are some polarized charges which give some repulsion forces (image force). Most importantly, these image charges have the same sign as ion and for this reason they are always repulsion. Therefore, the DSPM–DE model was proposed which includes this additional exclusion mechanism. This additional mechanism was included in DSPM–DE model which is called dielectric exclusion. The model allows researchers to overcome or solved the difficulties in modelling multivalent counter–ions (Geraldes and Alves, 2008).

Nevertheless, the concept of dielectric exclusion and mechanism has been debated over the past years by several researchers. Some authors are of the view that the Donnan exclusion mechanism is enough to explain rejection of ions including counter–ions. For instance, Higa et al. (1993) showed that a solution with Ca^{2+}, K^{+} and Cl^{-} ions passing through a negatively charged membrane can be modelled successfully by considering only Donnan exclusion (Roy et al., 2017). Other authors have found Donnan exclusion is not enough in modelling nanofiltration without considering dielectric exclusion as previously mentioned. Evidence from molecular dynamics simulation of membranes with nanopores shows that dielectric exclusion is an undeniable phenomenon which can never be neglected (Renou et al., 2013).

Extensive research work has been devoted to the dielectric effect in the membrane, which was done by Yaroshchuk and called as a ‘‘universal phenomenon’’ (Yaroshchuk, 2000, 2001, 2002). Bandini and Vezzani, 2003 noted two mechanisms are involved in DE (dielectric): (i) “image forces” forming as a result from the difference in the dielectric constant of an aqueous solution and membrane matrix, and (ii) differences in the structure and properties of the solvent in the membrane pores and the bulk resulting in excess solvation energy (Born effect). If the effective dielectric constant of the solution confined inside the pores is lower than that of the bulk solution, the excess solvation energy is positive and thus the ions are rejected by the membrane pores (Yaroshchuk, 2000). However, Bowen and Welfoot (2002) concluded that in nanofiltration, the Born effect of dielectric exclusion is more dominant than the effect of image charges that develop at the interface of the membrane and feed solution. This is because the small pores in nanofiltration membranes cause the intra–pore dielectric constant of the solvent to be almost equal to that of the membrane material itself. Moreover, the image charges are screened by electric double layers in electrolyte solutions (Roy et al., 2017; Bowen and Welfoot, 2002). In another research, Szymczyk et al. (2006) investigated the transport properties of NF membranes using an improved transport model. Their model incorporates the dielectric exclusion in terms of both Born dielectric and image force contributions. The authors concluded from the research that dielectric exclusion can never be neglected in the analysis of separation properties of the NF membrane.

5.5 Steric, Electric, and Dielectric Exclusion model (SEDE)

The Steric, Electric and Dielectric Exclusion (SEDE) model has been developed for nanofiltration by Szymczyk and Fievet (Szymcyzk and Fievet, 2005). This model is based on the extended Nernst–Planck equation to describe the mass transfer across the membrane and accounts for the ion’s distribution at the pore inlet and outlet through equilibrium partitioning relations. This model has been shown to provide a relatively good description of the experimental data for both symmetric and asymmetric single salts (Szymczyk and Fievet, 2005; Cavaco Marao et al., 2008; Szymczyk et al., 2006). The SEDE model includes the dielectric exclusion mechanism and the classical theory (steric/electric exclusion) and form the basis for the description of transport ions or solute inside the membrane. The dielectric exclusion mechanism can be obtained in terms image forces which were incorporated into NF model and Born effect (Vezzani and Bandini, 2002). The image forces which is due to interaction free energy are calculated numerically using approximate relations derived by

Yaroshchuk in 2000 and the solvent structure effects are considered by means of the revised approach of the Born model proposed by Rashin and Honig in 1985.

Various efforts have been made to include the excess solvation energy due to changes in solvent structure into the partitioning equation yielding the distribution of species at the membrane/solution interface. Indeed, the equilibrium and dynamical properties of a solvent in a confined geometry like pores of NF membranes can differ significantly from those in the bulk side (outside pores). The reason is because solvent molecules in such environments exhibit more spatial and orientational order. This ordered structure reduces the ability of the solvent molecules to respond to any external electric field and later, leads to a decrease in the solvent dielectric constant. The excess solvation energy produced resulting from the difference in dielectric constant between external and internal (inside pores) solutions can be evaluated based on the Born model. This energy has the advantage to be easily included in the steric/electric exclusion–based theory without increasing the complexity of calculations (Szymczyk and Fievet, 2005; Bowen and Welfoot, 2002).

Another way according to Yaroshchuk (2000) for the change in solvent structure inside pores of NF membranes is to consider the non–local dielectric response of the solvent. This can be done by using the non–local electrostatic theory which considers that the electric induction is dependent on the electric field strength not only at a given point but also within a zone around it. The interaction free energy of an ion inside a pore of nanometric dimensions is likely to be affected also by the interaction of the ion with the polarization charge induced by the ion itself at the interface between the membrane matrix and the solution inside the pore. This phenomenon results from the difference in dielectric constants between the membrane and the solution and is usually described as the production of image forces since the interaction between the ion and the polarized interface is formally equivalent to the interaction with a fictitious image charge located at the other side of the interface at the same distance from it as the ion. This has been reviewed extensively by Yaroshchuk (2000). It was clearly shown that the dielectric exclusion cannot be neglected in the analysis of the filtration properties of NF membranes. Indeed, the classical steric/electric exclusion theory is found to be unable to describe experimental rejection rates of the polyamide membrane under consideration. (Szymczyk and Fievet, 2005).

An experiment was performed by Szymczyk and Fievet (2005) to compare between the theoretical and experimental rejection rate of the SEDE model to the classical steric/electric exclusion model. The authors determined the effect of dielectric on the rejection properties and all experimental values were taken from Labbez et al. (2002). It was seen that

the experimental rejection and theoretical rate of SEDE were almost the same, but the steric/electric exclusion was different. This shows that dielectric plays a major role in the rejection mechanism of the NF polyamide membrane. In conclusion, the classical theory (i.e. based on steric and Donnan exclusions only) fails to describe experimental results and not suitable to describe transport properties of such a NF polyamide membrane. A good agreement was obtained for both electrolytes by involving dielectric effect using the SEDE model.

Cavaco Morão et al. (2008) used NF membrane Desal–DK to predict intrinsic rejection rate of five ions (K^+, Cl^-, NH_4^+, SO_4^{2-} and CA^-) by using SEDE. The authors found that the ion selectivity is governed by steric, Donnan and Born dielectric exclusion mechanisms. The predicted intrinsic rejections rates of the five ions were in good agreement with the experimental values. The major weakness of the present approach was the requirement to experimentally determine the effective membrane volume charge density for each electrolyte solution. However, the present challenge is to extend this SEDE model to the case of complex multi–component separations and to validate this predictive method with industrially relevant NF applications.

5.6 Teorell–Meyer–Sievers model (TMS)

The Teorell–Meyer–Sievers (TMS) model has been used successfully in many types of research works. It describes the transport characteristics of solutes through the NF membrane by the electrical properties (Hoffer and Kedem, 1967; Gherasim et al., 2014). It explains the transport of charged solutes through the membranes by only the electrostatic effects. The TMS assumes uniform distribution of fixed charges in a membrane and used to investigate the membrane potential, the effective fixed charged density, and salt rejection of a charged membrane (Wang et al., 1995). In addition, the model is widely used to determine the electrical properties (effective fixed charge density of the membrane φX).

Since is a salt solution of a 1–1 type electrolyte and a negative charged NF membrane, the TMS model equations which involve reflection coefficient (σ) and solute permeability (P) are given by the following equation (Wang et al., 1995):

$$\sigma = 1 - \frac{2}{(2\alpha - 1)\xi + (\xi^2 + 4)^{1/2}} \tag{18}$$

$$P = D_s(1 - \sigma)\frac{A_k}{\Delta x} \tag{19}$$

where ξ is the parameter which expresses the electrostatic effects and is defined as the ratio of the fixed charge density of the membrane (*X*) to the concentration of the 1–1 electrolyte *(c).*

The transport number of cations in the free solution (α) and diffusivity of the 1–1 electrolyte (D_s) found in Eqs. (20) and (21) are calculated based on the diffusion coefficients of the individual ions by using the following equation:

$$\alpha = \frac{D_{+,\infty}}{D_{+,\infty} + D_{-,\infty}} \tag{20}$$

$$D_s = \frac{2D_{+,\infty}D_{-,\infty}}{D_{+,\infty} + D_{-,\infty}} \tag{21}$$

It is well known that for most membrane, the fixed charge density varies with the concentration of the electrolyte. Therefore, to find the interpretation of the relationship between the fixed charge density and the concentration of the electrolyte *(c),* the effective fixed charge density is used instead of *X* (Kobatake et al., 1965; Wang et al., 2012; Gherasim et al., 2014).

In the case of electrical properties, charge solute such as NaCl and models (TSM and SKM) can be used for estimation. Gherasim et al. (2014) investigated the structural and charge properties by using a polyamide thin–film composite NF membrane (AFC 80). The membrane charge was found by using experiments of NaCl solutions with concentration in the range of 2.5–50 mM. By using the Teorell–Meyer–Sievers model together with the Spiegler–Kedem model, the effective membrane charge was calculated. These values fitted very well with the Freundlich isotherm equation. Similar values were obtained by various authors (Wang et al., 1995, Schaep et al., 1999). The Teorell–Meyer–Sievers model (TMS) has been effectively used in research employing ion–exchange membranes (Kobatake et al., 1965; Yuasa et al., 1968), and applied in describing the rejection of charged reverse osmosis membranes and ultrafiltration membranes (Tsuru et al., 1991; Hoffer and Kedem, 1967). The electrolyte rejections by charged reverse osmosis membranes both in single–electrolyte solutions and in mixtures as previously discussed were well predicted using the extended Nernst–Planck equation combined with the TMS model.

The extended Nernst–Planck equation includes the contribution of volume flux to ionic flux unlike the ordinary Nernst–Planck equation. The TMS model is not based on structural parameters such as pore radius but rather assumes uniform distribution of fixed charge. The mobile ion concentration and the electrical potential changed with the direction of

flow during the membrane process. This model simplifies mathematical analysis and gives an analytical equation of ionic transport. However, the range where the TMS model can be successfully applied is limited since one cannot assume uniform distribution of fixed charge, mobile ions, and electric potential especially for membranes with large pore radius (Wang et al., 1995).

5.7 Coupling of models

Coupling of models is useful to improve the accuracy of the values determined when compared to that of the experimental results. Roy et al. (2015) developed a DSPM with dielectric exclusion for different types of modules for NF process. A comparative study was performed for flat sheet and spiral wound modules for variable membrane characteristics. There was a comparison of the influence of operating conditions such as pressure, recovery ratio, and solute rejection of both modules. The result from the combination of model and experimental values was in good agreement.

Zafrilla and Moros (2008) investigated nanofiltration modelling based on the extended Nernst–Planck equation using different physical modes. These physical models are convenient in describing the interaction between the membrane and multi–ionic feed solution. These models determine the permeate characteristics at different operating conditions and feed concentration. The authors developed a model based on the combination of the extended Nernst–Planck equation and the Donnan steric equilibrium. They first used the iterative Runge–Kutta method followed by using COMSOL for Donnan Steric–Partitioning Pore model (DSPM) to overcome the union problem. COSMOL comparative study was beneficial when three different physical modes such as PDE (partial differential equation) coefficient form, convection and diffusion, and Nernst–Planck without electroneutrality were accomplished.

In conclusion, most of the NF model is based on the extended Nernst–Planck (ENP) equation. It combines contribution from diffusion, convection, and electrical migration to model ions across the membrane. Examples of such models are Donnan Steric Pore Model (DSPM) and Steric, Electrical and Dielectric Exclusion model (SEDE). These models have proven quite effective in predicting ion rejection in dilute solutions of both single and multi–ionic solution (Santafé–Moros et al., 2008; Bowen and Welfoot, 2002; Szymczyk and Fievet, 2005, 2006). However, these models have failed because they were developed specifically using a dilution solution assumption. In addition, these models discussed can be used to predict membrane characteristic with low solutions concentration where osmotic pressure is

negligible. Conversely, many applications of NF such as desalination which has high salt concentration and neglecting the effect of osmotic pressure cannot be possible. It is evident that these models for describing fluxes in solvent resistant application have not yet been conveyed. More research is needed before universal accepted model can be developed (Van der Bruggen et al., 2008).

6. Analysis of the problem and the objectives of the work

Removal of heavy metals from wastewater is paramount in this our 21st century due to its recalcitrance, persistence, and tendency to build–up in living organism. In addition, heavy metals cannot be degraded or destroyed in the environment without proper separation. Heavy metals and its effects in the environment have previously been discussed in this research (Fu and Wang, 2011; Gherasim et al., 2015; Murthy and Chaudhari, 2008). Numerous approaches have been employed for the development of cheaper and more effective technologies both to decrease the amount of wastewater produced and improve the quality of separation processes involved (Barakat, 2011). Diverse conventional technique has been carried out over the years to remove heavy metals from industrial effluents. These methods include chemical precipitation, solvent extraction, adsorption, ion exchange, coagulation–flocculation, electrochemical treatment, and floatation (Fu and Wang, 2011). Conversely, conventional separation processes involve high operational cost due to chemical consumption, high initial cost, and increased volume of sludge generated. Furthermore, these methods are slow and laborious due to collection of disposal sludge or addition of high level of chemicals. These chemicals have failed to meet regulation level set up by individual countries in terms of technical, economic, and environmental reasons (Malik et al., 2012).

Due to these limitations, much attention has been focused on membrane processes. This is because the processes are less expensive, efficient, and pollution free. For the removal of heavy metals from aqueous solution, membrane processes such as liquid membranes and pressure driven processes like nanofiltration, reverse osmosis, and hybrid processes have been used (Gherasim and Mikulášek, 2014). Among all this pressure driven processes, NF membrane has received greater attention and made tremendous progress since its introduction in the 1980's (Mohammad et al., 2015). NF membranes have been useful in many applications particularly in wastewater treatment as well as drinking water and process water production. The interest in the use of NF membrane can be explained by a combination of (i) growing demand for water with high quality, (ii) growing attention to reuse water due to rapid population globally (iii) better dependability and integrity of the membranes (iv) lower cost of membranes due to improved use and (v) more stringent water standards (Van der Bruggen et al., 2008). As nanofiltration application market is currently growing at a faster pace due to rapid development in technologies, an estimation of global sales had reach $450 million in 2019 (Zheng et al., 2016). Hence, it is significant to analyse proper separation process such as nanofiltration which can be useful to remove heavy metals from wastewater. In general, the

key factor for removal of heavy metal from wastewater depends on the characteristics of wastewater, operational cost, applicability, and process simplicity. In addition, the separation process should be suitable, appropriate, and meet the environmental–based treatment standard level set by the established country (Zhao et al., 2016).

Over the past decades, direct measurement methods were used to characterize membrane and have several setbacks. These physical methods include microscope techniques (electron and atomic force), permporometry, mercury intrusion, gas adsorption–desorption. For instance, atomic force microscopy (AFM) is used for direct measurement of the structural properties but does not give precise reading of NF membrane. This is because it has high roughness which may result in images that are difficult to understand and high forces that may damage the polymeric structure (Mulder, 1997; Johnson and Hilal, 2013). In addition, the pores are very small in nature and the images of the membrane surface cannot give enough information about the structure of the pores inside the membrane. Likewise, other methods used to estimate membrane charge density such as electro–kinetic measurement, measurement of membrane potential or determining of ion–exchange capacity usually give qualitative information (Mulder, 1997) and help to define the transport of solute in NF membrane. There are various characteristic techniques available for NF membrane and the key is choosing the right technique with the right resolution to have a desired result. A generally known method used to determine the characterization of the membrane is to carry out rejection experiments of neutral solutes and then using different mathematical models to estimate the pore size and membrane thickness to porosity (Mohammad et al., 2015). This is because of the minimal interaction of solutes found in the membrane. One of the criteria with this method is choosing neutral solutes of different sizes or nominal molecular weights closer to each other to ensure similar interaction with the membrane. It is necessary since the differences in interaction with the membrane material can have a significant effect on the differences in the solute rejection based on size exclusion (Garcia–Martin et al., 2014).

Numerous reports on the removal of heavy metals from wastewater by NF membrane had been made and the results are promising. Gherasim et al. (2013) studied the ability of a commercially available nanofiltration membrane (AFC 80) to remove polluting and toxic Pb (II) ions from aqueous solutions to meet the USEPA guidelines regarding the toxicity threshold limits. Gherasim and Mikulášek (2014) further analyse the separation process of lead ions from synthetic wastewater by NF using AFC 80 at different process parameters such as feed concentration, operating pressure, cross–flow velocity and pH. In addition, the authors researched the performance of the membrane with single Pb $(NO_3)_2$ and binary Pb–Cd salts

mixtures as found in a real mining effluent. In another experiment, Gherasim et al. (2015) investigated the performance of polyamide nanofiltration (AFC 40) in the rejection of Co (II) ions from aqueous solution. It was found that the operating variables (cross–flow velocity, operating pressure, feed pH and concentration) influence the permeate flux, rejection of Co (II) ions, and the separation mechanism. The AFC 40 membrane shows a very high cobalt nitrate rejection of 95–97 % at pH 3–4 feed solution and decreases at pH 5–6 for 100 mg Co/L. The maximum rejection normally for all concentration was at a low operating pressure of 20–25 bar which is the optimum range for NF process. This shows an advantageous condition of high flux and low energy consumption to achieve optimum operating conditions. In another research, Mikulášek and Cuhorka (2016) used two different polyamide NF membranes AFC 40 and AFC 80 for the removal of polluting and toxic Pb (II) ions under different operational conditions. In their research, the influence of operating conditions such as applied pressure, pH, and feed concentration on the ability of NF membranes to remove ions were evaluated. The same commercially nanofiltration membrane (AFC 40) was used by Kočanová et al. (2017) for the separation of zinc sulphate from aqueous solutions. The research mainly focuses on the influence of various operating conditions (transmembrane pressure, pH, and feed flow rate) on the membrane performance. During all the experiments with real samples of industrial wastewater, the achieved value of rejection was above 98 % which proves that the available nanofiltration membrane is suitable for removal of zinc.

Murthy and Chaudhari (2008) investigated the application of thin–film composite polyamide NF membrane for the rejection of nickel ions from aqueous wastewater with different feed concentration. They studied that the variation of pH does not have much effect on the rejection of nickel ion but on the flux as it increases. The maximum rejection of the metal was found to be 98 % and 92 % for an initial feed concentration of 5 and 250 ppm, respectively. In addition, Murphy and Chaudhari (2009) further researched on binary heavy metals such as nickel and cadmium separation capability of a commercial NF–300 membrane from aqueous solution. The maximum observed solute rejection of nickel and cadmium ions was 98.94 % and 82.69 % respectively for an initial feed concentration of 5 ppm. The observed rejection sequence was observed to be $R_O(Ni^{2+}) > R_O(Cd^{2+})$ for $NiSO_4$–$CdCl_2$–water system.

Daei Niaki et al. (2015) surveyed nanofiltration membrane technology in removal of heavy metals such as nickel, copper, and zinc from industrial wastewater. The effect of pressure, concentration, and separation time on removal efficiency was evaluated. The results show that the separation time was a positive agent in the heavy metal rejection. In another study,

Basaran et al. (2016) performed a comparative study of removal of nickel (II) and chromium (VI) heavy metals from metal plating wastewater by two nanofiltration membranes. The effects of both the transmembrane pressure (10, 20, and 30 bar) and the feed pH (3.5, 7, and 10) on the membrane performance were analysed. Under optimum conditions for NF90 and NF270 membranes, the rejection values of nickel were found to be 99.2 and 98.7 %, respectively. Alsalhy et al. (2018) estimated nanofiltration transport parameters for cobalt ions removal from aqueous solution. It was observed that the obtained cobalt ion rejection values increase with the decrease in initial concentration and increase in pH at constant feed flow rate.

The aim of this research is to investigate the performance of two commercially available thin–film composite polyamide NF membranes (AFC 30 and AFC 80) for separating of toxic heavy metals from wastewater. Structural parameters and electrical parameter of the membranes will be estimated. Experiments with neutral aqueous solutions in conjunction with two independent mathematical pore models (Donnan Steric Pore model – DSP model, and Steric Hindrance Pore model–SHP model) will be performed at various process conditions. The fixed charge density on the membrane surface will be determined from different concentrations of sodium chloride (NaCl) experiment by using the Spiegler–Kedem model together with the charge model called Teorell–Meyer–Sievers (TMS). In addition, the study disclosures the influence of different operating parameters to find the optimum condition for the removal of heavy metals from wastewater will be realized. These heavy metals to be considered are zinc sulphate ($ZnSO_4$), zinc nitrate ($Zn(NO_3)_2$), cobalt nitrate ($Co(NO_3)_2$) and nickel nitrate ($Ni(NO_3)_2$). The operating parameters evaluated are transmembrane pressure, feed concentration, cross–flow velocity, and pH.

Modelling of heavy metal rejection will be developed to select appropriate membrane, separation mechanism, design process, and improve the efficiency of membrane. Mathematical modelling plays a key role in the design and improves on efficiency of a membrane. This leads to a smaller number of experiments saving time, and in–depth knowledge of the separation mechanism (Agboola et al., 2015). Several authors have use Spiegler–Kedem model to attained reliable results. Therefore, the Spiegler–Kedem model will be used to evaluate the real rejection of heavy metals in all our experiments by finding the coefficient of reflection and solute permeability.

In summary, the objectives of this research are as follows:

- Evaluate the structural parameters (pore size and membrane porosity ratio) and electrical properties by modelling with DSPM model, SKM model with SHP model and SKM with TSM model.
- Evaluate the effect of operating variables for the removal of heavy metals (zinc, cobalt, and nickel) from wastewater.
- Modelling of rejection of heavy metals using Spiegler–Kedem model (SKM) and Steric Hindrance Pore (SHP) model.

7. Experimental part

7.1 Materials and methods

7.1.1 Membranes

Two kinds of NF tubular membranes (AFC 30 and AFC 80) from PCI membrane systems were used in these experiments. These membranes are thin–film composite consisting of aromatic polyamide skin–layer on polysulfone substrate. AFC 30 and AFC 80 membranes are capable of withstanding pressures up to 60 bar, temperatures below 70 ^{o}C and pH in 1.5–9.5 range. Table 7 shows the specification of both membranes (AFC 30 and AFC 80) used.

Table 7. Technical specification of membranes tested (PCI, 2018)

Structural parameters	AFC 30	AFC 80
Membrane type	Tubular	Tubular
Material	Polyamide film	Polyamide film
Maximum pH range	1.5–10.5	1.5–9.5
Operating pressure (bar)	60	60
Operating temperature (^{o}C)	70	60
NaCl or $CaCl_2$	80[a]	75[b]
MWCO (Da)	80[c]	100–150[d]
Membrane surface charge (pH =7)	Negative	Negative
NaCl or $CaCl_2$ rejection (%)	80	75

[a] Rejection of NaCl
[b] Rejection of $CaCl_2$
[c] Gherasim et al., 2013
[d] Wallace et al., 2018

7.1.2 Experimental equipment

Nanofiltration experiments were performed by a cross flow separation unit whose scheme is depicted in Fig. 11. A tubular MIC–RO module which was manufactured by PCI membrane system was used to carry out the experiment. The module was equipped with two tubular NF membranes of 1.25 cm internal diameter and 30 cm length, the effective membrane area of 240 cm^2.

Description of individual parts of experimental apparatus

The experimental apparatus consists of individual parts which have been explained below (see in Fig. 11).

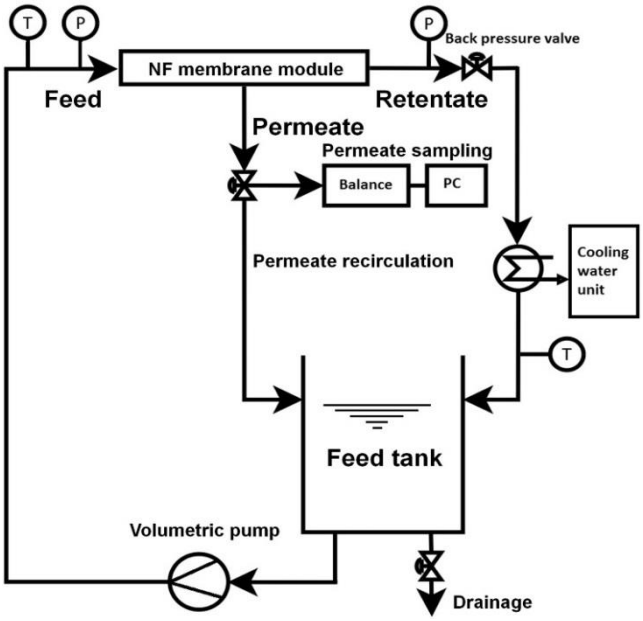

Fig. 11 Setup of nanofiltration experimental system.

Drainage valve: The valve is always provided at the lowest point of the experimental system.

Cooling water unit (TAEevi, Armfiled): The function of this unit is to remove heat from experimental system to maintain a temperature throughout the experiment. From our experiment, the cooling medium used was water.

Back pressure valve: A back pressure valve is a specific type of control valve that is designed to hold pressure on pressurized production vessels during experiment at relative constant value independent on volumetric flow rate.

Volumetric pump: The pump employs use 2 pumps both with 3 syringes which work by pushing a plunger to drive a syringe at a predetermined rate during experiment.

Pressure gauge: The function of the gauge is to measure and display pressure in an integral unit. Measuring the pressure of a substance is an important part of the manufacturing process.

Temperature gauge: A temperature gauge is a device used to indicate the temperature of feed during experiment.

Electronic scale balance (Balance KERN KB): The balance is used to weigh permeate at 200 mg during experiment which is connected to a personal computer. The fluxes are measured and recoded on the personal computer. The permeate is return to the feed tank to maintain a uniform feed concentration.

7.2 Chemicals

All the reagents used were of analytical reagent grade or of highest purity. The aqueous solution was prepared by dissolving the following reagents: glucose, glycerol, triethylene

glycol (TEG), lactose, ethanol, isopropyl alcohol, sec butyl alcohol, zinc sulphate ($ZnSO_4$), zinc nitrate ($Zn(NO_3)_2$), cobalt nitrate ($Co(NO_3)_2$), nickel nitrate ($Ni(NO_3)_2$), and sodium chloride (NaCl). All chemicals used were supplied by Penta Co., the Czech Republic. The individual solutions were prepared by dissolving the respective reagents in highly demineralised water (conductivity < 1 μS cm^{-1}, pH 6.0 ± 0.2). Neutral solutes diffusivities and Stokes radius can be found in Table 8.

Table 8. Diffusivities and Stokes radius of neutral solutes

Solute	Molecular weight g mol^{-1}	Diffusivity 10^{-10} m^2 s^{-1}	Stokes radius (nm)
Ethanol	46.0	12.40	0.198
Isopropyl alcohol	60.0	2.41	0.241
Sec butyl alcohol	74.1	9.40	0.261
Glycerol	92.1	9.50	0.258
TEG	150.0	7.31	0.336
Glucose	189.0	6.70	0.355
Lactose	340.0	4.90	0.501

7.3 Measurement procedure

7.3.1 Pure water flux (PWF)

The temperature of the feed solution during an experiment was at a constant value of 25 ° C by using the heat exchanger and transmembrane pressure which varies in a range of 5–30 bar. To reduce concentration polarization, the feed solution was pumped under a flow rate of 9 L min^{-1}. Firstly, membrane was compacted for at least 2 h to stabilize the active layer structure of membrane at the maximum transmembrane pressure (30 bar) used in the experiments. The membrane pure water permeability was obtained by measuring the pure water flux (PWF) at different transmembrane pressure in a range of 5–30 bar. PWF was measured by weighing of permeate using electronic balance connected to a personal computer. It was done twice for each membrane. Differences (experimental error) were below 5 %. The membrane pure water permeability L_p of the two different membranes was estimated.

7.3.2 Rejection of neutral solutes

The experiments were performed using 500 mg L^{-1} solution of all the neutral solutes seen in Table 8 at the natural pH of demineralized water (6.0 ± 0.2). The permeate and retentate were returned to the feed to maintain a constant concentration of feed throughout the experiment. The flux of the neutral solutes was recorded using an electronic balance connected to a personal computer. The samples of permeate and feed at each applied transmembrane pressure (5–30 bar) were taken for analysis after recirculation of permeate until the system reaches steady state.

To assure the reproducibility of the results, the experiments were performed in duplicate. The obtained results represented an average of two identical experiments and the relative standard deviation was up to 5 %. As the membrane characteristics were obtained by fitting models, the quality of fitting was found by calculating the correlation coefficient of determination (R^2) and the non–linear *chi–square* test (χ^2) by using the following relationship (Foo and Hameed, 2010):

$$\chi^2 = \sum \frac{\left(R_{exp} - R_{cal}\right)^2}{R_{cal}} \tag{22}$$

where R_{exp} and R_{cal} are the real rejections experimentally determined and calculated in accordance with the models, respectively. Very high values of R^2 and very small values of the parameter χ^2 indicate a good agreement between experimental values and theoretical model.

7.3.3 Rejection of heavy metals

In the case of heavy metal rejection experiments, the constant composition of permeate corresponding to the steady state was obtained by reaching a constant conductivity value in the permeate solution. Samples of both permeate and feed were taken for analysis at different applied transmembrane pressure (5–30 bar). Conductivity measurements were done by using a WTW Cond 340i conductometer for feed and WTW Cond 3210 conductometer for permeate equipped with a WTW 325 electrode, respectively. After each experiment, the system was cleaned with demineralized water for about 3 h at 30 bar and 45^{o} C until the water flux and permeability of the membrane has been restored back. In extreme cases, chemical cleaning by recirculation of 0.3 % HNO_3 solution was also used.

7.4 Determination of process streams characteristics

7.4.1 Determination of neutral solutes

The neutral solutes were determined by adding 500 mg L^{-1} of neutral solutes to deminerized water. The solution is stirred until all the solutes are dissolved. The neutral solutes concentration in feed and permeate was determined by the total organic carbon (TOC) technique (Skalar Formacs $^{HT/TN}$ TOC/TN Analyzer) (see Fig.12).

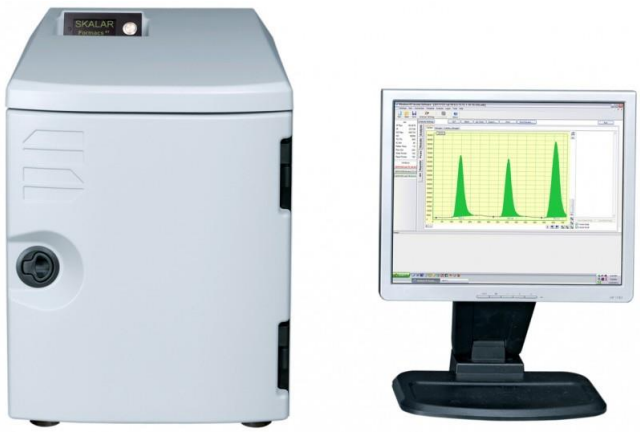

Fig. 12 Skalar Formacs HT/TN TOC/TN Analyzer)

The Formacs^{HT} Total Organic Carbon high temperature catalytic combustion system features a versatile modular design and excellent performance for the analysis of Total Carbon (TC), Total Inorganic Carbon (TIC), Total Organic Carbon (TOC), and Dissolved Organic Carbon (DOC). This design was developed not only to allow the determination of TOC in clean waters such as pharmaceutical and drinking waters, but also performing equally well for the analysis of waste, surface, seawater, and soil extracts. This intuitive and flexible software package is used for data acquisition and instrument control. The software package includes easy to use templates for routine analysis, multi point regression, automatic exclusion of results, recalculation, statistics etc. The Total Organic Carbon analyser can be operated as a stand–alone analyzer where sample and standard solutions are introduced directly through a rotary septum with less injection port for analysis of TC and TIC. TOC is calculated by subtraction of the TIC value from the TC the sample. For larger sample numbers, an optional random–access auto–sampler is available for complete automation of the TOC determination.

7.4.2 Determination of heavy metals content

Heavy metals at different feed concentration were circulated in the feed tank at different applied transmembrane pressure. The conductivity of permeate was measured by a

conductivity meter several times until the measurement was stable. The elemental analysis of heavy metals concentration in feed and permeate was carried out with the sequential, radially viewed ICP (Inductively Coupled Plasma) atomic emission spectrometer INTEGRA XL 2 (GBC, Dandenong Australia). The device was equipped with the concentric nebulizer and the glass cyclonic spray chamber (both Glass Expansion, Australia) (see Fig.13).

Fig. 13 ICP atomic emission spectrometer INTEGRA XL 2

The ICP atomic emission spectrometer is a type of emission spectroscopy that uses the inductively coupled plasma to produce excited atoms and ions that emit electromagnetic radiation at wavelengths characteristic of element (see Fig. 13) The sample often a liquid is sucked into the system by a peristaltic pump and the sample solution is transformed to a mist by a nebulizer. The burner combines air and fuel to produce flame. Then, the nebuliser and mixing chamber converts the liquid sample to mist and sprays the fine particles into the flame using the compressed jet of gases (fuel and air). A spray chamber is placed between the nebulizer and the torch. The primary function of the spray chamber is to remove large droplets from the aerosol. The monochrometer/filter allows only the chosen wavelength and absorbs all the other wavelengths. Then, detector is used to detect the intensity of the emitted light coming out of the cell and generates currents proportional to it. The meter displays the intensity of the emitted light (higher the concentration–higher is the intensity of the emitted light–higher the meter reading). Last not least, the blank sample was sprayed over the flame and the meter reading was set to zero.

7.4.3 Determination of membrane surface charge

The membrane surface charge is another parameter which is necessary for characterization of membrane. It was estimated by carrying out permeation experiments of NaCl solution at different concentrations in the range of 100–4500 mg L^{-1} at pH 6.0±0.2. Conductivity measurements were done by WTW Cond 340i conductometer (for bigger conductivity), WTW Cond 3210 (for smaller conductivity) equipped with a WTW TetraCon 325 electrode until the permeate conductivity reached the steady state conditions (three times constant value). The permeate and feed concentration of all concentration were measure using the total organic carbon technique and rejection was evaluated. By using mathematical models (in our case Spiegler–Kedem model together with Teorell–Meyer–Sievers model), the membrane fixed charge density of different concentrations of sodium chloride (NaCl) was evaluated.

8. Results and discussion

8.1 Pure water flux

The pure water fluxes were measured at various transmembrane pressures for both membranes and water permeability was then calculated. The water permeability of each membrane is the slopes of the straight lines. The Fig. 14 shows dependency of permeate flux on transmembrane pressure for both membranes. The values of pure water permeability *(L_p)* for both membranes (AFC 30 and AFC 80) at 25 ^{o}C are 5.926 L m^{-2} h^{-1} bar^{-1} and 1.526 L m^{-2} h^{-1} bar^{-1}, respectively. It has been observed that the flux linearly increases with increased transmembrane pressure for both membranes being considered. From differences in values of pure water permeability, it is clearly shown that AFC 80 membrane is denser than AFC 30 membrane. This revealed that AFC 80 membrane exhibited almost four times lower permeability than AFC 30 membrane.

Furthermore, Dudziak and Bodzek (2010) evaluated the permeability of the AFC 30 membrane; however, the obtained value was (4.97 L m^{-2} h^{-1} bar^{-1}) than our experimental value (5.93 L m^{-2} h^{-1} bar^{-1}). This difference can be explained by the different membrane batches used in each research (Cuhorka et al., 2020). The data supplied by the membrane manufacturer (PCI, 2018) includes typical and minimal values of the water flux. If the average value is calculated from our data and the data obtained by Dudziak and Bodzek (2010), then both of our results are in the range of ±16% around this average (5.45 L m^{-2} h^{-1} bar^{-1} ± 16%). Lastly, the permeability value (1.526 L m^{-2} h^{-1} bar^{-1}) of AFC 80 membrane in our experiment is comparable the data (1.45 ± 0.10 L m^{-2} h^{-1} bar^{-1}) obtained by Gherasim and Mikulášek (2014).

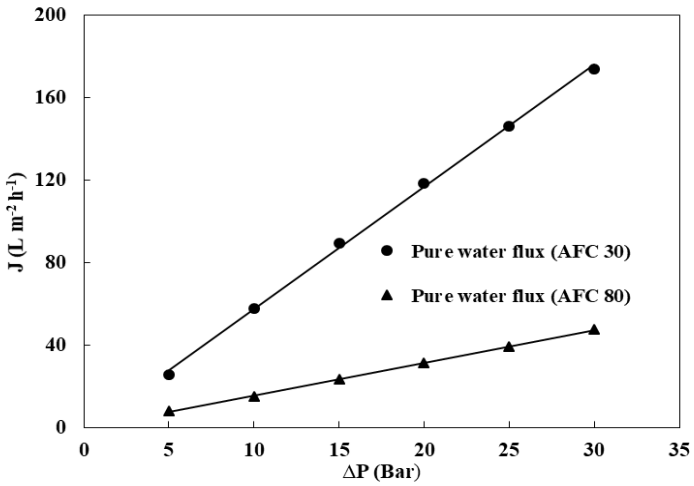

Fig. 14 Pure water fluxes against transmembrane pressures for both membranes used.

8.2 Evaluation of structure parameters

The NF experiments for the membrane structural characterization of both membranes (AFC 30 and AFC 80) were performed with neutral solutes (see Table 7) at feed concentration of 500 mg L^{-1}. The comparison of pure water flux and the fluxes during experiments with the solutions used against transmembrane pressure difference is shown in Fig. 15.

(a)

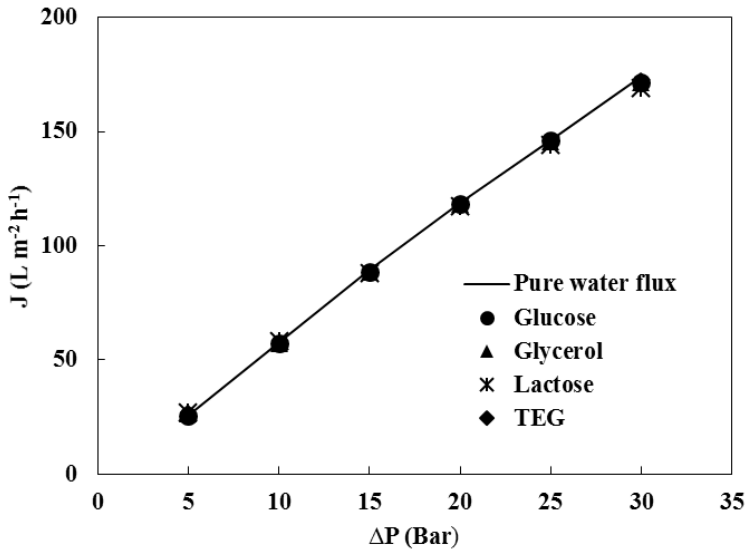

(b)

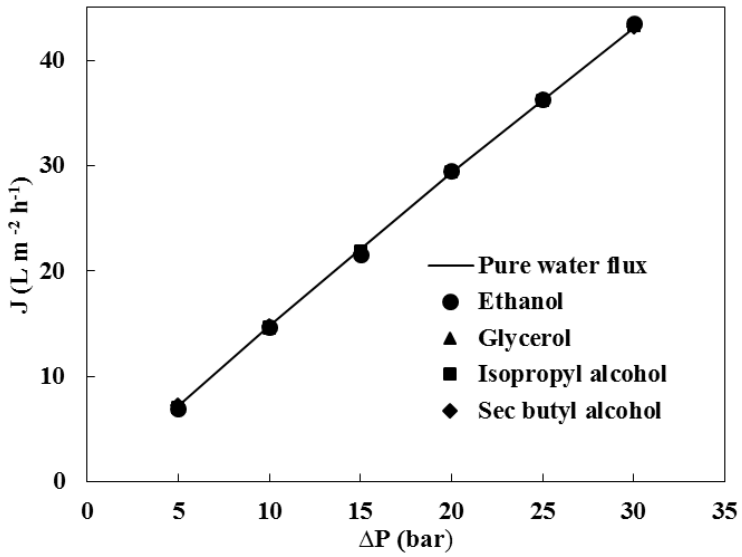

Fig. 15 Dependency of permeate flux on transmembrane pressure for neutral solutes. Pure water flux (solid lines), and neutral solutes (symbols). (a) AFC 30 and (b) AFC 80 membrane.

The measured permeate flux as a function of the transmembrane pressure differences for all neutral solutes used is similar to that of pure water flux irrespective of the solutes for both membranes. This shows that the osmotic pressure of the solution is negligible. The variations of properties (density, viscosity, and diffusion coefficients) are neglected. Such assumptions are useful for diluted solutions. As the fluxes of the neutral solutes are identical to pure water, no fouling was found in our case. It was observed that the flux linearly increases with increased transmembrane pressure differences for both membranes as seen in Fig. 13. This increase could be explained due to increase of the preferential sorption of water at higher transmembrane pressure (Salih and Al–Alawy, 2016).

8.2.1 Donnan Steric Partitioning model (DSPM)

By incorporating the expression for the thickness–to–porosity ratio into the Peclet number equation (Eq. 10), a new expression is obtained for real rejection depending only on the pore radius. By fitting the experimental rejection value for different transmembrane pressures with the real rejection from model, the pore radius (r_p) can then be estimated for both membranes (AFC 30 and AFC 80) using the cylindrical pores. This is followed by the corresponding values for the membrane thickness to porosity ratio ($\Delta x/A_k$) which is calculated from Eq. (11) and presented in Table 9. The application of these equations assume that the pressure drop through the microporous sublayer is negligible implying that the transmembrane pressure drop can be attributed to the active layer which is an assumption made in most literature (Lanteri et al., 2008).

Table 9. Estimation of structural parameters of NF membranes using DSP model

Membrane	Solutes	DSP model	
		r_p (nm)	$\Delta x/A_k$ (μm)
AFC 30	Glycerol	0.316	2.31
	TEG	0.365	3.08
	Glucose	0.355	3.18
	Average	**0.343**	**2.86**
AFC 80	Ethanol	0.212	4.17
	Isopropyl alcohol	0.245	5.53
	Glycerol	0.262	6.38
	Sec butyl alcohol	0.265	6.53
	Average	**0.246**	**5.65**

Also, NF membrane can be modelled using slit–like pores geometry. Selection of the neutral solutes for the experiment plays a pivotal role to obtain values to fit the DSP model. One of

the criteria with this method is choosing neutral solutes of varied sizes or nominal molecular weights closer to each other to assure similar interaction with the membrane. It is necessary since the differences in interaction with the membrane material can have a significant effect on the differences in the solute rejection based on size exclusion (Garcia–Mintin et al., 2014). From our results, the neutral solutes chosen for both AFC 30 and AFC 80 are glucose and glycerol, respectively. This is because both pore sizes are closer to each membrane and fit very well with the experimental values. From Table 10, the pore size and thickness to porosity for slit–like pore are 0.370 nm and 3.18 μm, respectively. The pore radius of glucose using slit–like geometry was closer to the Stokes radius of glucose (0.355 nm) and fit very well with the experimental values (see Fig. 16).

Table 10. Structure parameters of AFC 30 and AFC80 membranes for glucose and glycerol

Membranes	Pore geometry	Membrane structural parameters		Quality of fittings
		r_p (nm)	$\Delta x/A_k$ (μm)	(χ^2)
AFC 30	Slit–like	0.370	3.18	2.57×10^{-4}
	Cylindrical	0.486	2.05	8.42×10^{-3}
AFC 80	Slit–like	0.262	6.38	2.25×10^{-6}
	Cylindrical	0.329	3.23	2.38×10^{-3}

As seen in Table 10, it was observed that pore radius and thickness to porosity ratio of glycerol was 0.262 nm and 6.38 nm respectively for slit–like pore. From Fig. 17, the slit–like pore fit very well with the experimental values compared with the cylindrical pores. We can conclude that both slit–like pores and cylindrical pores can be used to model the structure of a membrane by DSP model. We can assume that the model fit very well by using the cylindrical pore when the average of the pore radius was used. However, selection of the neutral solute is also important when the model is used as a slit–like pore. It was noted that the Stokes radius or molecular weights of neutral solutes should be closer to each other and ideally near to the MWCO of membrane.

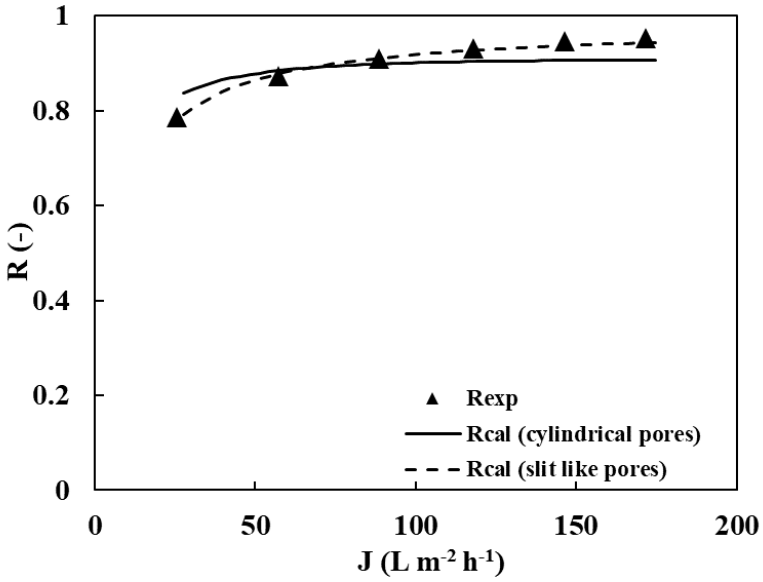

Fig. 16 Experimental data for glucose rejection by AFC 30 membrane. Experimental rejection (symbol), cylindrical pores geometry (full line), and slit–like pores (dotted line).

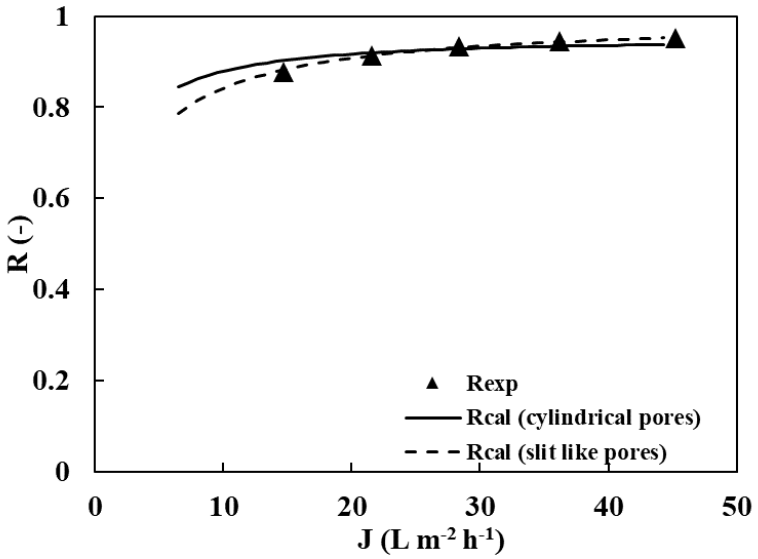

Fig. 17 Experimental data for glycerol rejection by AFC 80 membrane. Experimental rejection (symbol), cylindrical pores geometry (full line), and slit–like pores (dotted line).

8.2.2 Steric Hindrance Pore model (SHP)

The structural properties (r_p and $\Delta x/A_k$) were determined by using the following steps. First, the real rejection against the permeate flux was used to estimate the membrane parameters (σ and P) by the *chi–test* method to get best fit using the Spiegler–Kedem model found in Eqs. (20) and (21). Both obtained values of the membrane parameters can be found in Table 11. Then from reflection coefficients by using Eq. (16), based on SHP model, the ratio of the

solute radius (r_s) to pore radius (r_p) was obtained for each neutral solute (Nakao and Kimura, 1982). By using error function method, λ of each neutral solute was determined. Since λ and the solute radius are known, the pore radius can be calculated. Also, the membrane porosity ratios ($\Delta x/A_k$) were evaluated using Eq. (17) as the solute permeability of each neutral solutes and λ are known for both NF membranes.

Table 11. Estimation of structural parameters of NF membranes using SHP model

Membrane	Solutes	SHP model			
		σ (–)	P 10^{-6} m s^{-1}	r_p nm	$\Delta x/A_k$ μm
AFC 30	Glycerol	0.774	19.50	0.342	2.94
	TEG	0.915	4.20	0.389	3.21
	Glucose	0.950	1.64	0.392	3.65
	Average			**0.374**	**3.27**
AFC 80	Ethanol	0.914	4.32	0.229	5.36
	Isopropyl alcohol	0.983	0.68	0.256	5.39
	Glycerol	0.981	0.52	0.275	6.74
	Sec butyl alcohol	0.984	0.45	0.276	6.54
	Average			**0.259**	**6.00**

Also, the rejections of the neutral solutes of both membranes (AFC 30 and AFC 80) were compared to the two independent models (DSPM and SHP). It was observed from Fig. 18 that, the two independent models fit well with the experimental results of all the neutral solutes. The observed solute rejections increase continuously with increasing of permeates flux for neutral solutes which can be seen in Fig. 18. Selection of neutral solutes for the determining the pore radius is important when considering the molecular weight of each solute. Solutes with closer molecular weight will help achieve better results of pore radius and membrane porosity ratio. The SHP is not a good model for solutes with reflection coefficient very close to unity or highly restricted permeation. For instance, lactose has high rejection close to unity and this model is not useful for this solute (Nakao and Kimura, 1982). From our results, the molecular weight cut–off (MWCO) which corresponds to 90 % rejection of solutes is for AFC 30 between molecular weight of triethylene glycol and glucose and AFC 80 between ethanol and isopropyl alcohol (see Fig. 18). We can assume that the molecular weight cut–off (MWCO) of AFC 30 is approximately 150 g mol^{-1} and 60 g mol^{-1}

for AFC 80 membrane. By using interpolation, the obtained values are 153 g mol^{-1} (AFC 30), and 59.8 g mol^{-1} (AFC 80), respectively.

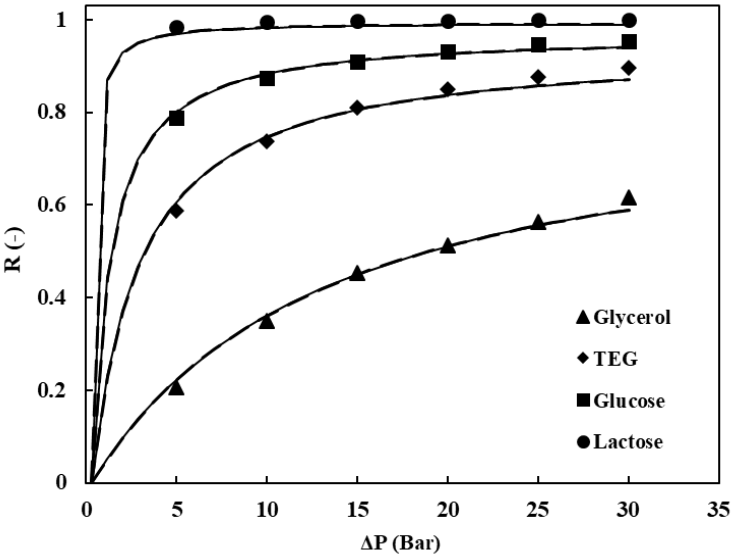

(a)

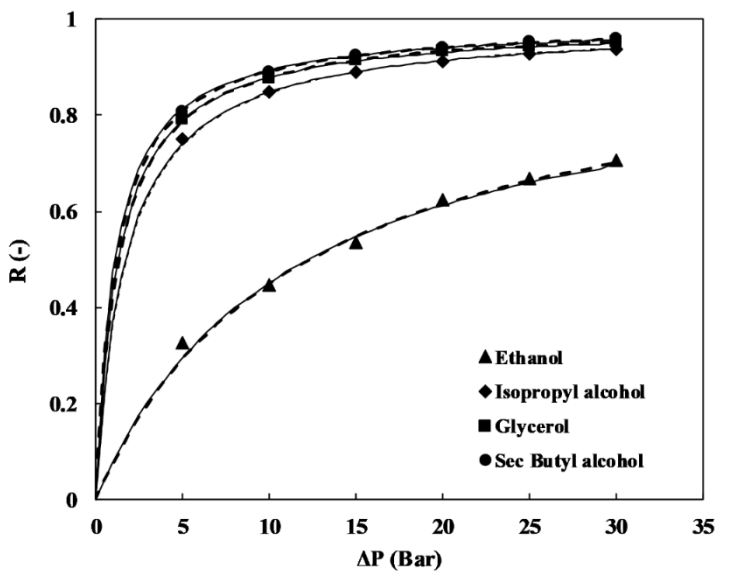

(b)

Fig. 18 Rejection of neutral solutes as a function of transmembrane pressure for membranes (a) AFC 30 and (b) AFC 80 using two independent models. Experimental (symbols), DSPM (lines) and SHP (dashed lines).

8.2.3 Membrane charge density

The membrane charge is an important parameter useful in the NF process. This is because the separation mechanism is a combination of size exclusion and electrical interaction (repulsion forces) between the ions in the feed (retentate) and the charged membrane. In addition, the membrane charge allows one to estimate, explain, and model the respective NF processes.

The membrane charge is determined by the type or chemical structure of the membrane material and is due to dissociation of the functional group(s) present in the membrane material, or adsorption of different charge or polarizable solutes from the solution (Gherasim et al., 2014). The AFC 30 membrane has a polyamide outer layer which gives raise the formation of ammonium ($–NH_3^+$) and carboxyl (–COOH) group. The isoelectric point is at pH of about 5.3 (AFC 30 membrane) and 3.6 (AFC 80 membrane) in KCl solution (Bouranene et al., 2008; Mikulášek and Cuhorka, 2016). If the pH <IEP the membrane is positively charged as the carboxyl groups are undissociated and the amino groups are protonated. Likewise, membrane is negatively charge at pH >IEP as the carboxyl groups are dissociated.

To estimate the membrane charge, different experiments were performed with NaCl solutions at various concentrations in the range 100–4500 mg L^{-1}. The Fig. 19 depicts the pure water flux and the permeate fluxes against the applied transmembrane pressure to the salt solutions. It has been observed that the permeate flux slightly decreases with increasing in NaCl concentration which can be explained by an increased in osmotic pressure.

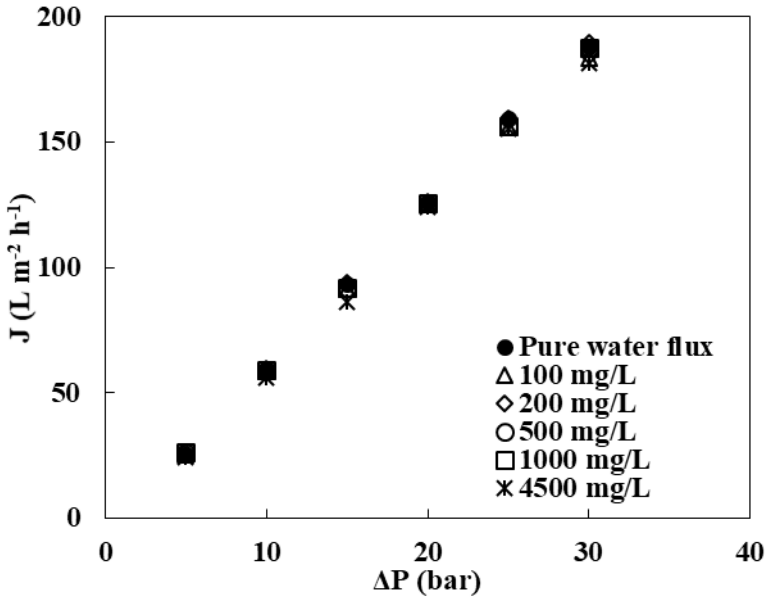

Fig. 19 Pure water flux and fluxes of NaCl solutions with different concentrations from 100–4500 mg L^{-1}

The reliance of real rejection against the permeate flux for NaCl solutions of different concentrations is presented in Fig. 20 for AFC 30 membranes. The salt diffusivity $D_s = 1.61 \times 10^{-9}$ m^2 s was used to analyse the real rejections by means of Eq. (16) accomplished by considering the diffusion coefficients of individual ions: $D_{\infty,Na^+} = 1.333 \times 10^{-9}$ m^{2}s^{-1} and $D_{\infty,Cl^-} = 2.031 \times 10^{-9}$ m^2 s^{-1} (Vanýsek, 2005).

As depicted in Fig. 20, the solute rejections gradually decrease with increasing of NaCl concentration in the feed solution. The decrease in rejection could be explained because of more solute ions being diffuse through the membrane. Several studies have been conducted on the decrease in rejection with increasing salt concentration (Wang et al., 1995; Tannien et al., 2006). Meanwhile, increase in transmembrane pressure extensively increases the solute rejection for all NaCl concentrations during the experiments. Salt rejections (symbols) in the experiments were fitted with Spiegler–Kedem model (dash). The good agreement between model and experimental data can be seen in Fig. 20. The values of the model parameters (reflection coefficient and solute permeability) can also be found in Table 12.

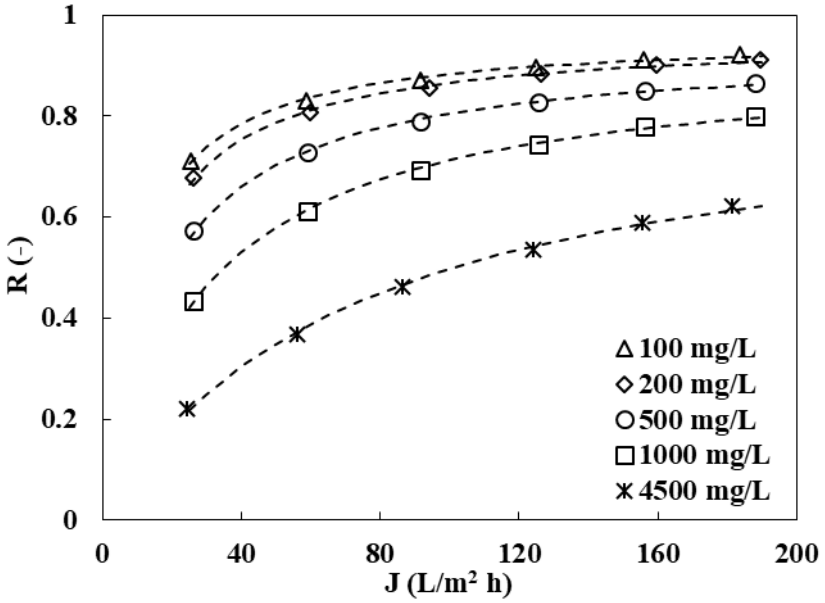

Fig. 20 Dependence of real rejection on permeate flux for AFC 30 membrane. Experimental data (points) and Spiegler–Kedem model (dashed lines).

The TMS model (see Eq. (18)) can be simplified when the transport number of cations in the free solution (α) being constant which can be calculated as 0.3954 (from Eq. (20)). When this value is inserted in the TMS model, it is further simplified to a quadratic expression. This equation is valid specifically for sodium chloride and is as follows:

$$0.9562\xi^2 + \frac{0.83712\xi}{(\sigma - 1)} + 4 - \left(\frac{2}{\sigma - 1}\right)^2 = 0 \qquad (23)$$

where ξ is the parameter which expresses the electrostatic effects and is defined as the ratio of the fixed charge density of the membrane (*X*) to the concentration of the 1–1 electrolyte (*c*).

By using the values of the reflection coefficient for each NaCl concentration, ξ can be determined using the quadratic Eq. (23). The value of the effective fixed charge density (Φ*X*) was calculated from Eq. (23) based on the reflection coefficient for each NaCl concentration. Reflection coefficient (σ) in Table 12 was calculated by Spiegler–Kedem model. Both positive and negative values were obtained for charge using Eq. (23). The negative values were used because it has physical meaning since the membrane is negatively charged.

Data seen in Fig. 20 and Fig. 21 as well as the values of the non–linear parameter χ^2 in Table 11 depict that the Spiegler–Kedem model describes very well the experimental rejection data for all NaCl concentrations considered. As can be observed in Fig. 21, the reflection coefficient (σ) decreases and the solute permeability (P) increases by increasing the salt concentration in the feed solution. This is in good agreement as the rejection gradually decreasing rejection when increasing NaCl concentrations in solutions as ascertained experimentally (Fig. 20). The Spiegler–Kedem model can estimate and describes very well the experimental results of NaCl rejection.

Table 12. Reflection coefficients (σ) and solute permeabilities (ω) determined byfittingexperimental data of NaCl rejection with Spiegler–Kedem model (AFC 30) and effective fixed charged density (ΦX).

NaCl concentration	Spiegler–Kedem model parameters		Effective fixed charge density	Quality of fitting
mg L^{-1}	σ (–)	P (L m^{-2} h^{-1})	–ΦX (mV)	χ^2
100	0.940	9.071	48.8	1.230×10^{-4}
200	0.936	10.967	87.9	9.247×10^{-5}
500	0.903	16.585	144.0	1.081×10^{-4}
1000	0.873	28.366	211.2	1.303×10^{-4}
4500	0.781	67.300	564.0	4.145×10^{-4}

The dependence of the effective fixed charge density (Φ*X*) of AFC 30 membrane can be seen in Fig. 21 which is estimated from Eq. (23) on various NaCl concentrations in the feed solution.

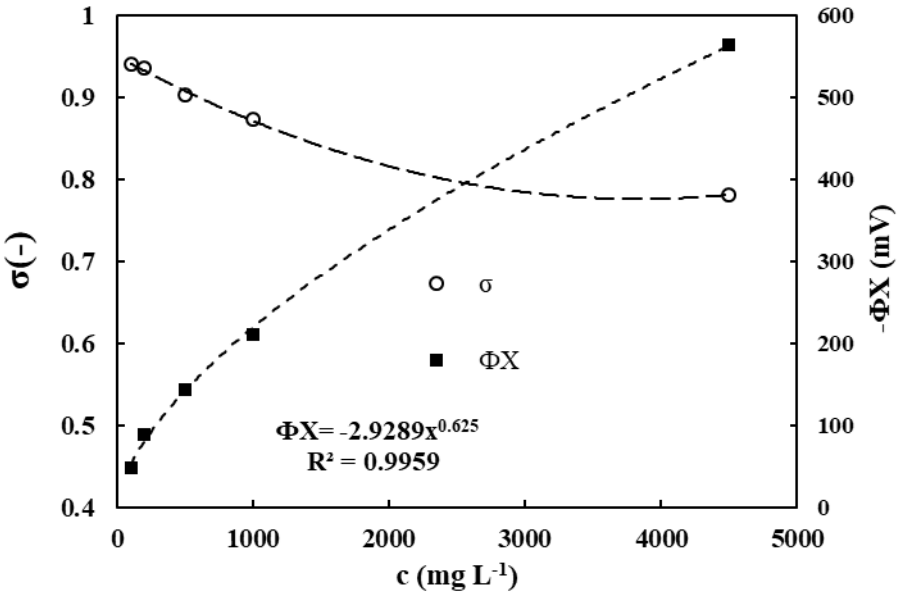

Fig. 21 Reflection coefficient and effective fixed charge density of AFC 30 membrane as a function of NaCl concentration in the feed solution. Effective charge density was fitted with Freundlich isotherm (dashed line).

It was observed that the membrane charge is strongly dependent on the concentration in the feed solution which was in contact to the membrane. The membrane charge was increasing when NaCl concentration of the solution increases. Thus, from experimental results, the increase in the negative membrane charge can be explained by adsorption of the chloride ions onto the membrane. A detailed explanation of AFC 80 membrane to estimate fixed charge density using TMS together with NaCl concentration has been performed by Gherasim et al. (2014). The authors observed that the membrane charge is strongly dependent on the concentration of the solution with which the membrane is in contact; the membrane negative charge is increasing monotonically when the NaCl concentration in the aqueous solution increases. This behaviour was attributed to the adsorption of ions from solution on the membrane surface. Other authors have noticed similar trend that can be attributed to spontaneous adsorption of ions from the solution to the membrane surface (Schaep et al., 1999; Bowen and Mukhtar, 1996; Zydney, 1997; Wang et al., 2012).

8.3 Influence of operating parameters on heavy metals separation

To select the optimum operating parameters for NF membrane, it is advisable to change operating conditions such as applied transmembrane pressure, feed concentration, cross–flow velocity, and pH. This is a useful technique used to investigate the transfer of solute as well as the separation properties of the membranes. Therefore, performing experimental works on

these operating parameters is important to predict the extent of heavy metals that can be concentrated in retentate.

8.3.1 Influence of transmembrane pressure

For a better understanding of NF membrane process, the influence of different applied transmembrane pressure on the rejection of heavy metals was investigated. This was done by carrying out rejection experiments with transmembrane pressure (5–30 bar) at constant cross–flow velocity of 1.25 m s^{-1} for both membranes (AFC 30 and AFC 80). The heavy metals to be considered are zinc sulphate ($ZnSO_4$), zinc nitrate ($Zn(NO_3)_2$), cobalt nitrate ($Co(NO_3)_2$) and nickel nitrate ($Ni(NO_3)_2$). Solutions properties (density, and viscosity) were taken from demineralized water and experimental temperature. Diffusion coefficients were used for infinite dilution. The measured pure water fluxes were similar to the fluxes for heavy metals considered at all feed concentration and for both membranes.

The increase in transmembrane pressure increases the real rejection for all feed concentrations used as seen in Fig. 22. Generally, the separation of ions at different transmembrane pressure condition can be explained by two phenomena. Firstly, an increase in transmembrane pressure leads to increase of solvent flux conversely the transport of solute in the membrane is hindered by steric and charge effect. Hence, the higher flux which leads to increase in solute rejection is because of permeate dilution. Secondly, an increase in transport of solute to the vicinity of the membrane surface is due to increase in applied transmembrane pressure which increases concentration polarization. This in turn leads to decrease in solute observed rejection by decreasing the charge effect (Seidel et al., 2002).

As observed in Fig. 22 a), the maximum real rejection of zinc sulphate was 99.3 % for AFC 30 membrane irrespective of the concentration range (50–200 mg Zn L^{-1}). At an even low transmembrane pressure of 5 bar, the real rejection was greater than 97 %. Considering AFC 80 membrane, the minimum real rejection of zinc sulphate was 98.7 % for 10 bar and maximum rejection was 99.6 % for feed concentration at 200 mg Zn L^{-1} (see Fig. 22 b)). From our results, both membranes have a good separating property for the separation of zinc sulphate from wastewater. However, the metal rejection has high value which slowly increases with increasing of applied transmembrane pressure.

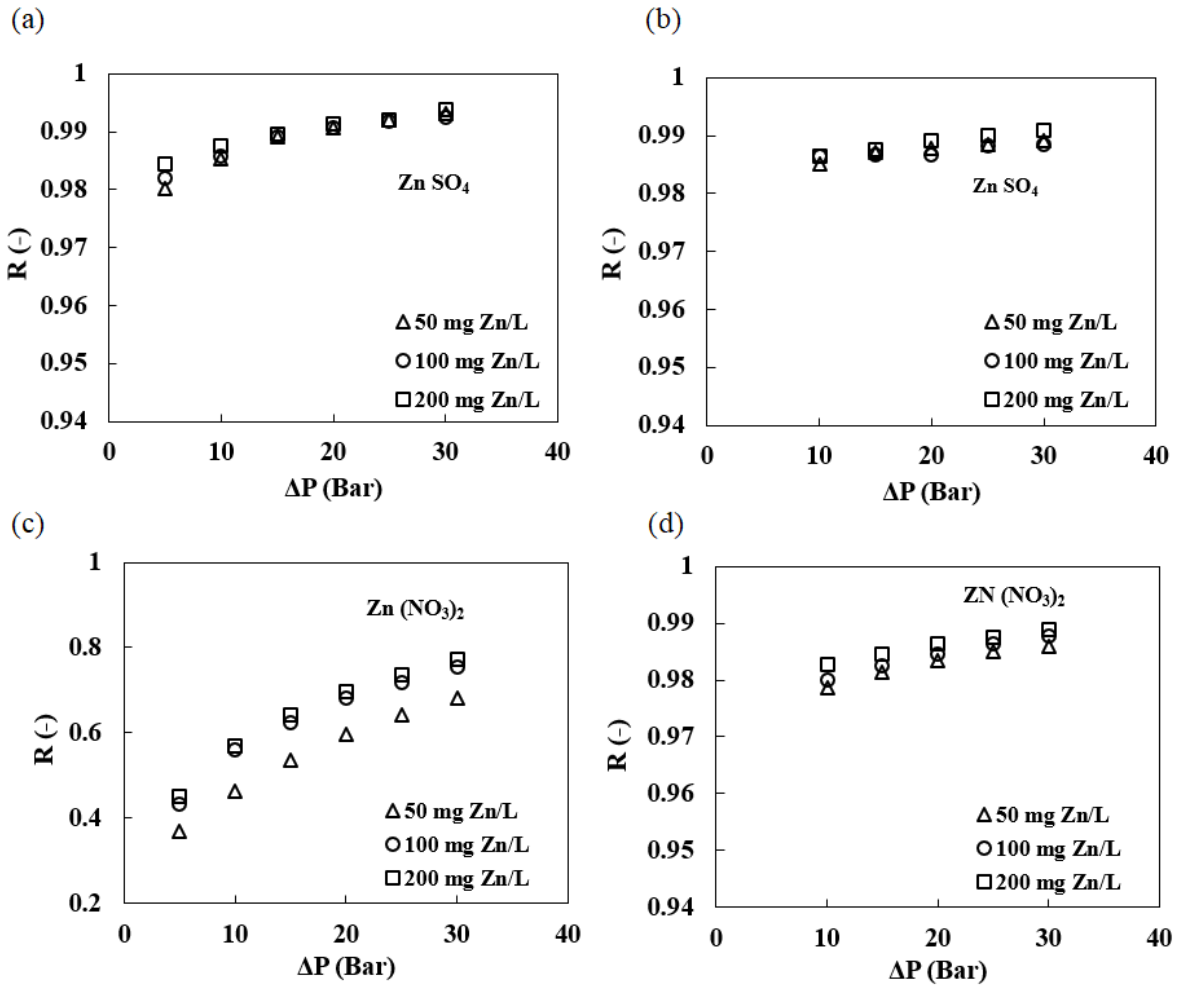

Fig. 22 Rejection of $ZnSO_4$ and $Zn(NO_3)_2$ against transmembrane pressure with different feed concentrations. AFC 30 membrane – a) and c), AFC 80 membrane – b) and d).

Regarding Fig. 22, it was found that increasing of transmembrane pressure increases the rejection of zinc nitrate for both membrane (AFC 30 and AFC 80). Even at low transmembrane pressure (10 bar) for AFC 80 membrane, the rejection was 97.7 % at 50 mg L^{-1} of feed concentration. But with AFC 30 membrane, rejection of zinc nitrate was observed to be 38.8 % at 5 bar (see Fig. 22 c)). Considering both membranes, it was concluded that AFC 80 membrane (as seen in Fig. 22 d)) is suitable for separating zinc nitrate from wastewater. From Fig. 22, zinc sulphate rejection is better than zinc nitrate for both membranes (AFC 30 and AFC 80). The order of rejections is as follow $Zn(SO_4)_{(AFC\ 80)}$ > $ZnSO_{4\ (AFC\ 30)}$> $Zn(NO_3)_{2\ (AFC\ 80)}$ >$Zn(NO_3)_{2\ (AFC\ 30)}$. It could be explained that both membranes have better rejection for the anions (in our case sulphate) than nitrate. Similar studies on the difference of rejection with transmembrane pressure have been reported by various authors (Gherasim and Mikulášek, 2014; Mikulášek and Cuhorka, 2016; Sablani et al., 2001).

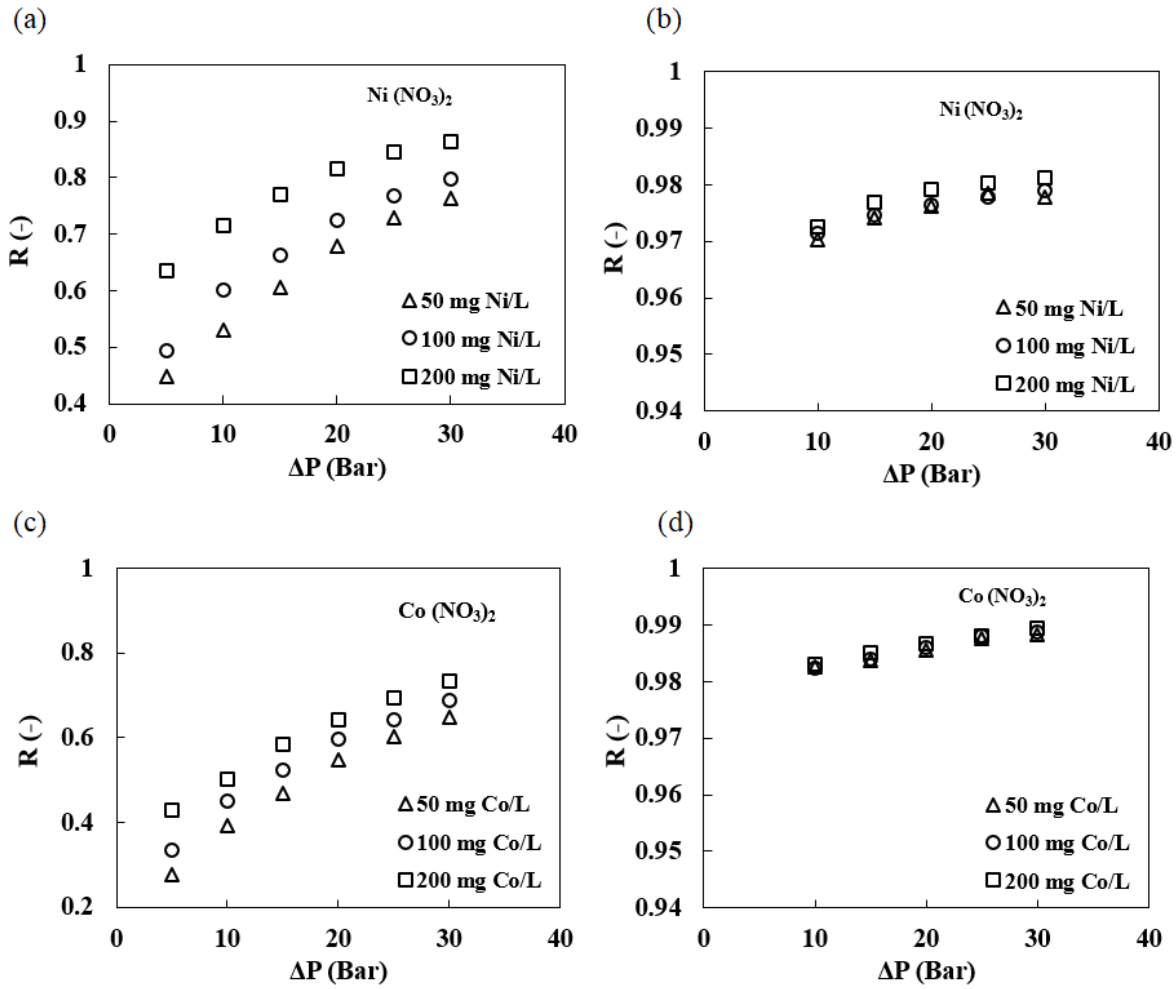

Fig. 23 Dependency of real rejection on transmembrane pressure for $Ni(NO_3)_2$ and $Co(NO_3)_2$ by both AFC 30 – a) and c), and AFC 80 – b) and d) membrane at different feed concentration.

Some remarks can be made based on the results of the transport mechanism of solutes in NF membrane process. As can be seen in Fig. 23, increase in transmembrane pressure gradually increases the rejection of all heavy metals for both membranes. The minimum rejection for nickel and cobalt ions for AFC 30 membrane was below 50 % and was above 25 % at 5 bar respectively (see Fig. 23 a) and c)). In addition, the maximum rejection of nickel nitrate was 98.6 % compared to cobalt ions of 98.9 % respectively for AFC 80 membrane. Considering AFC 80 membrane, the maximum rejection was 98.7 % which shows that the membrane has a better property than AFC 30 membrane in terms of separating nickel nitrate from wastewater. Even, the minimum rejection was above 98 % for all feed concentration (50–200 mg Ni L^{-1}) at 10 bars. Also, it was found that AFC 80 membrane is denser and has higher rejection at minimum transmembrane pressure than AFC 30 membrane. An increase in solvent flux when increasing the applied transmembrane pressure leads to increase in the solute rejection which could be attributed to dilution effect (Bowen et al., 1997; Paugham et al., 2004). Also, AFC

80 membrane has higher rejection of nickel and cobalt ions than AFC 30 membrane due to steric effect. This is because AFC 30 has larger pores than AFC 80 membrane which allow ions to pass through more easily. Similar results of rejection against transmembrane pressure were reported in several studies (Bouranene et al., 2008; 2009, Basaran et al., 2015; Gherasim et al., 2015).

8.3.2 Influence of feed concentration

The rejection performance of both membranes (AFC 30 and AFC 80) in the feed concentration range (50–200 mg L^{-1}) can be seen in Fig. 24 and Fig. 25. Feed concentration is very important parameter during separation as it directly affects efficiencies of the membranes. It can be observed that the rejection is improved when the feed concentration is increased for all heavy metals considered. This behaviour is usually not common because the concentration polarization and the shielding of the membrane charge at high concentrations decreases the rejection rate (Gherasim et al., 2015). It was observed in Fig. 24 that the rejection of zinc sulphate was higher than zinc nitrate with increasing feed concentration for both membranes. In our case, the other heavy metal rejection (nickel nitrate and cobalt nitrate) increase with feed concentration since AFC 80 is denser than AFC 30 membrane. Therefore, AFC 80 membrane rejection is higher than AFC 30 membrane for heavy metals such as nickel nitrate and cobalt nitrate (see Fig. 25). Comparable results were obtained by several authors (Ahn et al., 1999; Seidel et al., 2002; Sablani et al., 2011; Koter, 2006; Mikulášek and Cuhorka, 2016; Cuhorka et al., 2020). Gherasim and Mikulášek (2014) explained that the decrease in lead rejection when increasing the feed concentration could be mainly by the reduced solvent transport due to the increasing in osmotic effects. Paugham et al. (2004) attributed the decrease of nitrate rejection to the characteristics of the charged membrane which is by the shielding phenomenon. This involves increasing formation by the cations of the screen which gradually neutralises the negative charge of the membrane. In addition, the rejection increases at low concentration because the screen effect is very weak with the repulsion of anions playing a significant role in the process. Bouranene et al. (2008) reported that the decrease of the rejection when increasing the lead and cobalt concentration of AFC 30 membrane was not strongly influenced by the ionic concentration but was mainly steric hindered. In our case, heavy metals rejection increases with feed concentration. Bowen and Welfoot (2002) explained the increasing of $MgCl_2$ rejection with increasing feed concentration which can be because of decrease in the normalized negative charged density of the membrane with increasing electrolyte concentrations. In another studies, Seidel et al.

(2002) attributed the enhancing rejection with increasing concentration to the presence of more permeable ions of like charge that preferentially permeate through the membrane.

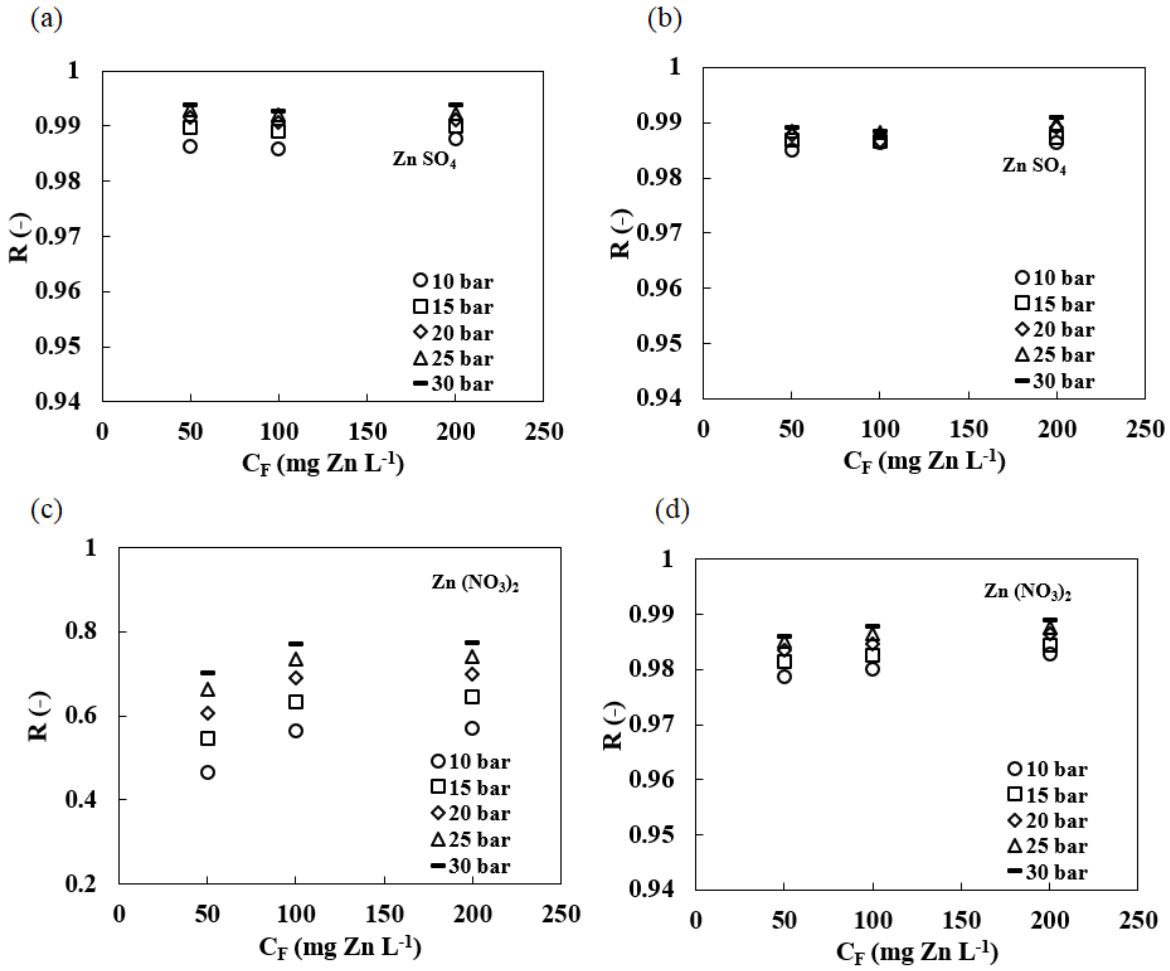

Fig. 24 Rejection of $ZnSO_4$ (a) and b)) and $Zn(NO_3)_2$ (c) and d)) for AFC 30 (left pictures) and AFC 80 (right pictures) as a function of various feed concentration.

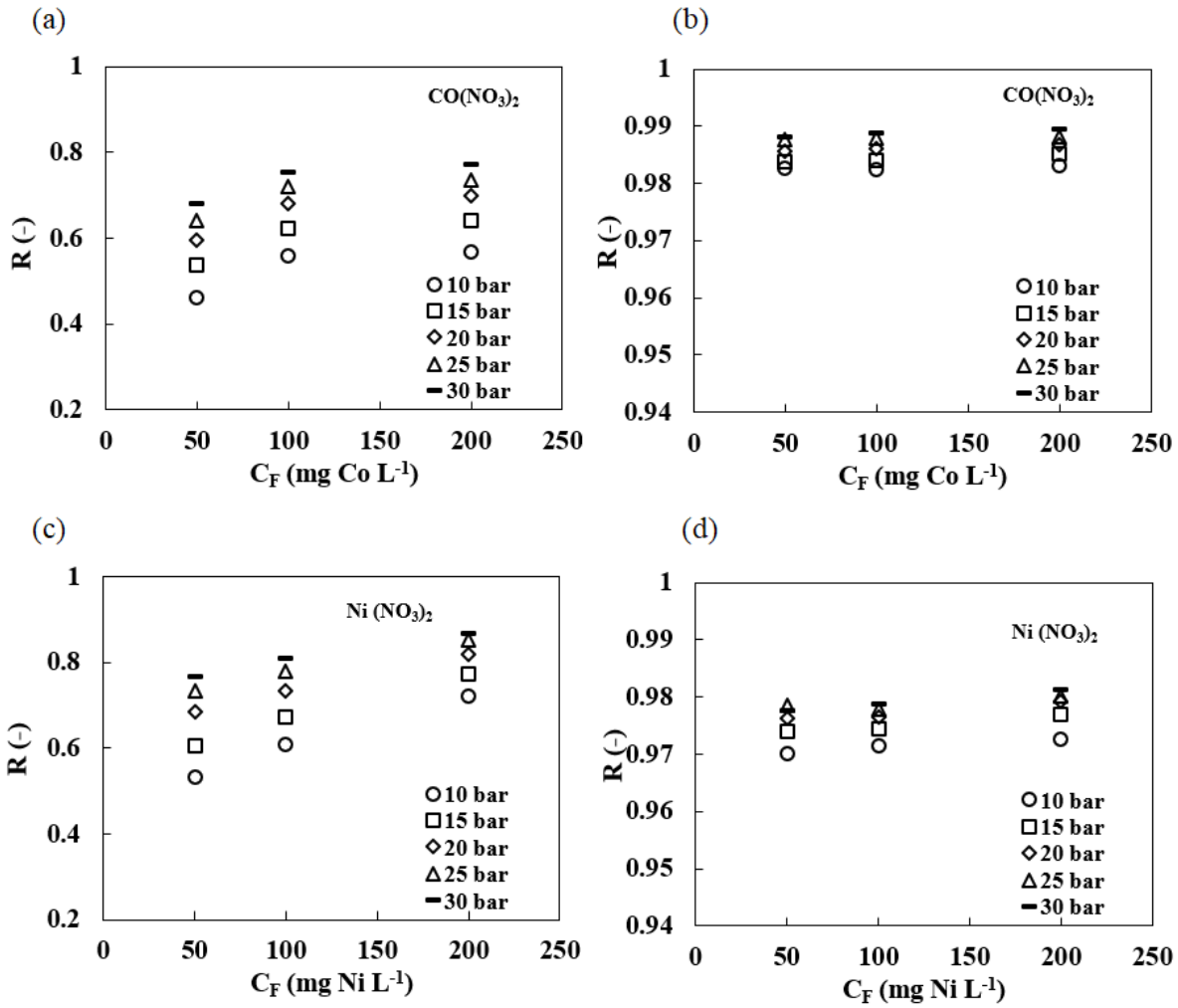

Fig. 25 Dependency of rejection on feed concentration. ($Co(NO_3)_2$) (upper pictures) and ($Ni(NO_3)_2$) (lower pictures) for AFC 30 (left pictures) and AFC 80 (right pictures) membrane.

8.3.3 Influence of pH

One of the important parameters of the NF membrane process is the pH of the solution. The pH of the feed influences the membrane charge and then the rejection properties of NF membrane. The type of chemical structure of the membrane material determines the membrane charge. Change of charge is due to dissociations of the functional group of the membrane material or adsorption of charge polarizable solutes (cations or anions) from the solution (Bouranene et al., 2009; Gherasim et al., 2013). However, enough information is not provided by the manufacturer about the membrane charge which can be useful in characterization of a membrane. Both AFC 30 and AFC 80 membrane used have a polyamide top layer and amphoteric character. The partial hydrolysis of polyamide leads to formation of ammonium ($–NH_3^+$) and carboxyl (–COOH) groups. When the membrane is below the IEP, the carboxyl groups are dissociated, and the amino groups are protonated, and the membrane charge is positive. On the other hand, when the membrane is above the IEP the carboxyl

groups are dissociated and the membrane is charged negatively. Szymcyzk et al. (2007) performed experiment with KCl solution and found out that IEP of AFC 30 membrane was at pH about 5.3. The same behaviour was found for AFC 80 membrane. Gherasim et al. (2013) performed experiment with solution of $Pb(NO_3)_2$ and found out that the IEP of AFC 80 membrane was shifted from pH of 3.6 to a higher value of about 5.7. This behaviour could be explained due to the adsorption of lead ions on the membrane surface which can switch the membrane charge from negative to positive in the range of pH 4–6 (Bouranene et al., 2008).

The influence of pH on rejection was considered for feed solution of 50 mg Zn L^{-1} with pH (5.3, 6.0, 6.5) adjusted by H_2SO_4. From our result (see Table 13) it was observed that zinc rejection of AFC 30 membrane was very high for all pH range considered. Rejection slightly increases with increasing in pH value. At isoelectric point with pH 5.3, the membrane is neutral which makes a solute rejection of 96.8 % at 30 bars. In addition, AFC 30 membrane has pores (0.374 nm) which are larger than Stokes radii of zinc and sulphate ions. Stokes radii are 0.348 nm and 0.229 nm for zinc and sulphate, respectively. Comparing the pores radius of AFC 30 membrane to that of Stokes radii of the ions, we can deduce that the zinc ions will be retained more than sulphate ions. This shows that AFC 30 membrane is governed by steric hindrance in our case otherwise; the reverse order would be expected. It can be expected that the steric effect plays a major role in rejection with respect to the electric interaction (Mehdipour et al., 2015). When the pHs (6.0 and 6.5) are above IEP, the carboxyl groups are dissociated and the membrane becomes more negatively charged which increases the rejection of anion and reaching electroneutrality condition, zinc is retained too. The maximum rejection of 98.7 % was reached at the highest value of pH at 30 bars. This behaviour could be explained by a decrease in pore size dimension when the membrane is charged by the increased repulsion between the charged functional groups of the membrane (Childress and Elimelech, 2000). In our case, the electrostatic repulsion that occurs between sulphate and charged membrane in turn increases the rejection rate with increase in pH (see Fig. 26).

Concerning AFC 80 membrane, Mikulášek and Cuhorka (2016) researched on the effects of pH (3.0 and 5.7) on lead nitrate at 50 mg Pb L^{-1}. It was observed that AFC 80 has smaller pores and therefore the steric effects will play more important role in the rejection than electric effects. The rejection of lead for AFC 80 was very high and more than 98 % for almost both pH values investigated. It was concluded that the membrane rejects predominantly the lead ions due to the steric effects determined by the hindered transport of ions in small pores of about 0.246 nm. The same explanation could be used when comparing

the different Stokes radii of our heavy metals (see Table 13) to that of the AFC 80 membrane found in Table 7.

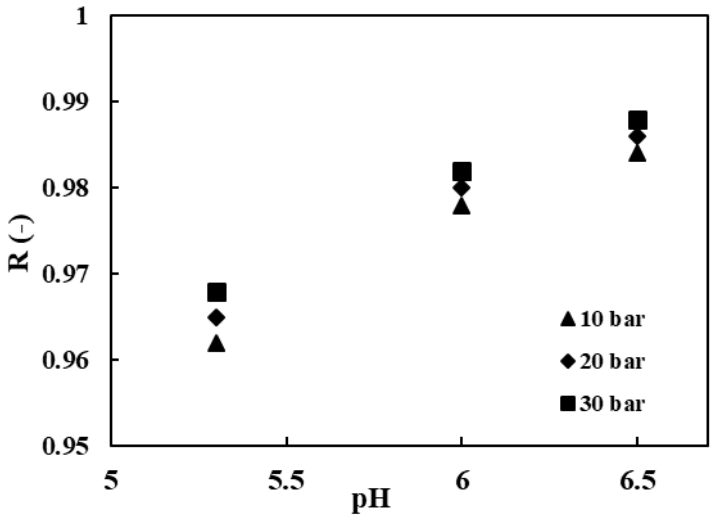

Fig. 26 Observed rejection against pH for $ZnSO_4$ feed solution with concentration of 50 mg Zn L^{-1} at different applied transmembrane pressure for AFC 30 membrane.

Table 13. Observed rejection at different value of pH for AFC 30 membrane

	ΔP (bar)		
pH (–)	**10**	**20**	**30**
	Rejection (–)		
5.3	96.2	96.5	96.8
6.0	97.8	98.0	98.2
6.5	98.4	98.6	98.7

8.3.4 Influence of cross–flow velocity

One of the major drawbacks in NF membrane separation is the concentration polarization phenomenon. This phenomenon reduces the membrane performance process by increasing the osmotic pressure at the membrane surface due to the accumulation of retained solutes near the membrane on the high–pressure side. During the process, the concentration of solutes at the membrane surface is higher than in the bulk of the feed. A boundary layer is builds up because of the equilibrium established between the transport of solutes towards the membrane by convection and the slower back diffusion of the retained species. The concentration polarization phenomenon affects the flux, the rejection, and the fouling of the membranes

which limit in the application of NF treatment of highly feed concentration side (Gherasim et al., 2015; Bowen et al., 1997; Bowen and Mukhtar, 1996; Sablani et al., 2001).

The influence of the cross–flow velocity was investigated and applied with the aim to create a high shear condition at the surface of the membrane (Bian et al., 2000). The feed velocity through the tubular NF membrane was set at 0.420, 0.833, and 1.250 m s^{-1} with concentration of feed solution chosen for these experiments as 100 mg Zn L^{-1} (zinc sulphate and zinc nitrate). Real and observed rejections were calculated using Eqs. (1) – (8). For calculation of real rejections, the solution properties (density and viscosity) were considered as identical to those of pure water which is valid for dilution solutions.

The difference between the observed and real rejections decreases when increasing the cross–flow velocity as seen in Fig. 27. The equivalent calculated Reynolds numbers from the cross–flow velocities of 0.420, 0.833 and 1.250 m s^{-1} are 5,890, 11,670, and 17,500, respectively. The calculated Reynolds numbers are greater than 2,300 at all cross–flow velocity which guarantee a turbulent flow in the membrane module (AFC 30) under investigation. By using Eq. (8), diffusion coefficient (D) of zinc nitrate and zinc sulphate was calculated as 2.51×10^{-6} and 8.47×10^{-6} m^2 s^{-1}, respectively. The mass transfer coefficients of zinc nitrate and zinc sulphate in the polarization layer (k) were calculated using Eq. (7). Table 14 shows the values of mass transfer coefficient of both zinc sulphate and zinc nitrate at different cross–flow velocity. It can be observed that the mass transfer coefficient increases as the cross–flow velocity increase as described by the Sherwood relationship in Eq. (6).

Table 14. Mass transfer coefficients at various cross–flow velocities

Cross–flow velocity	**Mass transfer coefficient**	
	Zinc nitrate	**Zinc sulphate**
m s^{-1}	$k \times 10^{-5}$ m^2 s^{-1}	
0.420	1.05	2.47
0.833	1.94	4.57
1.250	2.78	6.52

(a)

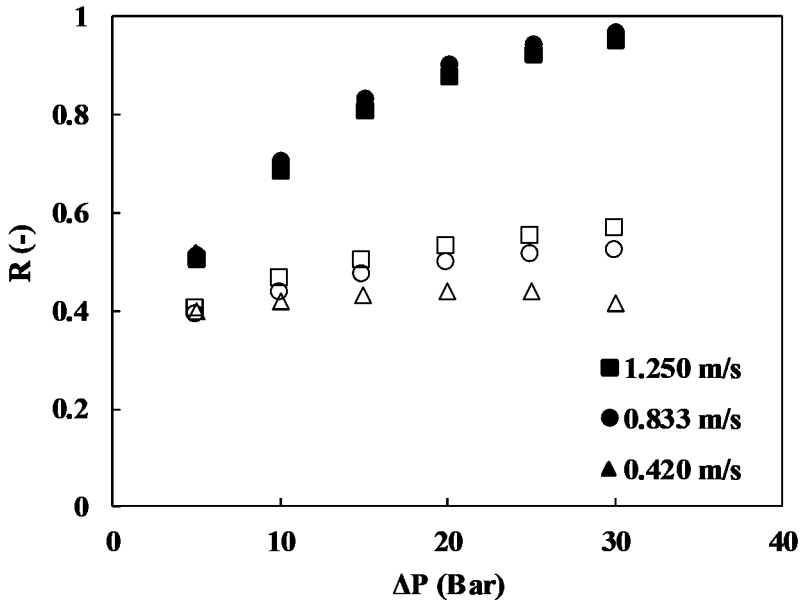

(b)

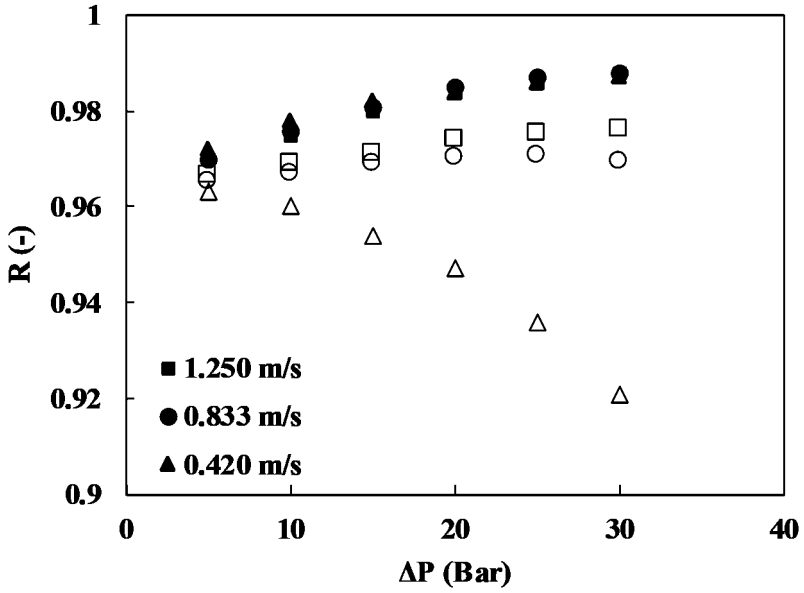

Fig. 27 Rejection of AFC 30 membrane as a function of cross–flow velocity – a) zinc nitrate, b) zinc sulphate; (observed rejections–empty symbols, real rejection–full symbols).

As described in Fig. 27 (b), real rejection increases with increase in permeate flux at constant cross–flow velocity. Furthermore, as the cross–flow velocity of the feed solution increases, the difference between observed and real rejection decreases. At the lowest cross–flow velocity of 0.42 m s^{-1}, the observed rejection decreases when increasing the applied transmembrane pressure (see Fig. 27). This could be explained that more solutes (in our case zinc sulphate and zinc nitrate) are transported to the membrane by convection as the transmembrane pressure increases and eventually accumulates near the membrane. Due to the low cross–flow velocity, the concentration polarization increases and decreases the observed rejection significantly. Differences in observed and real rejection give clear indication that the

concentration polarization effect decreases when increasing the cross–flow velocity. From Table 14, it was observed that the mass transfer coefficient in the polarization increases when increasing the feed cross–flow velocity rate from 0.42 to 1.25 m s^{-1}. The reason for the increase in the mass transfer coefficient in the polarization layer is because of the decrease in the thickness of the boundary layer in the membrane surface when increasing the cross–flow velocity. From our results obtained, we can possibly conclude that enhancing the hydrodynamics by increasing the cross–flow velocity decreases the concentration polarization of AFC 30 membrane. This will lead to increasing of rejection and permeate flux. The maximum real rejection of both zinc nitrate and zinc sulphate (see Fig. 27) are above 95 % which proves that the membrane has a good property for the separation of heavy metals. The minimum real rejection of zinc nitrate was about 52 % compared to 97 % of zinc sulphate.

Regarding AFC 80 membrane, Gherasim and Mikulášek (2014) studied the influence of cross–flow velocity on the removal of heavy metal by nanofiltration. The authors found that the metal rejection (250 mg Pb L^{-1} at pH 5.8) slightly increases with increase in feed cross–flow velocity. The increase of rejection was explained by differences in concentration polarization and mass transfer coefficient. Liu et al. (2011) revealed that an increase in the cross–flow velocity would lead to an increase in the equilibrium permeate flux for the NF and hence increase the rejection. They observed that the increase in the stabilized permeate flux at increasing cross–flow velocity is likely caused by the decrease in concentration polarization and foulants adsorption on membrane surface. However, the permeate flux increase as a function of cross–flow velocity for the NF membrane. In another research, Choi et al. (2005) explained increase in cross–flow velocity increases the permeate flux due to the increase in solute back–transport to the bulk solution. The authors further explained that increasing the cross–flow velocity will decrease the flux decline and solutes accumulation by sweeping away the solute from the membrane surface. Several authors had similar results when increasing the cross–flow velocity (Gherasim et al., 2015; Koo et al., 2014).

8.4 Effect of solution composition

It is important to note that the solution composition play a significant role during rejection of ions. The rejection of ions mostly depends on several factors during separation process. Such factors are ion concentration, valence, and chemical nature of components along with membrane surface charge and charge density. To fully understand the separation mechanism, it is of foremost importance to know the effect of anions and cations on the membrane surface charge and its relation to chemical nature of the solution (Batels et al., 2015). Experiment was

conducted for both AFC 30 and AFC 80 membrane being negatively charged exhibited different rejection behaviours at similar feed conditions to investigate the solution composition. The effects of cations and anions were examined for both membranes. The different cations having the same anions considered in our case are as follow; zinc nitrate ($Zn(NO_3)_2$), cobalt nitrate ($Co(NO_3)_2$) and nickel nitrate ($Ni(NO_3)_2$). Also, same cation with the different anions are zinc sulphate ($ZnSO_4$) and zinc nitrate ($Zn(NO_3)_2$).

8.4.1 Effect of cations

The nanofiltration membranes (AFC 30 and AFC 80) being investigated is negatively charged and have different rejection behaviours at similar feed conditions. In our case, the cations are having the same anions as nitrate. The heavy metals considered are zinc nitrate ($Zn(NO_3)_2$), cobalt nitrate ($Co(NO_3)_2$) and nickel nitrate ($Ni(NO_3)_2$). It was observed from the two membranes that AFC 80 membrane has a better rejection than AFC 30 membrane. The reason being that AFC 80 membrane is denser than AFC 30 membrane.

The sequence of AFC 80 membrane interfering cations with the same anions on the rejection was Co^{2+}> Zn^{2+}> Ni^{2+} as observed in Fig. 22 d), Fig. 23 b), and Fig. 23 d) when considering these three different divalent cations with the same type of anions (NO_3^-). We can deduce that rejection is a very complex mechanism where the cations types, cations concentration, membrane charge could play their perspective role among other factors during separation process (Qadir et al., 2017). Also, difference of cations with equal valences is always associated to hydration energies of cations and their hydrated radii (Gherasim et al., 2013; Mehiguene et al., 1999; Paugham et al., 2004; Mehdipour et al., 2015), and diffusivities of ions (Bouranene et al., 2008; Al–Rashdi et al., 2013). From Table 3, the order of cations considering the hydration radii is as follows: Co^{2+}< Zn^{2+}< Ni^{2+}. Considering the order of hydrated radii, we can observe that hydration radii do not play any key role in the rejection of cations since the order shows the opposite rejection with the same anions. Another reason of the rejection order can be attributed by comparing the coefficients of diffusion of different cations in the solution (see Table 15). The order of coefficient of diffusion is Co^{2+}> Zn^{2+}> Ni^{2+}. Since Co^{2+} has the highest diffusivity and rejection of all cations, we could conclude that the electromigration effect against a negative potential gradient is more dominant than the convective and diffusive effects (Bowen et al., 1997).

The order of rejection of ions for AFC 30 membrane are Ni^{2+} >Zn^{2+} > Co^{2+} (see Fig. 22 and Fig. 23). In our case, we have different cations with equal valences which are always related to hydration energies of cations, hydrated radii, and diffusivities of ions. From Table 15, the

order of cations with respect to hydrated radii are as follows; Ni^{2+} >Zn^{2+} > Co^{2+} which proves that Co^{2+} has the smallest value. The results show that the smallest size hydrated cation can be transported through the membrane. The results of AFC 30 membrane should be opposite to AFC 80 membrane in terms of rejection. The electric effect will play a significant role in rejection of AFC 30 with respect to steric effects. The pores of the membrane (0.374 nm) are much larger than those of Stokes radii of heavy metals in our case (Bouranene et al., 2009). Another explanation of sequence of rejection could be the diffusivities coefficient of cations. As can be seen in Table 15, the order was Co^{2+} >Zn^{2+} > Ni^{2+}. From our results, Co^{2+} has lower rejection because it could pass through the membrane easily due to its higher diffusion rate. It was observed that when the hydration radii decrease, the convection flow increases which turns to decrease the rejection. Also, as the diffusion coefficient increases, it increases the diffusion flow as the rejection rate decreases (Mehdipour et al., 2015).

Table 15. Diffusion coefficient, hydration radii and hydration energy of ions (Mehdipour et al.,2015)

Ion	$D_{i,\infty} \times 10^{-9}$ ($m^2 s^{-1}$)	R_H (nm)	Hydration energy (kJ mol^{-1})
Ni^{2+}	0.616	0.371	–2096
Zn^{2+}	0.703	0.348	–2047
Co^{2+}	0.732	0.335	–2010
NO^{3-}	1.902	0.128	– 314
SO_4^{2-}	1.065	0.229	–1047

8.4.2 Effect of associated anions

The effect of co–ions such as sulphate and nitrate were investigated for both membranes (AFC 30 and AFC 80). The rejection of ions was enhanced when the charged of the associated ions increased which indicate that the surface forces are stronger when divalent anions are present. The rejection was increased by increasing the valence of a co–ion (in our case, anion) due to the growing repulsion between the membrane surface and higher valence ions. Since the valency of sulphate is higher than that of nitrate, the highest rejection for both membranes was above 99 % for $ZnSO_4$ irrespective of the different cations being considered (Mehiguene et al., 1999; Childress and Elimelech, 2000). It could be explained that anions with higher valence are easily rejected than the lower valence anions. This is because of the less repulsion forces pushing away the anions from membrane surface which is negatively charged. In our case, the membrane is negatively charged and the anion with higher valency (sulphate) had higher rejection than that of lower valences (nitrate). Indeed, the charge of the

membrane is important to membrane performance because charge affects the electrostatic repulsion between the ions or charged molecules and the membrane surface (Childress and Elimelech, 2000). This behaviour of anions in charged membrane was explained by many authors as Donnan exclusion phenomenon (Qadir et al., 2017; Mehdipour et al., 2015). By considering $ZnSO_4$ and $Zn(NO_3)_2$, hydration energy plays an important role in the separation process. The nitrate ions for both membranes were compared to that of sulphate ions. It was found that the nitrate ions are less hydrated than the sulphate ions (314 and 1047 kJ mol^{-1} for nitrate and sulphate, respectively as seen in Table 15) resulting in less rejection with cations of nitrate ions. Similar results were achieved by different authors (Ballet et al., 2004; Murphy and Chaudhari, 2009; Garba et al., 2003).

As seen in Fig. 24 and Fig. 25, the order of rejection of ions for AFC 80 was $ZnSO_4$ > $Co(NO_3)_2$ > $Zn(NO_3)_2$ > $Ni(NO_3)_2$. This order was observed because the divalent anions (SO_4^{2-}) was strongly rejected by the negatively charged functional groups of membrane compared to monovalent anions (NO_3^-) for different cations (Co^{2+}, Zn^{2+}, Ni^{2+}). Nevertheless, the cations are rejected to ensure electro neutrality at both sides of the membrane. Another possible explanation is that by considering of $ZnSO_4$ and $Zn(NO_3)_2$, the differences in rejection was not affected by the same cations but rather different anions in our case. It was found that the hydration radii are principal factor that influence the selectivity of a nanofiltration membrane. The hydration radii of SO_4^{2-} and NO_3^- are 0.229 and 0.128 nm, respectively, as seen in Table 15. The sulphate ions are retained more than nitrate as the hydration radius was greater than nitrate. This means that the nitrate will permeate through the membrane since the radius was smaller than the pore radius (0.246 nm). Therefore, sulphate ions will be retained more than nitrate comparing to the pore radius. The results obtained show that the transport of solute was due to the steric effects. The rejection sequence can be determined by comparing the diffusion coefficient of different anions too. The order of diffusion coefficient of anions was NO_3^- > SO_4^{2-} in water at 25 ^oC (see Table 15). It was assumed that the diffusion of coefficient in the membrane can be approximated to that in the aqueous water. From Table 15, the higher diffusion coefficient will increase the diffusion flow through both membranes. For this reason, decreased rejection of anions (in our case NO_3^-) can be approximated by diffusion coefficient in aqueous solutions (Mehdipour et al., 2015).

8.5 Modelling of heavy metals rejection

8.5.1 Spiegler–Kedem model (SKM)

The experimental rejections were fitted with the Spiegler–Kedem model to give more information about the membranes used (AFC 30 and AFC 80). The experimental data together with the model prediction can be seen in Table 16 and Table 17. In addition, Fig. 28 and Fig. 29 depict rejection against transmembrane pressure for various feed concentrations of heavy metals considered for both membranes. The heavy metals considered were zinc sulphate, zinc nitrate, cobalt nitrate, and nickel nitrate.

From Fig. 28, it was observed that the model shows high accuracy in comparison to the experimental data of heavy metals rejection for all feed concentration considering AFC 30 membrane. The high rate of reflection coefficients (σ) and low solute permeability (P) were estimated by fitting the experimental data with the Spiegler–Kedem model. The model of rejection of heavy metals agree to the experimental rejection which can be confirmed by quality of fittings presented in Table 16.

Table 16. Reflection coefficients (σ) and solutes permeabilities (P) obtained by fitting of experimental data using the Spiegler–Kedem model for AFC 30 membrane

Solute	Concentration (mg L^{-1})	Reflection coefficient σ (–)	Solute permeability P (L m^{-2} h^{-1} bar^{-1})	Quality of fittings (χ^2)
Zinc sulphate	50	0.997	0.82	1.58×10^{-6}
	100	0.995	1.20	2.05×10^{-7}
	200	0.993	1.36	1.42×10^{-7}
Zinc nitrate	50	0.875	21.70	3.92×10^{-2}
	100	0.926	15.20	4.81×10^{-3}
	200	0.952	8.10	1.59×10^{-2}
Nickel nitrate	50	0.773	24.34	1.24×10^{-2}
	100	0.807	20.23	1.06×10^{-3}
	200	0.857	11.29	7.43×10^{-4}
Cobalt nitrate	50	0.753	51.92	6.51×10^{-3}
	100	0.796	44.02	1.38×10^{-3}
	200	0.827	23.97	8.49×10^{-3}

As can be seen in Table 16, when the feed concentration increases the reflection coefficients gradually decrease and the membrane permeabilities slightly increases for zinc sulphate only.

In the case of the rest of the heavy metals (zinc nitrate, cobalt nitrate, and nickel nitrate) considered, an opposite trend was found (see Table 16). The reflection coefficients increase whiles the solute permeability decreases when increasing the feed concentration of zinc nitrate, cobalt nitrate, and nickel nitrate. Increasing of reflection coefficient can be explained by more convention transport of nitrates compared to sulphates, which are separated directly by steric mechanism and transport is mainly due the diffusion. The convection transport was influence by absorption of ions in membrane pores (in the case of nitrates) and it increase the reflection coefficient (or in similar meaning limiting rejections at infinite high flux). This can lead to some type of "fouling".

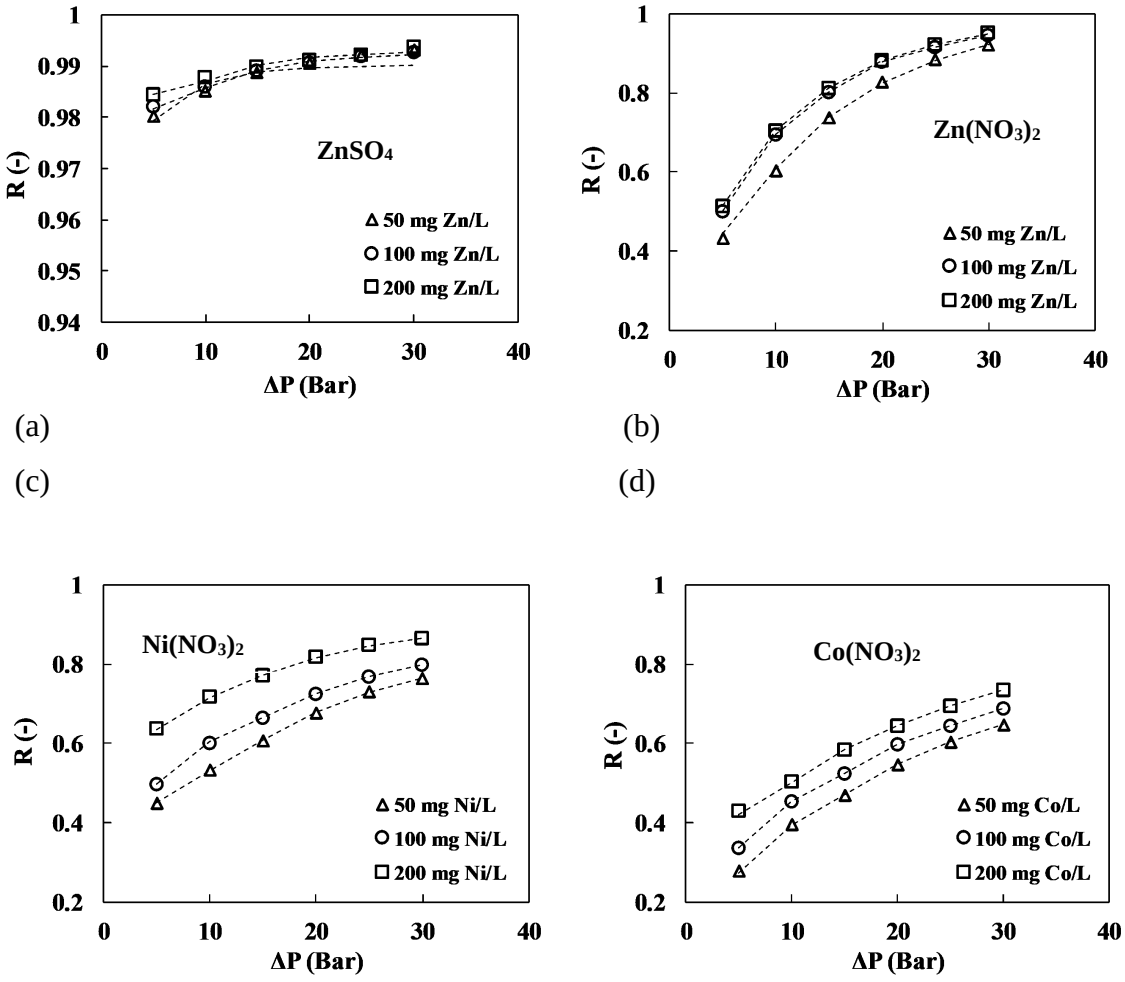

Fig. 28 Rejection as a function of transmembrane pressure for various feed concentrations for AFC 30 membrane (a) zinc sulphate (b) zinc nitrate (c) nickel nitrate (d) cobalt nitrate.

For AFC 80 membrane, the reflection coefficients (σ) decreases as the solute permeability (*P*) increase for all heavy metals considered (see Table 17). From Fig. 29 (a), the results achieved

by AFC 80 membrane were similar to that of sulphate ions (see Fig. 28 (a)) in the case of AFC 30 membrane. Here all ions were retained by steric mechanism (very low permeabilities) by membrane and transport was mainly due to diffusion. It was found that the experimental values fit very well with the model. Mikulášek and Cuhorka (2016) studied the removal of lead nitrate with different feed concentration (25, 150, 400 mg Pb L^{-1}) from aqueous solution. The authors fit the experimental data with the Spiegler–Kedem model. It was observed that the reflection coefficients slightly decrease as the feed concentration increases, thus predicting a decrease in the rejection with increase in feed concentration. Similar results were obtained by several authors (Abdullah et al., 2019; Gherasim et al., 2015; Gherasim and Mikulášek, 2013). Therefore, the Spiegler–Kedem model can explain and predict NF process of heavy metals by both membranes over a wide range of concentration.

Table 17. Reflection coefficients (σ) and solutes permeabilities (P) obtained by fitting of experimental data using the Spiegler–Kedem model for AFC 80 membrane

Solute	**Concentration (mg L^{-1})**	**Reflection coefficient σ (–)**	**Solute permeability P (L m^{-2} h^{-1} bar^{-1})**	**Quality of fittings (χ^2)**
Zinc sulphate	50	0.995	0.129	2.32×10^{-6}
	100	0.992	0.157	1.83×10^{-6}
	200	0.991	0.175	2.47×10^{-6}
Zinc nitrate	50	0.995	0.355	8.05×10^{-5}
	100	0.992	0.368	1.33×10^{-5}
	200	0.985	0.385	2.59×10^{-5}
Nickel nitrate	50	0.983	0.258	7.79×10^{-6}
	100	0.980	0.302	4.20×10^{-6}
	200	0.979	0.343	7.19×10^{-5}
Cobalt nitrate	50	0.994	0.234	5.40×10^{-5}
	100	0.992	0.252	4.56×10^{-6}
	200	0.989	0.279	1.17×10^{-5}

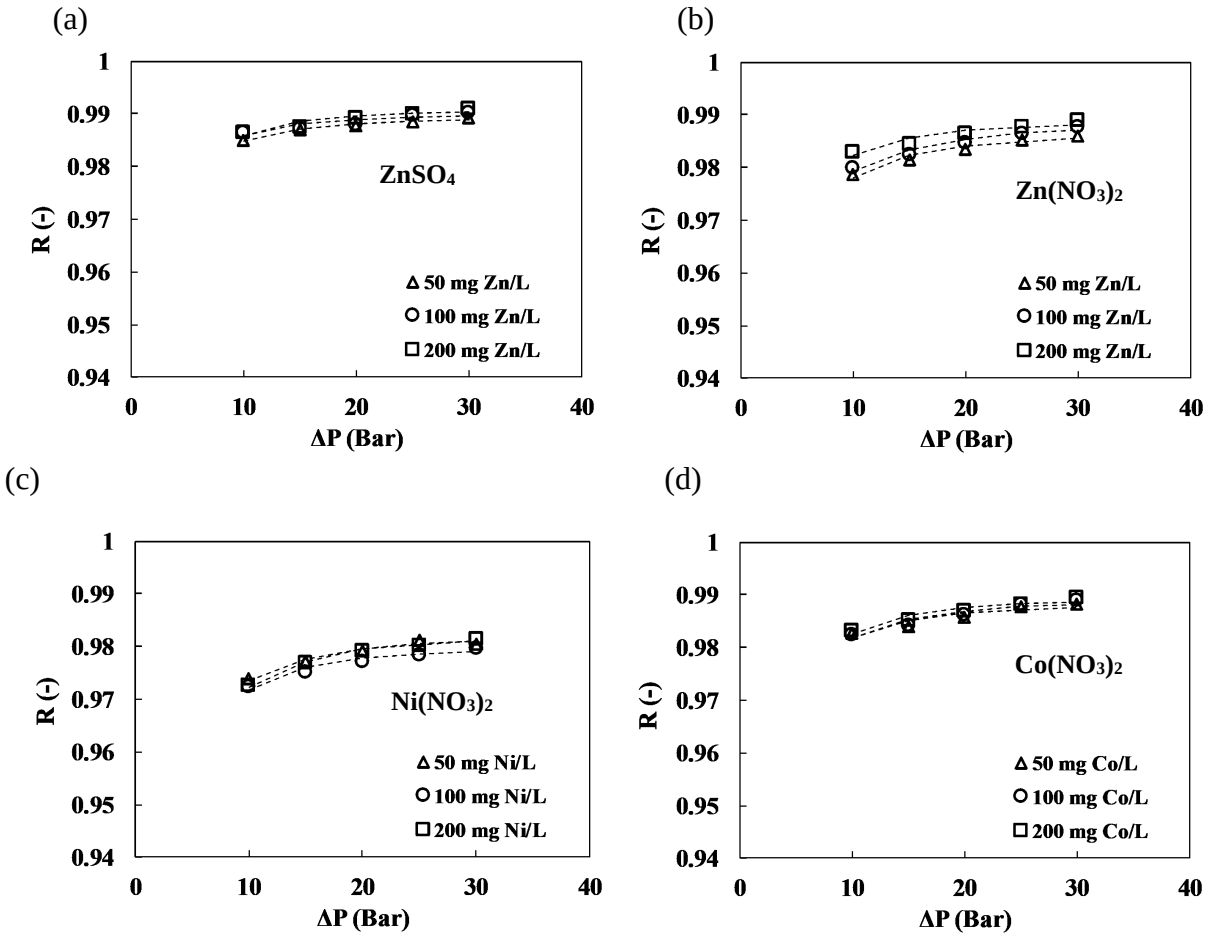

Fig. 29 Rejection as a function of transmembrane pressure for various feed concentrations for AFC 80 membrane (a) zinc sulphate (b) zinc nitrate (c) nickel nitrate (d) cobalt nitrate.

8.5.2 Steric Hindrance Pore model (SHP)

The effective pore radius for each solute at 200 mg L^{-1} was calculated from the transport parameters based on SHP model and is presented in Table 18. The pore radii of these membranes were calculated using the Stokes radius of the solute. These Stokes radii were 0.290, 0.202, 0.210, 0.198 nm for $ZnSO_4$, $Zn(NO_3)_2$, $Ni(NO_3)_2$, and $Co(NO_3)_2$ respectively. Also, the reflection coefficient of the divalent ions is high in both membranes compared to monovalent ions (see Table 18). However, the reflection coefficients were high for all solutes considered. By obtaining the membrane transport parameters, the SHP model was used to determine the effective pore radii of these membranes calculated using Stokes radius of each solute tested.

Table 18. Calculated values of σ, λ, and r_p for both membranes used

Membrane	**Solute**	**σ (–)**	**λ (–)**	**r_p (nm)**
AFC 30	$ZnSO_4$	0.966	0.966	0.300
	$Zn(NO_3)_2$	0.924	0.959	0.210
	$Ni(NO_3)_2$	0.868	0.969	0.217
	$Co(NO_3)_2$	0.855	0.964	0.221
AFC 80	$ZnSO_4$	0.990	0.985	0.294
	$Zn(NO_3)_2$	0.985	0.948	0.213
	$Ni(NO_3)_2$	0.979	0.940	0.223
	$Co(NO_3)_2$	0.989	0.955	0.219

It was found that the effective pore radius was similar to each other considering both membranes (AFC30 and AFC 80) in our case. Since the reflection coefficient is almost close to unity for AFC 80 membrane (see Table 18), the pore radius has been similar. This is because the equation of the SHP determines the effective pore radius with the reflection coefficient. The effective pore is not physical true since the membrane absorbed the ions which in turn may change the charged and eventually decrease the pores. Both membranes show better rejection for divalent ions since the reflection coefficient was high compared to monovalent ions. A similar result was achieved when different polyamide membranes were studied (Nair et al., 2018).

9. Conclusions

Separation of heavy metals from wastewater is paramount as these metals cannot be degraded or destroyed and pose a great treat to living organism including human beings. Nanofiltration membrane has been used in recent years to separate heavy metals due to its pollution free nature over these conventional methods. Modelling of both neutral and charged solutes in the separation process is necessary as limited information is given by the manufacturer in terms of membrane permeability, solute rejection, and neutral solute rejection. These models are used to describe and predict flux as well as rejection at different operating conditions of both neutral and charge species by NF membrane. Modelling is developed to select appropriate membrane, separation mechanism, design process, and improve the efficiency of membrane. A good predictive model is necessary to facilitate the performance of the membrane to be predicted accurately without involving tedious and complicated procedures. Using reliable modelling will result in a smaller number of experiments and consequently a reduction in cost and time.

In this study, the AFC 30 and AFC 80 membranes were first characterized by pure water flux (PWF). The pure water permeabilities for both membranes (AFC 30 and AFC 80) were 5.926 L m^{-2} h^{-1} bar^{-1} and 1.526 L m^{-2} h^{-1} bar^{-1}, respectively. It was observed that AFC 80 membrane was denser than AFC 30 membrane due to difference in pure water permeability. In addition, both NF membranes (AFC 30 and AFC 80) have been characterized by using modelling of rejection experiment of different neutral solutes. The structural parameters — pore radius (r_p) and membrane thickness to porosity ratio ($\Delta x/A_k$) — were calculated by using two independent models (Steric Hindrance Pore and Donnan Steric Partitioning). Based on the obtained results, the structural parameters prove to be useful as the data fit well with the experimental values of different neutral solutes for both AFC 30 and AFC 80 membranes. It was observed that the pore radius of neutral solutes using Donnan steric partitioning model can be calculated as slit–like or cylindrical geometry. One important criterion was the selection of the neutral solutes used for modelling. Selection of neutral solutes for the determination of pore radius is vital when considering the molecular weight of each solute. Solutes with close molecular weight will help achieve better results of pore radius and membrane thickness to porosity ratio. However, the SHP model cannot be applied to neutral solute with reflection coefficient almost close to unity. The pore radii (r_p) for AFC 30 and AFC 80 membranes using two independent models (DSP and SHP) were in the ranges (0.340–0.375 nm) and (0.245–0.265 nm), respectively. In addition, the membrane thickess to

porosity ratios ($\Delta x/A_k$) were in the ranges (2.80–3.50 μm) and (5.60–6.50 μm) for both AFC 30 and AFC 80 membrane. From our results, the two independent models can be used to predict and interpret the structural properties of NF membrane using different neutral solutes.

The fixed charge density on the membrane surface was determined using sodium chloride experiments with different concentrations in the range 100–4500 mg L^{-1}. First, it was observed that the permeate flux slightly decreased with increasing in NaCl concentrations which was explained by increase in osmotic pressure. In addition, the solute rejection gradually decreases with increasing of NaCl concentration in the feed solution. It was found that the decrease in rejection could be because of more solute ions being diffuse through the membrane. The data from sodium chloride experiment were used to calculate the effective charge density (ΦX) by using Spiegler–Kedem model together with the simplified quadratic equation formed from the Teorell–Meyer–Sievers model. The Spiegler–Kedem model describes very well the experimental rejection values for all NaCl concentration considered. As was observed, the reflection coefficient (σ) decreases and the solute permeability (P) increases by increasing the salt concentration in the feed solution. It was also revealed that the charge density of the membrane depends solely on the concentration of the electrolyte solution. This means that the charge density (absolute values) gradually increased with the increasing concentration of solution(s), which can be described by the Freundlich isotherm. The chloride ions from the solution are absorbed preferably on the membrane surface, thus increasing the membrane negative charge. It was observed that the membrane charge is strongly dependent on the concentration in the feed solution which was in contact to the membrane. This behaviour was attributed to the adsorption of ions from solution on the membrane surface.

The influence of process parameters such as transmembrane pressure, feed concentration, pH, and cross–flow velocity were examined. As observed, a linear relationship was found between transmembrane pressure and fluxes for both membranes. Also, increase in transmembrane pressure differences gradually increase the rejection of all solutes considered. The order of rejections was as follows: $ZnSO_{4\ (AFC\ 80)} > Zn(SO_4)_{(AFC\ 30)} > Zn(NO_3)_{2\ (AFC\ 80)} > Zn(NO_3)_{2\ (AFC\ 30)}$. Both membranes exhibit almost the same rejection which was greater than 98.5 % when considering zinc sulphate. It could be explained that both membranes have better rejection for the divalent anions (in our case sulphate) than monovalent ion (nitrate). It was seen that steric effect played a major role for AFC 30 than AFC 80 membrane. For AFC 30 membrane, there was greater effect of charge for this reason there was bigger differences between sulphate and nitrate rejection at minimum pressure of 5 bar. The rejection of sulphate

and nitrate were 98 % and 30 %, respectively. With AFC 80 membrane, comparing zinc sulphate and zinc nitrate rejection, there was small effect of concentration polarization due to smaller flux. In the case of zinc nitrate, it was concluded that AFC 80 membrane was suitable for separating zinc nitrate from wastewater as the minimum rejection was above 98 % compared to 35 % of that of AFC 30 membrane. It was observed that the maximum rejection of AFC 80 membrane was 98.7 % which shows that the membrane has a better property than AFC 30 membrane in terms of separating nickel nitrate from wastewater. Another reason was that AFC 80 membrane was denser and has higher rejection at minimum transmembrane pressure than AFC 30 membrane. The minimum rejection for nickel and cobalt ions for AFC 30 membrane was below 50 % but was above 25 % at 5 bar, respectively. In terms of AFC 80, it was found that the maximum rejection of nickel nitrate was 98.6 % compared to cobalt ions of 98.9 % respectively.

Furthermore, it was observed that increase in feed concentration increases the heavy metal rejection and directly affects the separation efficiency of AFC 30 membrane. It was explained that increasing feed concentration increases rejection for all heavy metal considered. This could be because of decrease in the normalized negative charged density of the membrane with increasing electrolyte concentrations. Another reason is that the rejection was increase with increasing concentration due to the presence of more permeable ions of like charge that preferentially permeate through the membrane.

Differences between observed and real rejection give clear indication that the concentration polarization effect decreases when increasing the cross–flow velocity for AFC 30 membrane. It was observed that the mass transfer coefficient in the polarization increases when increasing the feed flow rate from 0.42 to 1.25 m s^{-1}. With increasing in cross–flow velocity, the mass transfer coefficient increases due to increasing of the thickness of the polazied layer near the membrane surface. Back transport sweeps away the solutes which in turn decrease the osmotic pressure and increases net driving force. From our results obtained, we could possibly conclude that enhancing the hydrodynamics by increasing the cross–flow velocity decreases the concentration polarization of AFC 30 membrane. Regarding AFC 80 membrane, the increase of rejection was explained by differences in concentration polarization and mass transfer coefficient. It was seen that increase in the cross–flow velocity leads to an increase in the equilibrium permeate flux for NF and hence increase the rejection. It was observed that increase in cross–flow velocity increases the permeate flux due to the increase in solute back–transport to the bulk solution. It could be explained that increasing the

cross–flow velocity will decrease the flux decline and solutes accumulation by sweeping away the solute from the membrane surface.

The value of pH was found to influence both the rejection and the permeation flux since the charge properties of the surface layer of the NF membrane changes with pH. The flux by AFC 30 membrane was significantly higher than that of AFC 80 membrane and therefore the steric effects will play more important role in the rejection than electric effects. It was seen that AFC 80 membrane has smaller pores in comparison with AFC 30 membrane. This shows that AFC 30 membrane is governed by steric hindrance with respect to the electric interaction in our case otherwise; the reverse order would be expected.

From our results, it was observed that the divalent anions (SO_4^{2-}) was strongly rejected by the negatively charged functional groups of membrane compared to monovalent anions (NO_3^-) for different cations (Co^{2+}, Zn^{2+}, Ni^{2+}) mainly for AFC 30 membrane. For our case, both membranes exhibited a maximum rejection above 99 % for zinc sulphate. This was due to the growing repulsion between the membrane surface and higher valence ions. We can deduce that rejection is a very complex mechanism where the cations types, cations concentration, membrane charge could play their perspective role among other factors during nanofiltration separation process. Also, it was found that the difference of cations with equal valences was always associated to hydration energies of cations, their hydrated radii, and diffusivities of ions. Membrane transport parameters were found by fitting the Spiegler–Kedem model which produces high accuracy using flux and rejection values from experiments. Also, the membrane transport was fitted by the Steric Hindrance Pore model and found the effective pore radius of each heavy metal for both membranes. The model values show good correlation with experimental values of NF process for a wider range of concentration. It is important to know the feed content before selecting the desired membrane for separation of heavy metals. Experiments with dense membrane (AFC 80) resulted in higher rejection of over 98 % for different anions (sulphate and nitrate) selected. Rejection of the solutes by the AFC 80 membrane was predominantly due to steric effect. However, the AFC 30 (loose membrane) reached high real rejection of over 98 % for sulphate only. For nitrate anions, low to moderate real rejection (20–80 %) was achieved. This allows us to recommend the dense membrane (AFC 80) as a better alternative for nitrate or loose membrane (AFC 30) if we separate sulphate.

References

ABU SEMAN, M.N., KHAYET, M., HILAL, N. Development of antifouling properties and performance of nanofiltration membranes modified by interfacial polymerisation. *Desalination*, 2011, 273, 36–47.

AGBOOLA, O., MAREE, J., KOLESNIKOV, A., MBAYA, R., SADIKU, R. Theoretical performance of nanofiltration membranes for wastewater treatment. *Environmental Chemistry Letters*, 2015, 13, 37–47.

Agency for Toxic Substances and Disease Registry (ATSDR). Toxicological Profile for Cobalt. Public Health Service, U.S. Department of Health and Human Services, Atlanta, GA. 2004.

AGENSON, K. O., URASE, T. Change in membrane performance due to organic fouling in nanofiltration (NF)/reverse osmosis (RO) applications. *Separation and Purification Technology*, 2007, 55, 147–152.

AHMAD, A.L., OOI, B.S. A study on acid reclamation and copper recovery using low pressure nanofiltration membrane. *Chemical Engineering Journal*, 2010, 56, 257–263.

AHMAD, R., BEGUM, S., HOEK, E. M. V., KARANFIL, T., GENCELI, E.A., YADAV, A., TRIVEDI, P., ZHANG, C. Physico–chemical processes, *Water Environment Research*, 2004, 76, 829–1002.

ANG, W.L., MOHAMMAD, A.W. Mathematical modelling of membrane operations for water treatment. *Advances in Membrane Technologies for Water Treatment*, 2015, 379–407.

AHN, K.–H., SONG, K.G., CHA, H.Y., YEOM, I.–T. Removal of ions in nickel electroplating rinse water using low–pressure nanofiltration. *Desalination*, 1999, 122, 77–84.

AHUJA, S., 2014. Overview of Sustainability of Water Quality Worldwide. In: Comprehensive Water Quality and Purification, Ahuja, S. (Ed.). Elsevier, USA, ISBN: 978–0–12–382183–6, 1–10.

AL–MALACK, M.H., ANDERSON, G.K., ALMASI, A. Treatment of anoxic pond effluent using crossflow microfiltration. *Water Research*, 1998, 32, 3738–3746.

AL–RASHDI, B.A.M., JOHNSON, D.J., HILAL, N. Removal of heavy metals ions by nanofiltration. *Desalination*, 2013, 315, 2–17.

ALSALHY, Q.F., MOHAMMED, A.A., AHMED, S.H., RSAHID, T., ALSAADI, M.A. Estimation of nanofiltration transport parameters for cobalt ions removal from aqueous solutions. *Desalination and Water Treatment*, 2018, 108, 235–245.

AL–ALAWY, A., SALIH, M.H.Theoretical and experimental study of nanofiltration and reverse osmosis membranes for removal of heavy metals from wastewater. *International Journal of Science and Research*, 2016, 6, 778–788.

AOUNI, A., FERSI, C., CAURTAS–URIBE, B., BES–PIA, A., ALCAINA–MIRANDA, M.I., DHAHBI, M. Reactive dyes and textile effluent treatment study using ultrafiltration and nanofiltration processes. *Desalination*, 2012, 297, 87–96.

ARGUN, M.E. Use of clinoptilolite for the removal of nickel ions from water: kinetics and thermodynamics. *Journal of Hazardous Materials*, 2008, 150, 587–595.

AROUA, M.K., ZUKI, F.M., SULAIMAN, N.M. Removal of chromium ions from aqueous solutions by polymer–enhanced ultrafiltration. *Journal of Hazardous Materials*, 2007, 147, 752–758.

ASHRAF, R., ALI, T.A. Effect of heavy metals on soil microbial community and mung beans seed germination. *Pakistan Journals of Botany*, 2007, 39, 629–636.

AL–RASHDI, B., SOMERFIELD, C., HILAL, N. Heavy metals removal using adsorption and nanofiltration techniques. *Separation and Purification Reviews*, 2011, 40, 209–259.

ALYÜZ, B., VELI, S. Kinetics and equilibrium studies for the removal of nickel and zinc from aqueous solutions by ion exchange resins. *Journal of Hazardous Materials,* 2009, 167, 482–488.

AZIMI, A., AZARI, A., REZAKAZEMI, M., ANSARPOUR, M. Removal of heavy metals from industrial wastewaters: A review. *Chem Bio Eng Reviews*, 2017, 4, 37–59.

BABY, J., RAJ, J.S., BIBY, E.T., SANKARGANESH, P., JEEVITHA, M.V., AJISHA, S.U., RAJAN, S.S. Toxic effect of heavy metals on aquatic environment. *International Journal of Biological and Chemical Science*, 2010, 4, 939–952.

BAKER, R.W. Membrane Technology and Applications, 2nd edition, John Wiley & Sons Ltd, Chichester, United Kingdom, 2004. ISBN: 9780470854457.

BALLET, G.T., GZARA, L., HAFIANE, A., DHAHBI, M. Transport coefficients and cadmium salt rejection in nanofiltration membrane, *Desalination*, 2004, 167, 369–376.

BANDINI, S., VEZZANI, D. Nanofiltration modeling: the role of dielectric exclusion in membrane characterization. *Chemical Engineering Science*, 2003, 58, 3303–3326.

BANO, S., MAHMOOD, A., KIM, S.J., LEE, K.H. Graphene oxide modified polyamide nanofiltration membrane with improved flux and antifouling properties. *Journal of Materials Chemistry A*, 2015, 3, 2065–2071.

BARAKAT, M. A. New trends in removing heavy metals from industrial wastewater. *Arabian Journal of Chemistry*, 2011, 4, 361–377.

BARAKAT, M.A., SCHMIDT, E. Polymer–enhanced ultrafiltration process for heavy metals removal from industrial wastewater. *Desalination*, 2010, 256, 90–93.

BASARAN, G., KAVAK, D., DIZGE, N., ASCI, Y., SOLENER, M., OZBEY, B. Comparative study of the removal of nickel (II) and chromium (VI) heavy metals from metal plating wastewater by two nanofiltration membranes. *Desalination and Water Treatment*, 2016, 57, 21870–21880.

BATELS, C., FRANKS, R., RYBAR, S., SCHIERACH, M., WILF, M. The effect of feed ionic strength on salt passage through reverse osmosis membranes. *Desalination*, 2005, 184, 185–195.

BENNANI, C.F., M'HIRI, O. Comparative study of the removal of heavy metals by two nanofiltration membranes. *Desalination and Water Treatment*, 2013, 53, 1024–1030.

BES–PIA, A., CUASTAS–URIBE, B., MENDOZA–ROCA, J.A., ALCAINA–MIRANDA, M.I. Study of the behaviour of different NF membranes for the reclamation of a secondary textile effluent in rinsing processes. *Journal of Hazardous Materials*, 2010, 178, 341–348.

BELKHOUCHE, N.–E., DIDI, M.A., TAHA, S., FARES, N.B. Zinc rejection from leachate solutions of industrial solid waste–effects of pressure and concentration on nanofiltration membrane performance. *Desalination*, 2009, 239, 58–65.

BLOCHER, C., DORDA, J., MAVROV, V., CHMIEL, H., LAZARIDIS, N.K., MATIS, K. A. Hybrid flotation–membrane filtration processes for the removal of heavy metal ions from wastewater. *Water Research*, 2003, 37, 4018–4026.

BIAN, R., YAMAMOTO, K., WATANABE, Y. The effect of shear rate on controlling the concentration polarization and membrane fouling. *Desalination*, 2000, 131, 225–236.

BOCCA, B., PINO, A., ALIMONTI, A., FORTE, G. Toxic metals contained in cosmetics: a status report. *Regulatory Toxicology and Pharmacology*, 2014, 68, 447–467.

BOJIC, A.L., BOJIC, D., ANDJELKOVIC, T. Removal of Cu^{2+} and Zn^{2+} from model wastewaters by spontaneous reduction coagulation process in flow conditions. *Journal of Hazardous Materials*, 2009, 168, 813–819.

BOURANENE, S., FIEVET, P., SZYMCZYK, A. Investigating nanofiltration of multi–ionic solutions using the steric, electric and dielectric exclusion model. *Chemical Engineering Science*, 2009, 64, 3789–3798.

BOURANENE, S., FIEVET, P., SZYMCZYK, A., SAMER EL–HADI, M., VIODONNE, A. Influence of operating conditions on the rejection of cobalt and lead ions aqueous solutions by nanofiltration polyamide membrane. *Journal of Membrane Science*, 2008, 325, 150–157.

BOUSSU, K., VANDECASTEELE, C., VAN DER BRUGGEN, B. Relation between membrane characteristics and performance in nanofiltration. *Journal of Membrane Science*, 2008, 310, 51–65.

BOWEN, W.R., MOHAMMAD, A.W. Diafiltration by nanofiltration: prediction and optimization. *American Institute of Chemical Engineers Journal*, 1998, 44, 1799–1812.

BOWEN, W.R., MOHAMMAD, A.W., HILAL, N. Characterization of nanofiltration membranes for predictive purposes—use of salts, uncharged solutes, and atomic force microscopy. *Journal of Membrane Science*, 1997, 126, 91–105.

BOWEN, W.R., MUKHTAR, H. Characterisation, and prediction of separation performance of nanofiltration membranes. *Journal of Membrane Science*, 1996, 112, 263–274.

BOWEN, W.R., WELFOOT, J.S. Modelling the performance of membrane nanofiltration—critical assessment and model development. *Chemical Engineering Science*, 2002, 57, 1121–1137.

BUNANI, S., YÖRÜKOĞLU, E., YÜKSEL, Ü., KABAY, N., YÜKSEL, M., SERT, G. Application of reverse osmosis for reuse of secondary treated urban wastewater in agricultural irrigation. *Desalination*, 2015, 364, 68–74.

CAMARILLO, R., LLANOS, J., GARCÍA–FERNÁNDEZ, L., PÉREZ, A., CAÑIZARES, P. Treatment of copper (II)–loaded aqueous nitrate solutions by polymer enhanced ultrafiltration and electrode position. *Separation and Purification Technology*, 2010, 70, 320–328.

CATH, T.Y., CHILDRESS, A.E., ELIMELECH, M. Forward osmosis: Principles, applications, and recent developments. *Journal of Membrane Science*, 2006, 281, 70–87.

CAVACO MORÃO, A.I., SZYMCZYK, A., FIEVET, P., BRITES ALVES, A.M. Modelling the separation by nanofiltration of a multi–ionic solution relevant to an industrial process. *Journal of Membrane Science*, 2008, 322, 320–330.

CEMPEL, M., NIKEL, G. Nickel: A review of its sources and environmental toxicity. *Polish Journal of Environmental Studies*, 2006, 15, 375–382.

CORCORAN, E., NELLEMANN, C., BAKER, E., BOS, R., OSBORN, D., SAVELLI, H. Sick Water? The central role of wastewater management in sustainable development. A Rapid Response Assessment. UNEP/UNHABITAT, 2010. ISBN: 978–82–7701–075–5.

COUTINHO, C., CHIU, M.C., BASSO, R.C., RIBEIRO, A.P.B., GONÇALVES, L.A.G., VIOTTO, L. A. State of art of the application of membrane technology to vegetable oils: A review. *Food Research International*, 2009, 42, 536–550.

CHANG, Q., WANG, G. Study on the macromolecular coagulant PEX which traps heavy metals. *Chemical Engineering Science*, 2007, 62, 4636–4643.

CHIBUIKE, G.U., OBIORA, S.C. Heavy metal polluted soils: Effect on plants and bioremediation methods. *Applied and Environmental Soil Science*, 2014, 1–12.

CHILDRESS, A.E., ELIMELECH, M. Effect of solution chemistry on the surface charge of polymeric reverse osmosis and nanofiltration membranes. *Journal of Membrane Science*, 1996, 119, 253–268.

CHILDRESS, A.E., ELIMELECH, M. Relating nanofiltration membrane performance to membrane charge (Electro kinetic) characteristics, *Environmental Science and Technology*, 2000, 34, 3710–3716.

CHOI, H., ZHANG, K., DIONYSIOU, D.D., OERTHER, D.B., SORIAL, G.A. Influence of cross–flow velocity on membrane performance during filtration of biological suspension. *Journal of Membrane Science*, 2005, 248, 189–199.

CHON, K., SARP, S., LEE, S., LEE, J. H., LOPEZ–RAMIREZ, J. A., CHO, J. Evaluation of a membrane bioreactor and nanofiltration for municipal wastewater reclamation: trace contaminant control and fouling mitigation. *Desalination*, 2011, 272, 128–134.

CHOUDHURY, R.R., GOHIL, J.M., MOHANTY, S., NAYAK, S.K. Antifouling, fouling release and antimicrobial materials for surface modification of reverse osmosis and nanofiltration membranes. *Journal of Material Chemistry*, A, 2018, 6, 313–333.

CUHORKA, J., WALLACE, E., MIKULÁŠEK, P. Removal of micropollutants from water by commercially available nanofiltration membranes. *Science of the Total Environment*, 2020, 720, 137474.

CUI, Z.F., MURALIDHARA, H.S. Membrane Technology. A practical guide to membrane technology and application. In: Food Bioprocessing Fundamentals of Pressure–Driven Membrane Separation Processes. Butterworth–Heinemann, 2010. ISBN: 978–85617–632–3.

DAEI NIAKI, S.M., TAKDASTAN, A., BAZAFKAN, M.H., ZAZOUL, M.A. Survey of nanofiltration technology in removal heavy metals (Ni, Cu and Zn) from industrial wastewater. *International Conference on Chemical Environmental and Biological Sciences*, 2015, 45–50.

DAS, K.K., BUCHNER V. Effect of nickel exposure on peripheral tissues: role of oxidative stress in toxicity and possible protection by ascorbic acid. *Reviews on Environmental Health*, 2007, 22, 157–173.

DEEN, W.M. Hindered transport of large molecules in liquid–filled pores. *American Institute of Chemical Engineers Journal*, 1987, 33, 1409–1425.

DECHADILOK, P., DEEN, W.M. Hindrance factors for diffusion and convection in pores. *Industrial & Engineering Chemistry Research*, 2006, 45, 6953–6959.

DIALYNAS, E., DIAMADOPOULOS, E. Integration of a membrane bioreactor coupled with reverse osmosis for advanced treatment of municipal wastewater. *Desalination*, 2009, 238, 302–311.

DIAWARA, C.K. Nanofiltration process efficiency in water. *Desalination*, 2008, 37, 302–324.

Directive 2013/39/EU of the European parliament and of the council of 12 August 2013 amending Directives 2000/60/EC and 2008/105/EC as regards priority substances in the field of water policy official J L 226, 24/8/2013, 9–11.

DONNAN, F.G. Theory of membrane equilibria and membrane potentials in the presence of non–dialysing electrolytes. A contribution to physical–chemical physiology. *Journal of Membrane Science*, 1995, 100, 45–55.

DRIOLI, E., QUIST–JENSEN, C., GIORNO L. (2016) Molecular Weight Cut–off. In: Drioli E., Giorno L. (eds), Encyclopaedia of Membranes. Springer, Berlin, Heidelberg, 2016 ISBN: 978–3–662–44324–8.

DUDZIAK, M., BODZEK, M. Removal of phytoestrogens from water solutions using tubular nanofiltration membranes. *Ecological Chemistry and Engineering A*, 2010, 17, 289–296.

EL SAMRANI, A.G., LARTIGES, B.S., VILLIÉRAS, F. Chemical coagulation of combined sewer overflow: heavy metal removal and treatment optimization. *Water Research*, 2008, 42, 951–960.

ENNIGROU, D.J., GZARA, L., BEN ROMDHANE, M.R., DHAHBI, M. Cadmium removal from aqueous solutions by polyelectrolyte enhanced ultrafiltration. *Desalination*, 2009, 246, 363–369.

FADAEI, F., HOSHYARGAR, V., SHIRAZIAN, S., ASHRAFIZADEH, S.N. Mass transfer simulation of ion separation by nanofiltration considering electrical and dielectrical effects. *Desalination*, 2012, 284, 316–323.

FAN, X., DONG, Y., SU, Y., ZHAO, X., LI, Y., LIU, J., JIANG, Z. Improved performance of composite nanofiltration membranes by adding calcium chloride in aqueous phase during interfacial polymerization process. *Journal of Membrane Science*, 2014, 452, 90–96.

FANE, A.G., WANG, R., HU, M.X. Synthetic membranes for water purification: Status and future. *Angewandte Chemie International Edition*, 2015, 54, 3368–3386.

FANE, A.G., WANG, R., JIA, Y. Membrane technology: Past, present, and future. *Membrane and Desalination Technologies*, 2010, 13, 1–45.

FANG, W., SHI, L., WANG, R. Interfacially polymerized composite nanofiltration hollow fiber membranes for low–pressure water softening. *Journal of Membrane Science*, 2013, 430, 129–139.

FANG, W., SHI, L., WANG, R. Mixed polyamide–based composite nanofiltration hollow fiber membranes with improved low–pressure water softening capability. *Journal of Membrane Science*, 2014, 468, 52–61

FEHER, J. Osmosis and osmotic pressure. *Quantitative Human Physiology*, 2012, 141–152.

FOO, K.Y., HAMEED, B.H. Insights into the modelling of adsorption isotherm systems. *Chemical Engineering Journal*, 2010, 156, 2–10.

FRARES, N.B., TAHA, S., DORANGE, G. Influence of the operating conditions on the elimination of zinc ions by nanofiltration. *Desalination*, 2005, 185, 245–253.

FU, F., WANG, Q. Removal of heavy metal ions from wastewaters: A review. *Journal of Environmental Management*, 2011, 92, 407–418.

GARBA, Y., TAHA, S., CABON, J., DORANGE, G. Modelling of cadmium salts rejection through a nanofiltration membrane: relationships between solute concentration and transport parameters. *Journal of Membrane Sciences*, 2003, 211, 51–58.

GARCÍA–MARTIN, N., SILVA, V., CARMONA, F.J., PALACIO, L., HERNADEZ A., PRÁDANOS, P. Pore size analysis from retention of neutral solutes through nanofiltration membranes. The contribution of concentration polarization. *Desalination*, 2014, 344, 1–11.

GEENS, J., DE WITTE, B., VAN DER BRUGGEN, B. Removal of API's (Active Pharmaceutical Ingredients) from organic solvents by nanofiltration. *Separation Science and Technology*, 2007, 42, 2435–2449.

GERALDES, V., ALVES, A.M.B. Computer program for simulation of mass transport in nanofiltration membranes. *Journal of Membrane Science*, 2008, 321,172–182.

GHAEMI, N., MADAENI, S.S., ALIZADEH, A., DARAEI, P., BADIEH, M.M.S., FALSAFI, M., V. VATANPOUR, V. Fabrication and modification of polysulfone nanofiltration membrane using organic acids: morphology, characterization, and performance in removal of xenobiotics. *Separation and Purification Technology*, 2012, 96, 214–228.

GHERASIM, C.V., CUHORKA, J., MIKULÁŠEK, P. Analysis of lead (II) retention from single salt and binary aqueous solutions by a polyamide nanofiltration membrane: experimental results and modelling. *Journal of Membrane Science*, 2013, 436, 132–144.

GHERASIM, C.V., HANCKOVÁ, K., PALARČIK, J., MIKULÁŠEK, P. Investigation of cobalt (II) retention from aqueous solutions by a polyamide nanofiltration membrane. *Journal of Membrane Science,* 2015, 490, 46–56.

GHERASIM, C.V., MIKULÁŠEK, P. Influence of operating variables on the removal of heavy metals ions from aqueous solution by nanofiltration. *Desalination,* 2014, 343, 67–74.

GHERASIM, C.V., MIKULÁŠEK, P., CHÝLKOVÁ J., KREJČOVÁ, A. Evaluation of structural and charge properties of polyamide nanofiltration membrane. *Scientific Papers of the University of Pardubice, Series A*, 2014, 20, 343–352.

GIORNO L., PIACENTINI, E., BAZZARELLI, F. The Principle of Microfiltration. In: Drioli E., Giorno L. (Eds) Encyclopaedia of Membranes. Springer, Berlin, Heidelberg. 2015. ISBN 978–3–662–44323–1.

GODE, F., PEHLIVAN, E. Removal of chromium (III) from aqueous solutions using Lewatit S 100: the effect of pH, time, metal concentration and temperature. *Journal of Hazardous Material*, 2006, 136, 330–337.

GOH, P.S., ISMAIL, A.F., HILAL, N. Nano–enabled membranes technology: Sustainable and revolutionary solutions for membrane desalination. *Desalination*, 2016, 380, 100–104.

GUNATILAKE, S.K. Methods of removing heavy metals from industrial wastewater. *Journal of Multidisciplinary Engineering Science Studies*, 2015, 1, 2912–1309.

HAN, B., RUNNELLS, T., ZIMBRON, J., WICKRAMASINGHE, R. Arsenic removal from drinking water by flocculation and microfiltration. *Desalination,* 2002, 145, 293–298.

HIDALGO, A.M., LEÓN, G., GÓMEZ, M., MURCIA, M.D., GÓMEZ, E., GÓMEZ, J.L. Application of the Spiegler–Kedem–Kachalsky model to the removal of 4–chlorophenol by different nanofiltration membranes. *Desalination*, 2013, 315, 70–75.

HIGA, M., KIRA, A., TANIOKA, A., MIYASAKA, K. Ionic partition equilibrium in a charged membrane immersed in a mixed ionic solution. *Journal of the Chemical Society, Faraday Transactions,* 1993, 89, 3433–3435.

HILAL, N., AL–ZOUBI, H., DARWISH, N. A., MOHAMMAD, A. W., ARABI, M. A. A comprehensive review of nanofiltration membranes: Treatment, pre–treatment, modelling, and atomic force microscopy. *Desalination,* 2004, 170, 281–308.

HOFFER, E., KEDEM, O. Hyperfiltration in charged membranes: The fixed charge model. *Desalination*, 1967, 2, 25–39.

HOMAYOONFAL, M., AKBARI, A., MEHRNIA, M.R. Preparation of polysulfone nanofiltration membranes by UV–assisted grafting polymerization for water softening. *Desalination*, 2010, 263, 217–225.

HOSSEINI, S. S., BRINGAS, E., TAN, N. R., ORTIZ, I., GHAHRAMANI, M., SHAHMIRZADI, M. A. A. Recent progress in development of high–performance polymeric membranes and materials for metal plating wastewater treatment: A review. *Journal of Water Process Engineering*, 2016, 9, 78–110.

HU, M., MI, B. Layer–by–layer assembly of graphene oxide membranes via electrostatic interaction. *Journal of Membrane Science*, 2014, 469, 80–87.

HUANG, J.H., ZENG, G.M., ZHOU, C.F., LI, X., SHI, L.J., HE, S.B. Adsorption of surfactant micelles and Cd^{2+}/Zn^{2+} in micellar–enhanced ultrafiltration. *Journal of Hazardous Materials*, 2010, 183, 287–293.

HUANG, Y., DU, J.R., ZHANG, Y., LAWLESS, D., FENG, X. Removal of mercury (II) from wastewater by polyvinyl amine–enhanced ultrafiltration. *Separation and Purification Technology*, 2015, 154, 1–10.

HUNG, D.C., NGUYEN, N.C., UAN, D.K., SON, L.H. Membrane processes and their potential applications for freshwater provision in Vietnam. *Vietnam Journal of Chemistry*, 2017, 55, 533–544.

INGLEZAKIS, V.J., STYLIANOU, M.A., GKANTZOU, D., LOIZIDOU, M.D. Removal of Pb (II) from aqueous solutions by using clinoptilolite and bentonite as adsorbents. *Desalination*, 2007, 210, 248–256.

IPEK, U. Removal of Ni (II) and Zn (II) from aqueous solution by reverse osmosis. *Desalination*, 2005, 174, 161–169.

IVNITSKY, H., MINZ, D., KAUTSKY, L., PREIS, A., OSTFELD, A., SEMIAT, R., DOSORETZ, C.G. Biofouling formation and modelling in nanofiltration membranes applied to wastewater treatment. *Journal of Membrane Science*, 2010, 360, 165–173.

JHAVERI, J.H., MURTHY, Z.V.P. A comprehensive review on anti–fouling nanocomposite membranes for pressure driven membrane separation processes. *Desalination*, 2016, 379, 137–154.

JI, Y., QIAN, W., YU, Y., AN, Q., LIU, L., ZHOU, Y., GAO, C. Recent developments in nanofiltration membranes based on nanomaterials. *Chinese Journal of Chemical Engineering*, 2017, 25, 1639–1652.

JOHNSON, D.J., HILAL, N. Membrane characterization by atomic force microscopy. *Encyclopaedia of Membrane Science and Technology*, 2013, 16, 394–399.

KOČANOVÁ, V., CUHORKA, J., DUŠEK, L., MIKULÁŠEK, P. Application of nanofiltration for removal of zinc from industrial wastewater. *Desalination and Water Treatment*, 2017, 75, 342–347.

KANG, S.Y., LEE, J.U., MOON, S.H., KIM, K.W. Competitive adsorption characteristics of Co^{2+}, Ni^{2+}, and Cr^{3+} by IRN–77 cation exchange resin in synthesized wastewater. *Chemosphere*, 2004, 56, 141–147.

KIM, H.A., CHOI, J. H., TAKIZAWA, S. Comparison of initial filtration resistance by pre–treatment processes in the nanofiltration for drinking water treatment. *Separation and Purification Technology*, 2007, 56, 354–362.

KIM, I.S., JANG, N. The effect of calcium on the membrane biofouling in the membrane bioreactor (MBR). *Water Research*, 2006, 40, 2756–2764.

KIM, J.F., SZEKELY, G., VALTCHEVA, I.B., LIVINGSTON, A.G. Increasing the sustainability of membrane processes through cascade approach and solvent recovery–pharmaceutical purification case study. *The Royal Society of Chemistry*, 2014, 16, 133–145.

KOBATAKE, Y., TAKEGUCHI, N., TOYOSHIMA, Y., FUJITA, H. Studies of membrane phenomena. *Journal of Physical Chemistry*, 1965, 69, 3981–3987.

KOO, C.H., MOHAMMAD, A.W., SUJA, F. Effect of cross–flow velocity on membrane filtration performance in relation to membrane properties. *Desalination and Water Treatment*, 2014, 55, 678–692.

KOROS, W.J., MA, Y.H., SHIMIDZU, T. Terminology for membranes and membrane processes (IUPAC Recommendations 1996). *Pure Applied Chemistry*, 1996, 68, 1479–1489.

KOTER, S. Determination of the parameters of the Spiegler–Kedem–Katchalsky model for nanofiltration of single electrolyte solutions. *Desalination*, 2006, 198, 335–345.

KOTTE, M.R., CHO, M., DIALLO, M.S. A facile route to the preparation of mixed matrix polyvinylidene fluoride membranes with in–situ generated polyethyleneimine particles. *Journal of Membrane Science*, 2014, 450, 93–102.

KUCERA, J. *Reverse osmosis: Design, processes, and application for Engineers*. John Wiley & Sons Inc. Hoboken, New Jersey, 2010. ISBN 978–0–470–618431.

KUMARAN, M., BAJPAI, S. Application of extended Nernst–Planck model in nanofiltration process—A critical review. *International Journal of Engineering Research and Reviews*, 2015, 3, 40–49.

KÜMMERER, K. Sustainable from the very beginning: rational design of molecules by life cycle engineering as an important approach for green pharmacy and green chemistry. *Green Chemistry*, 2007, 9, 899–907.

KÜMMERER, K. The presence of pharmaceuticals in the environment due to humans' use–present knowledge and future challenges. *Journal of Environmental Management*, 2009, 90, 2354–2366.

KURIHARA, M., TOMIOKA, H. Preparation of industrial RO, NF membranes, and their membrane modules and applications, in Drioli, E., Giorno, L. (Eds), Comprehensive Membrane Science and Engineering, Elsevier: Oxford, U.K., 2010, ISBN: 9780080932507.

KURNIAWAN, T. A., CHAN, G.Y.S., LO, W.Y., BABEL, S. Physico–chemical treatment techniques for wastewater laden with heavy metals. *Chemical Engineering Journal*, 2006, 118, 83–98.

LABBEZ, C., FIEVET, P., SZYMCZYK, A., VIDONNE, A., FOISSY, A., PAGETTI, J. Analysis of the salt retention of a titania membrane using the "DSPM" model: effect of pH, salt concentration and nature. *Journal of Membrane Science*, 2002, 208, 315–329.

LADEWIG, B., AL–SHAELI, M.N.Z. *Fundamentals of Membrane Bioreactors*, Springer Transactions in Civil and Environmental Engineering, 2016, ISBN 978–981–10–2014–8.

LANTERI, Y., SZYMCZYK, A., FIEVET, P. Influence of steric, electric, and dielectric effects on membrane potential. *Langmuir*, 2008, 24, 7955–7962.

LAJIMI, R.H., FERJANI, E., ROUDESLI, M.S., DERATANI, A. Effect of LbL surface modification on characteristics and performances of cellulose acetate nanofiltration membranes. *Desalination*, 2011, 266, 78–86.

LANDABURU–AGUIRRE, J., GARCÍA, V., PONGRÁCZ, E., KEISKI, R.L. The removal of zinc from synthetic wastewaters by micellar–enhanced ultrafiltration: statistical design of experiments. *Desalination*, 2009, 240, 262–269.

LANDABURU–AGUIRRE, J., PONGRÁCZ, E., PERÄMÄK, P., KEISKI, R.L. Micellar enhanced ultrafiltration for the removal of cadmium and zinc: use of response surface methodology to improve understanding of process performance and optimisation. *Journal of Hazardous Materials*, 2010, 180, 524–534.

LEE, J.C., SON, Y.O., PRATHEESHKUMAR P., SHI X.L. Oxidative stress and metal carcinogenesis. *Free Radical Biology and Medicine*, 2012, 53, 742–757.

LEVENSTEIN, R., HASSON, D., SEMIAT, R. Utilization of the Donnan effect for improving electrolyte separation with nanofiltration membranes. *Journal of Membrane Science*, 1996, 116, 77–92.

LEYSSENS, L., VINCK, B., VAN DER STRAETEN, C., WUYTS, F., MAES, L. Cobalt toxicity in humans—A review of the potential sources and systemic health effects. *Toxicology*, 2017, 387, 43–56.

LI, X., CAO, Y., YU, H., KANG, G., JIE, X., LIU, Z., YUAN, Q. A novel composite nanofiltration membrane prepared with PHGH and TMC by interfacial polymerization. *Journal of Membrane Science*, 2014, 466, 82–91.

LI, Y.F., MAO, H., ZHANG, H.Q., YANG, G.H., DING, R., WANG, J.T. Tuning the microstructure and permeation property of thin film nanocomposite membrane by functionalized inorganic nanospheres for solvent resistant nanofiltration. *Separation and Purification Methods*, 2016, 165, 60–70.

LIN, C–J, CHIRAZI, S., RAO, P. Mechanistic model for $CaSO_4$ fouling on nanofiltration membrane. *Journal of Environmental Engineering*, 2005, 131, 1387–1391.

LIN, J.C.T., LEE, D.J., HUANG, C. Membrane fouling mitigation: Membrane cleaning. *Separation of Science Technology*, 2010, 45, 858–872.

LINGGAWATI, A., MOHAMMAD, A.W., LEO, C.P. Effects of APTEOS content and electron beam irradiation on physical and separation properties of hybrid nylon–66 membranes. *Materials Chemistry and Physics*, 2012, 133, 110–117.

LUO, J., WAN, Y. Effects of pH and salt on nanofiltration–a critical review. *Journal of Membrane Science*, 2013, 438, 18–28.

MALAEB, L., AYOUB, G.M. Reverse osmosis technology for water treatment: State of the art review. *Desalination*, 2011, 267, 1–8.

MALIK, M.A., HASHIM, M.A., NABI, F. Extraction of metal ions by ELM separation technology. *Journal of Dispersion Science and Technology*, 2012, 33, 346–356.

MÄNTTÄRI, M., PIHLAJAMÄKI, A., NYSTRÖM, M. Effect of pH on hydrophobicity and charge and their effect on the filtration efficiency of NF membranes at different pH. *Journal of Membrane Science*, 2006, 280, 311–320.

MEHDIPOUR, S., VATANPOUR, V., KARIMINIA, H–R. Influence of ion interaction on lead removal by a polyamide nanofiltration membrane, *Desalination*, 2015, 362, 84–92.

MEHIGUENE, K., GARBA, Y., TAHA, S.; GONDREXON, N., DORANGE, G. Influence of operating conditions on the retention of copper and cadmium in aqueous solutions by nanofiltration: experimental results and modelling. *Separation and Purification Technology*, 1999, 15, 181–187.

MIKULÁŠEK, P., CUHORKA, J. Removal of heavy metals from aqueous solutions by nanofiltration. *Chemical Engineering Transactions*, 2016, 47, 379–384.

MIRBAGHERI, S.A., BIGLARIJOO, N., AHMADI, S., RAZMARA, P., DOOST, A.Y. Removing Fe, Zn and Mn from steel making plant wastewater using RO and NF membranes. *Iranian Journal of Health Sciences*, 2016, 4, 41–55.

MOAREFIAN, A., GOLESTANI, H. A., BAHMANPOUR, H. Removal of amoxicillin from wastewater by self–made polyethersulfone membrane using nanofiltration. *Journal of Environmental Health Science and Engineering*, 2014, 12, 1–10.

MOHAMMAD, A.W., TEOW Y.H., ANG W.L., CHUNG Y.T., OATLEY–RADCLIFFE D.L., HILAL N. Nanofiltration membrane review: Recent advances and future prospects. *Desalination*, 2015, 356, 226–254.

MÓLGORA, C.C., DOMÍNGUEZ, A.M., AVILA, E.M., DROGUI, P., BUELNA, G. Removal of arsenic from drinking water: A comparative study between electrocoagulation–microfiltration and chemical coagulation–microfiltration processes. *Separation and Purification Technology*, 2013, 118, 645–651

MOROS, A.S., GOZA´LVEZ–ZAFRILLA, J.M., GARCIA, J.L. Application of the DSPM with dielectric exclusion to high rejection nanofiltration membrane in separation of nitrate solutions. *Desalination*, 2008, 221, 268–276.

MULDER, M. Basic Principles of Membrane Technology, 2nd ed., Kluwer Academic Publishers, 1997. ISBN: 978–94–009–1766–8.

MURTHY, Z. V. P., CHAUDHARI, L. B. Application of nanofiltration for the rejection of nickel ions from aqueous solutions and estimation of membrane transport parameters. *Journal of Hazardous Materials*, 2008, 160, 70–77.

MURTHY, Z.V.P., CHAUDHARI, L.B. Separation of binary heavy metals from aqueous solutions by nanofiltration and characterization of the membrane using Spiegler–Kedem model. *Chemical Engineering Journal*, 2009, 150, 181–187.

MUSBAH, I., CICÉRON, D., SABONI, A., ALEXANDROVA, S. Characterization of nanofiltration membranes: pore radius estimation using two models. *Journal of Chemical Technology and Metallurgy*. 2014, 49, 435–441.

NAIR, R.R., PROTASOVA, E., STRAND, S., BILSTAD, T. Implementation of Spiegler–Kedem and Steric Hindrance Pore models for analyzing nanofiltration membrane performance for smart water production. *Membranes (Basel)*, 2018, 8, 1–16.

NAKAO, S., KIMURA, S. Models of membrane transport phenomena and their applications for ultrafiltration data. *Journal of Chemical Engineering of Japan*, 1982, 15, 200–205.

NATH, K. Membrane separation processes. Raj Press, New Delhi–110012. 2017, ISBN 978–81–203–5291–9.

NGUYEN, C.M., BANG, S., CHO, J., KIM, K.W. Performance, and mechanism of arsenic removal from water by a nanofiltration membrane. *Desalination*, 2009, 245, 82–94.

NUNES, S. P., PEINEMANN, K–V. Membrane Technology in the Chemical Industry. WILEY–VCH Verlag GmbH & Co. KGaA, Weinheim, 2006. ISBN: 3–527–31316–8.

O'CONNELL, D.W., BIRKINSHAW, C., O'DWYER, T.F. Heavy metal adsorbents prepared from modification of cellulose: a review. *Bioresource Technology*, 2008, 15, 6709–6724.

QADIR, D., MUKHTAR, H.B., KEONG, L.K. Rejection of divalent ions in commercial tubular membranes: Effect of feed concentration and anion type. *Sustainable Environmental Research*, 2017, 27, 103–106.

OATLEY, D. L., LLENAS, L., PÉREZ, R., WILLIAMS, P. M., MARTÍNEZ–LLADÓ, X., ROVIRA, M. Review of the dielectric properties of nanofiltration membranes and verification of the single oriented layer approximation, *Advances in Colloid and Interface Science*, 2012, 173, 1–11.

OLIVEIRA, C.R., SILVA, C.M., MILANEZ, A.F. Application of ultrafiltration in the pulp and paper industry: metals removal and white–water reuse. *Water Science and Technology*, 2007, 55, 117–123.

OTERO, J. A., LENA, G., COLINA, J. M., PRÁDANOS, P., TEJERINA, F., HERNÁNDEZ, A. Characterisation of nanofiltration membranes. Structural analysis by the DSP model and microscopically techniques. *Journal of Membrane Science*, 2006, 279, 410–417.

OYARO, N., JUDDY, O., MURAGO, E.N.M., GITONGA, E. The contents of Pb, Cu, Zn and Cd in meat in Nairobi, Kenya. *International Journal of Agriculture and Environment*, 2007, 5, 119–121.

PAPADOPOULOS, A., FATTA, D., PARPERIS, K., MENTZIS, A., HARALAMBOUS, K. J., LOIZIDOU, M. Nickel uptake from a wastewater stream produced in a metal finishing industry by combination of ion–exchange and precipitation methods. *Separation and Purification Technology*, 2004, 39,181–188.

PAUGHAM, L., TAHA, S., DORANGE, G., JAOUEN, P., QUEMENEUR F. Mechanism of nitrate ions transfer in nanofiltraton depending on pressure, pH, concentration, and medium composition. *Journal of Membrane Science*, 2004, 231, 37–46.

PEINERMANN, K–V., NUNES, S.P. Membranes for Water Treatment. Wiley–VCH, 2010. ISBN: 9783527314836.

PENDERGAST, M.M., HOEK, E.M.V. A review of water treatment membrane nanotechnologies. *Energy & Environmental Science*, 2011, 4, 1946–1971.

PLATTES, M., BERTRAND, A., SCHMITT, B., SINNER, J., VERSTRAETEN, F., WELFRING, J. Removal of tungsten oxyanions from industrial wastewater by precipitation, coagulation, and flocculation processes. *Journal of Hazardous Materials*, 2007,148, 613–615.

PLUM, L. M., RINK, L., HASSE, H. The essential toxin: Impact of zinc on human health. *International Journal of Environmental Research and Public Health*, 2010, 7, 1342–1365.

POLAT, H., ERDOGAN, D. Heavy metal removal from waste waters by ion flotation. *Journal of Hazardous Materials*, 2007, 148, 267–273.

QADIR, D., MUKHAR, H.B., KEONG, L.K. Rejection of divalent ions in commercial membranes: Effects of feed concentration and anion type. *Sustainable Environmental Research*, 2017, 27, 103–106.

RAHIMPOUR, A., JAHANSHAHI, N., MORTAZAVIAN, N. Preparation and characterization of asymmetric polyethersulfone and thin–film composite polyamide nanofiltration membranes for water softening. *Applied Surface Science*, 2010, 256, 1657–1663.

RAJESWARI, R. T., SAILAJA, N. Impact of heavy metals on environmental pollution. *Journal of Chemical and Pharmaceutical Sciences*, 2014, 3, 175–181.

RASHIN, A.A., HONIG, B. Revaluations of the born model of ion hydration. *Journal of Physical Chemistry*, 1985, 89, 5588–5593.

RENOU, R., GHOUFI, A., SZYMCZYK, A., ZHU, H., NEYT, J., MALFREYT, P. Nano confined electrolyte solutions in porous hydrophilic silica membranes. *The Journal of Physical Chemistry C*, 2013, 117, 11017–11027.

RENU, B., AGARWAL, M., SING, K. Methodologies for removal of heavy metal ions from wastewater: an overview. *Interdisciplinary Environmental Review*, 2017, 18, 124–140.

ROGANOVIC–ZAFIROVA, D., JORDANOVA, M., PANOV, S., VELKOVA–JORDANOSKA, L. Hepatic capillariasis in the Mediterranean barbell (Barbus meridionalis petenyi Heck.) from lake Ohrid. *Folia Veterinaria*, 2003, 47, 35–37.

ROOHANI, N., HURRELL, R., KELISHADI, R., SCHULIN J. R. Zinc and its importance for human health: An integrative review. *Journal of Research in Medical Sciences,* 2013, 18, 144–157.

ROY, Y., SHARQAWY, M.H., LIENHARD, J.H. Modelling of flat–sheet and spiral–wound nanofiltration configurations and its application in seawater nanofiltration. *Journal of Membrane Science*, 2015, 493, 360–372.

ROY, Y., WARSINGER, D.M., LIENHARD, J.H. Effect of temperature on ion transport in nanofiltration membranes: Diffusion, convection and electromigration. *Desalination*, 2017, 420, 241–257.

RUBIO, J., TESSELE, F. Removal of heavy metal ions by adsorptive particulate flotation. *Minerals Engineering*, 1997, 10, 671–679.

SABLANI, S.S., GOOSEN, M.F.A., AL–BELUSHI, R., WILF, M. Concentration polarization in ultrafiltration and reverse osmosis: a critical review. *Desalination*, 2001, 141, 269–289.

SALIH, M.H., AL–ALAWY, A.F. Mathematical modelling of zinc removal from wastewater by using nanofiltration and reverse osmosis membranes. *International Journal of Science and Research*, 2016, 7, 45–51.

SANTAFÉ–MOROS, A., GOZÁLVEZ–ZAFRILLA, J.M. Applicability of the DSPM with dielectric exclusion to a high rejection NF membrane in the separation of nitrate solutions. *Desalination*, 2008, 221, 268–276.

SCHAEP J., VANDECASTEELE, C., MOHAMMAD A. W., BOWEN W. R. Analysis of the salt retention of nanofiltration membranes using the Donnan steric partitioning pore model. *Separation Science and Technology*, 1999, 34, 3009–3030.

SCHAEP, J., VANDECASTEELE, C., MOHAMMAD, A.W., BOWEN, W.R. Modelling the retention of ionic components for different nanofiltration membranes. *Separation and Purification Technology*, 2001, 22, 169–179.

SCHAFER, A.I., FANE, A.G., WAITE, T.D. Nanofiltration–Principles and Applications Elsevier, Oxford, 2005. ISBN: 1–85617–405–0.

SEIDEL, A., ELIMELECH, M. Coupling between chemical and physical interactions in natural organic matter (NOM) fouling of nanofiltration membranes: Implications for fouling control, *Journal of Membrane Science*, 2002, 203, 245–255.

SEOANE, B., CORONAS, J., GASCON, I., BENAVIDES, M.E., KARVAN, O., CARO, J., GASCON, J. Metal–organic framework based mixed matrix membranes: a solution for highly efficient CO_2 capture. *Chemical Society Reviews*, 2015, 44, 2421–2454.

SHAHTALEBI, A., SARRAFZADEH, M.H., RAHMATI, M.M.M. Application of nanofiltration membrane in the separation of amoxicillin from pharmaceutical wastewater. *Iranian Journal of Environmental Health Science and Engineering*, 2011, 8, 109–116.

SHENVI, S.S., ISLOOR, A.M, ISMAIL, A.F. A review on RO membrane technology: Developments and challenges. *Desalination*, 2015, 368, 10–26.

SHON, H.K., VIGNESWARAN, S., BEN AIM, R., NGO, H.H., KIM, I.S., CHO, J. Influence of flocculation and adsorption as pre–treatment on the fouling of ultrafiltration and nanofiltration membranes: Application with biologically treated sewage effluent. *Environmental & Science Technology*, 2005, 39, 3864–3871.

SILVA, V., GERALDES, V., BRITES ALVES, A.M., PALACIO, L., PRÁDANOS, P., HERNÁNDEZ, A. Multi–ionic nanofiltration of highly concentrated salt mixtures in the seawater range, *Desalination*, 2011, 277, 29–39.

SIMON, A., MCDONALD, J.A., KHAN, S.J., PRICE, W.E., NGHIEM, L.D. Effects of caustic cleaning on pore size of nanofiltration membranes and their rejection of trace organic chemicals. *Journal of Membrane Sciences*, 2013, 447, 153–162.

SINGH, J., KALAMDHAD, A.S. Review paper effects of heavy metals on soil, plants, human health, and aquatic life. *International Journal of Research in Chemistry and Environment*, 2011, 1, 15–21.

SONG, Y., GAO, X., GAO, C. Evaluation of scaling potential in a pilot–scale NF–SWRO integrated seawater desalination system. *Journal of Membrane Science*, 2013, 443, 201–209.

SPIEGLER, K.S., KEDEM, O. Thermodynamics of hyperfiltration (reverse osmosis): Criteria for efficient membranes. *Desalination*, 1966, 1, 311–326.

SRIVASTAVA, N. K, MAJUMDER, C. B. Novel biofiltration methods for the treatment of heavy metals from industrial wastewater. *Journal of Hazardous Materials*, 2008, 151, 1–8.

STRATHMANN, H. 2011. Introduction to Membrane Science and Technology. Wiley–VCH, Weinheim, 2011. ISBN: 978–3–527–32451–4.

STRATHMANN, H., GIORNO, L., DRIOLI, E. An introduction to membrane science and technology. In: Consiglio Nazionale delle Recherché, Rome, 2006. ISBN: 978–3–527–32451–4.

SZYMCZYK, A., AOUBIZA, B., FIEVET, P., PAGETTI, J. Electrokinetic phenomena in homogeneous cylindrical pores. *Journal of Colloid and Interface Science*, 1999, 216, 285–296.

SZYMCZYK, A., FIEVET, P. Investigating transport properties of nanofiltration membranes by means of steric, electric, and dielectric exclusion model. *Journal of Membrane Science*, 2005, 252, 77–88.

SZYMCZYK, A., FIEVET, P. Ion transport through nanofiltration membranes: the steric, electric, and dielectric exclusion model. *Desalination*, 2006, 200, 122–124.

SZYMCZYK, A., FATIN–ROUGE, N., FIEVET, P. Tangential streaming potential as a tool in modelling of ion transport through nano porous membranes. *Journal of Colloid and Interface Science*. 2007, 309, 245–252.

TANNINEN, J., MÄNTTÄRI, M., NYSTRÖM, M. Effect of salt mixture concentration on fractionation with NF membranes. *Journal of Membrane Science*, 2006, 283, 57–64.

TAFFAREL, S.R., RUBIO, J. On the removal of Mn^{2+} ions by adsorption onto natural and activated Chilean zeolites. *Minerals Engineering*, 2009, 22, 336–343.

TCHOUNWOU, P.B., YEDJOU, C.G., PATLOLLA, A.K., SUTTON, D.J. Heavy metals toxicity and the environment. *National Institute of Health*, 2012, 101, 140–162.

TSURU, T., NAKAO, S., KIMURA, S. Calculation of ion rejection by extended Nernst–Planck equation with charged reverse osmosis membranes for single and mixed electrolyte solutions, *Journal of Chemical Engineering of Japan*, 1991, 24, 511–517.

TSURU, T., SASAKI, S., KAMADA, T., SHINTANI, T., OHARA, T., NAGASAWA, H., NISHIDA, K., KANEZASHI, M., YOSHIOKA, T. Multi–layered polyamide membranes by spray–assisted 2–step interfacial polymerization for increased performance of trimesoyl chloride (TMC)/m–phenylenediamine (MPD)–derived polyamide membranes. *Journal of Membrane Science*, 2013, 446, 504–512.

TUNAY, O., KABDASLI, N.I. Hydroxide precipitation of complexed metals. *Water Research*, 1994, 28, 243–245.

TUNG, K.–L., CHANG, K.–S., WU, T.–T., LIN, N.–J., LEE, K.–R., LAI, J.–Y. Recent advances in the characterization of membrane morphology. *Current Opinion in Chemical Engineering*, 2014, 4, 121–127.

UN–WATER 2009, Water annual report World Water http://www.unwater.org /publications/ un–water–annual–report–2009/ (Accessed: August 2018).

URAGAMI, T., YANAGISAWA, S., MIYATA, T. Water/Ethanol selectivity of new organic–inorganic hybrid membrane fabricated from poly (vinyl alcohol) and oligosilane. *Macromolecular Chemistry and Physics*, 2007, 208, 756–764.

UZAL, N., JAWORSKA, A., MIŚKIEWICZ, A., ZAKRZEWSKA–TRZNADEL, G. AND COJOCARU, C. Optimization of Co^{2+} ions removal from water solutions via polymer enhanced ultrafiltration with application of PVA and sulfonated PVA as complexing agents. *Journal of Colloid and Interface Science*, 2011, 362, 615–624.

VAN DER BRUGEN, B., MÄNTTÄRI, M., NYSTRÖM, M. Drawback of applying nanofiltration and how to avoid them: A review. *Separation and Purification Technology*, 2008, 63, 251–263.

VAN DER BRUGGEN, B., VANDECASTEELE, C. Modelling of the retention of uncharged molecules with nanofiltration. *Water Research*, 2002, 36, 1360–1368.

VAN DER BRUGGEN, B., VANDECASTEELE, C., VAN GESTEL, T., DOYEN, W., LEYSEN, R. A Review of pressure driven membrane processes in wastewater treatment and drinking water production. *Environmental Progress*, 2003, 22, 46–56.

VANÝSEK, P. Ionic conductivity and diffusion at infinite dilution, in: D.R. Linde (Ed.), CRC Handbook of Chemistry and Physics, 84th ed., CRC Press, Boca Raton, 2005.

VEERABABU, P., VYAS, B.B., SINGH, P.S., RAY, P. Limiting thickness of polyamide–polysulfone thin–film–composite nanofiltration membrane. *Desalination*, 2014, 346, 19–29.

VEZZANI, D., BANDINI, S. Donnan equilibrium and dielectric exclusion for characterization of nanofiltration membranes. *Desalination*, 2002, 149, 477–483.

VIAL, D., DOUSSAU, G. The use of microfiltration membranes for seawater pre–treatment prior to reverse osmosis membranes. *Desalination*, 2003, 153, 141–147.

VRIJENHOEK, E.M., WAYPA, J.J. Arsenic removal from drinking water by a "loose" nanofiltration membrane. *Desalination*, 2000, 130, 265–277.

WALLACE, E., CUHORKA, J., MIKULÁŠEK, P. Investigation of the structural and charge properties of a polyamide nanofiltration membrane, *Scientific Papers of the University of Pardubice, Series A*, 2017, 23, 225–243.

WALLACE, E, CUHORKA, J, MIKULÁŠEK, P. Characterization of nanofiltration membrane and its application for the separation of heavy metals from wastewater. *Waste Forum*, 2018, 2, 314–325.

WANG, X.L., WANG, W.N., WANG, D.X. Experimental investigation on separation performance of nanofiltration membranes for inorganic electrolyte solutions. *Desalination*, 2002, 145, 115–122.

WANG X.L., FANG Y.Y., TU C.H., VAN DER BRUGGEN, B. Modelling of the separation performance and electrokinetic properties of nanofiltration membranes. *International Reviews in Physical Chemistry*, 2012, 31,111–130.

WANG X.L., TSURU T., TOGOH M., NAKAO S., KIMURA S. Evaluation of pore structure and electrical properties of nanofiltration. *Journal of Chemical Engineering of Japan*, 1995, 28, 186–192.

WANG, L.Y., FANG, M.Q., LIU, J., HE, J., LI, J.D., Lei, J.D. Layer–by–layer fabrication of high–performance polyamide/ZIF–8 nanocomposite membrane for nanofiltration applications. *American Chemical Society Applied Materials & Interfaces*, 2015, 7, 24082–24093.

WANG, Z., LIU, G., FAN, Z., YANG, X., WANG, J., WANG, S. Experimental study on treatment of electroplating wastewater by nanofiltration. *Journal of Membrane Science*, 2007, 305, 185–195.

WEI, X. KONG, X., YANG, J., ZHANG, G., CHEN, J., WANG, J. Structure influence of hyperbranched polyester on structure and properties of synthesized nanofiltration membranes. *Journal of Membrane Science*, 2013, 440, 67–76.

WEI, X., KONG, X., WANG, S., XIANG, H., WANG, J., CHEN, J. Removal of heavy metals from electroplating wastewater by thin–film composite nanofiltration hollow–fiber membranes. *Industrial and Engineering Chemistry Research*, 2013, 52, 17583–17590.

WEI, X., WANG, Z., FAN, F., WANG, J., WANG, S. Advanced treatment of a complex pharmaceutical wastewater by nanofiltration: membrane foulant identification and cleaning. *Desalination*, 2010, 251, 167–175.

WERBER, J.R., OSUJI, C.O., ELIMELECH, M. Materials for next–generation desalination and water purification membranes. *Nature Reviews Materials*, 2016, 1, 16018–16033.

YANG, Z., ZHOU, Y., FENG, Z., RUI, X., ZHANG, T., ZHANG, Z. A Review on reverse osmosis and nanofiltration membranes for water purification. *MDPI Polymers*, 2019, 11, 1–22.

YAROSHCHUK, A. E. Dielectric exclusion of ions from membranes. *Advances in Colloid and Interface Science*, 2000, 85, 193–230.

YAROSHCHUK, A.E. Non–steric mechanisms of nanofiltration: superposition of Donnan and dielectric exclusion. *Separation and Purification Technology*, 2001, 22, 143–158.

YAROSHCHUK, A.E. Recent progress in the transport characterisation of nanofiltration membranes. *Desalination*, 2002, 149, 423–428.

YUASA, M., KOBATAKE, Y., FUJITA, H. Studies of membrane phenomena. VII. Effective charge densities of membrane. *Journal of Physical Chemistry*, 1968, 72, 2871–2879.

ZAFRILLA, J.M.G., MOROS, A.S. Nanofiltration modelling based on the extended Nernst–Planck equation under different physical modes. Proceedings of the European COMSOL Conference, Hannover, Germany, 2008.

ZHANG, S., LIU, L., PANG, X. Use of microfiltration to improve quality and shelf life of ultra–high temperature milk. *Journal of Food Processing and Preservation*, 2015, 40, 707–704.

ZHAO, F.Y., JI, Y.L., WENG, X.D., MI, Y.F., YE, C.C., AN, Q.F., GAO, C.J. High–flux positively charged nanocomposite nanofiltration membranes filled with poly(dopamine) modified multiwall carbon nanotubes. *ACS Applied Materials & Interfaces*, 2016, 8, 6693–6700.

ZHAO, K., LI. Y. Dielectric characterization of a nanofiltration membrane in electrolyte solutions: its double–layer structure and ion permeation. *Journal of Physical Chemistry*, 2006, 110, 2755–2763.

ZHENG, X., WEI, Y.S., WANG, Z.W., ZHANG, Z.X. Report for sustainable development strategy of China water treatment industry, Membrane and Industry II, China Renmin University Press, Beijing (in Chinese), 2016.

ZHU, W.–P., SUN, S.–P., GAO, J., FU, F.–J., CHUNG, T.–S. Dual–layer polybenzimidazole/polyethersulfone (PBI/PES) nanofiltration (NF) hollow fiber membranes for heavy metals removal from wastewater. *Journal of Membrane Science*, 2014, 456, 117–127.

ZYDNEY, A.L. Stagnant film model for concentration polarisation in membrane systems. *Journal of Membrane Science*, 1997, 130, 275–281.

Appendix

Protocols from analyses (Original in Czech language)

Note: *P is the permeate sample and F is the feed concentration sample*

Table 1. Sample of both permeate and feed concentration at 50 mg L^{-1} (AFC 80) – 07.09.2017

Sample	Ni [mg L^{-1}]
P1	0.916
P2	0.834
P3	0.746
P4	0.655
P5	0.698
F1	42.57
F2	43.56

Table 2. Sample of both permeate and feed concentration at 100 mg L^{-1} (AFC 30) – 10.10.2018

Sample	Ni [mg L^{-1}]
P1	51.62
P2	44.75
P3	41.61
P4	38.24
P5	35.53
P6	33.49
F1	95.76
F2	97.05

Table 3. Sample of both permeate and feed concentration at 50 mg L^{-1} (AFC 30) – 04.10.2018

Sample	Ni [mg L^{-1}]
P1	28.48
P2	26.25
P3	24.24
P4	21.96
P5	20.47
P6	19.77
F1	48.77
F2	49.41

Table 4. Sample of both permeate and feed concentration at 100 mg L^{-1} (AFC 30) – 20.11.2018

Sample	Zn [mg L^{-1}]	Sample	Zn [mg L^{-1}]
P1	57.09	P13	58.83
P2	51.13	P14	57.00
P3	47.75	P15	55.51
P4	44.86	P16	54.45
P5	42.92	P17	55.04
P6	41.56	P18	56.32
P7	58.00	F1	81.56
P8	53.54	F2	82.23
P9	50.27	F3	82.62
P10	47.92	F4	83.75
P11	46.19	F5	84.63
P12	45.25	F6	86.52

Table 5. Sample of both permeate and feed concentration at 50 mg L^{-1} (AFC 80) – 27.09.2017

Sample	Zn [mg L^{-1}]	Sample	Zn [mg L^{-1}]	Sample	Zn [mg L^{-1}]
F1	57.69	P3	1.134	P11	0.749
F2	60.11	P4	1.077	P12	1.184
F3	51.37	P5	1.111	P13	3.200
F4	54.26	P6	1.154	P14	2.511
F5	66.12	P7	1.277	P15	2.333
F6	69.53	P8	0.939	P16	2.041
P1	1.593	P9	0.876	P17	1.889
P2	1.293	P10	0.846	P18	1.850

Table 6. Sample of both permeate and feed concentration at 50 mg L^{-1} (AFC 80) – 27.09.2017

Sample	Zn [mg L^{-1}]	Sample	Zn [mg L^{-1}]
P1	0.624	F1	50.65
P2	0.543	F2	51.92
P3	0.590	F3	53.13
P4	0.490	F4	53.44
P5	0.492	F5	55.19
P6	0.405	F6	45.19
P7	0.355	F7	52.56
P8	0.643		

Table 7. Sample of both permeate and feed concentration at 50 and 100 mg L^{-1} (AFC 80) – 23.09.2018

Sample	Ni [mg L^{-1}]	Sample	Ni [mg L^{-1}]
P1	1.374	P8	2.636
P2	1.238	P9	2.572
P3	1.169	P10	2.534
P4	1.287	F1	50.41
P5	1.372	F2	53.38
P6	2.988	F3	96.59
P7	2.766	F4	99.30